# The art of calorimetry part V

Erika Garutti
DESY

# Remaining topics to discuss

MC models & validation

Calorimeters around the world: the most popular ones

Calibration and monitoring

# Validation of MC models

To design a calorimeter often people use MC simulation

Question:

➔ How reliable is “the simulation”?

➔ For which aspect of a calorimeter it can be safely used?

Answer:

➔ EM processes are generally modeled at 1-2% level accuracy in the energy rage relevant for most of HEP calorimeters

➔ Hadronic processes… let’s discuss about that…

# Models comparison in GEANT

## Integrated quantities

Energy correction coefficient = E_generated / E_reconstructed

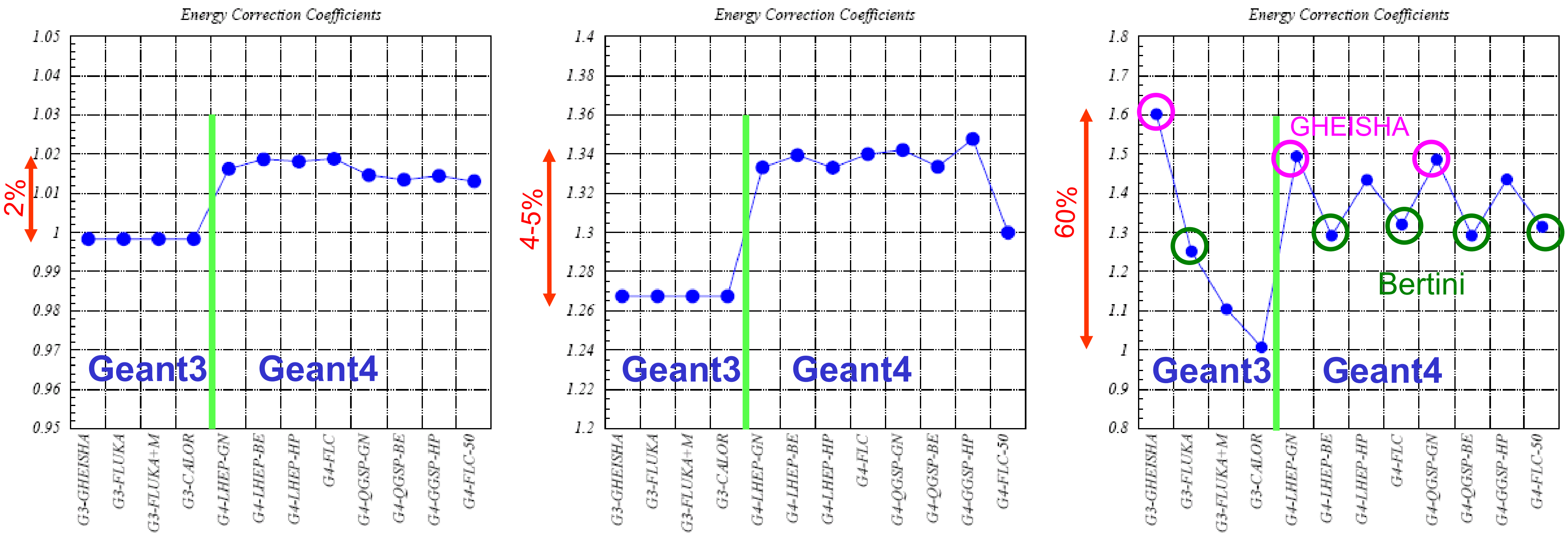


Muon 2 GeV

Electron 2 GeV

Pion + 10 GeV

Materials, geometry, energy cutoff optimized to be as similar as possible (@ 2% level, see muon)

# Models comparison

## Integrated quantities

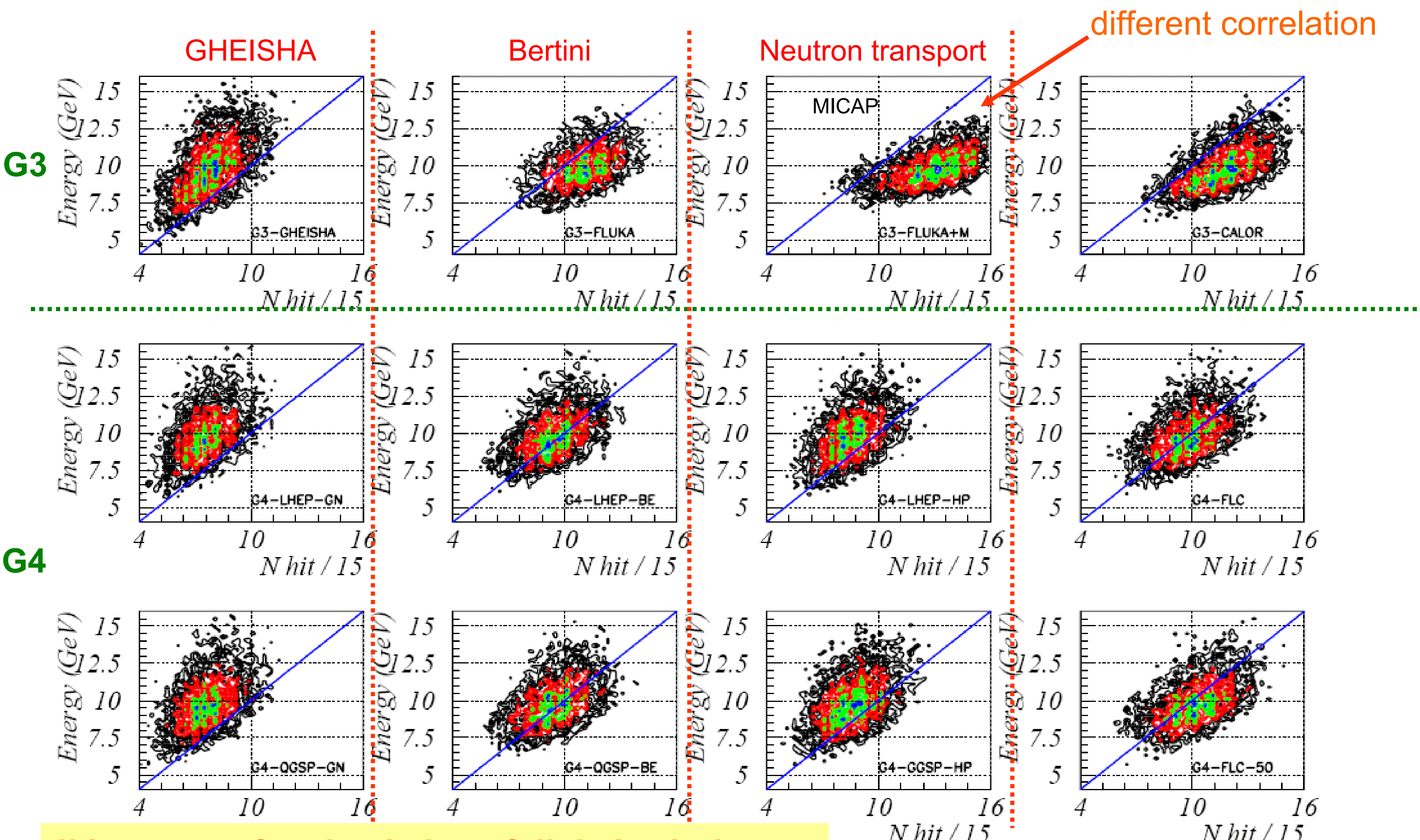


**!! Important for simulation of digital calorimeter**

# Models comparison

## Differential quantities

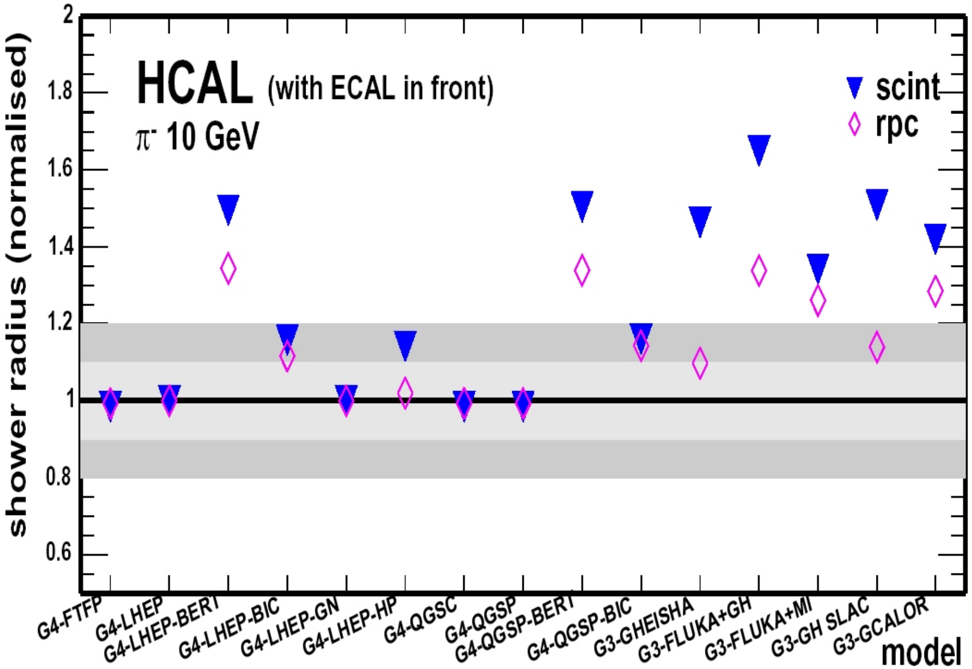


**IMPORTANT!**

**This picture changes dramatically when including realistic time cut from electronics**

**➔ Main differences in neutron content (> 200 ns)**

**High granularity offers the possibility to investigate longitudinal and lateral shower shapes with unprecedented precision**

➔Up to 60% variation between different models

➔More typical ~20%

# A deeper comparison

## Shower composition

**Binding / Lost Energy = $E_{beam} - (E_{EM} + E_{HAD})$ .vs. # of reconstructed neutrons**

**New benchmark for data/MC comparison**

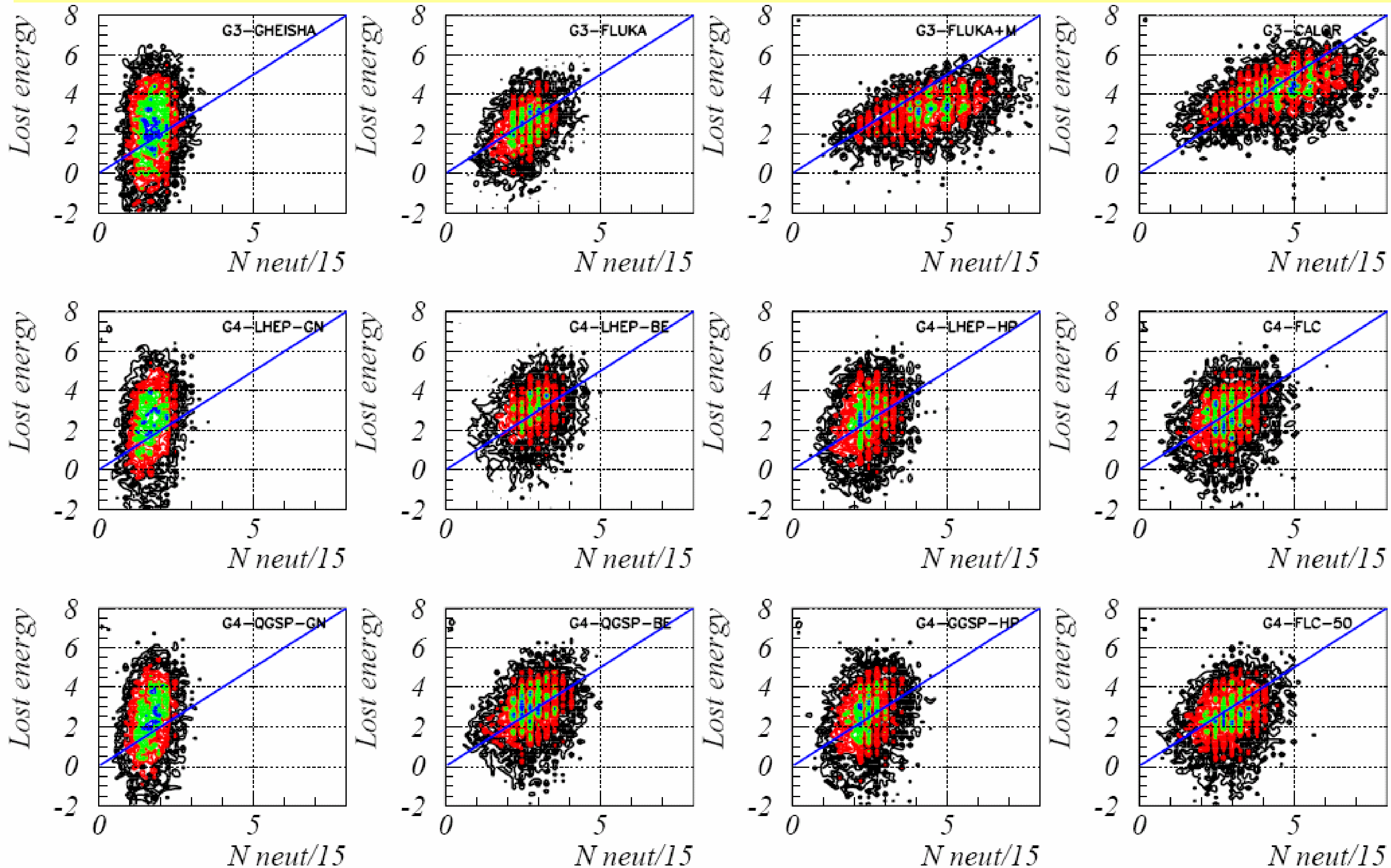

# Medium energy differences between models

Preliminary studies for the KOPIO project (from Joseph Comfort) $K_L$ and n beam-line under consideration for future experiment (secondary beam production from 30 GeV/c protons on Ni)

➔ Simulate 4 GeV/c $K_L$ , $K^+$, $p^+$, n beams on 1cm cube lead, look momentum and $\Theta$ spread "differences such as these (up to 2-4 between FLUKA and GEANT4) can be very disturbing for proposals for experiments, …, in our application the FLUKA results were more favorable."

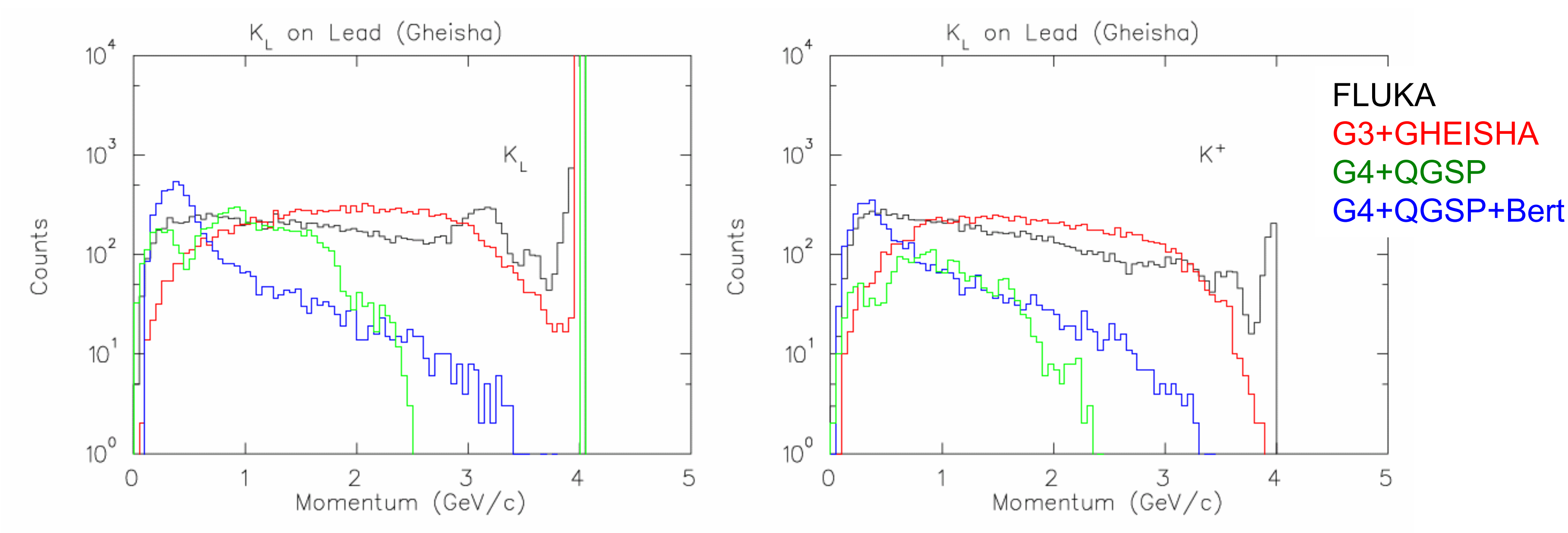


**Large differences between models at medium energies**

# Hadronic Inelastic Model Inventory

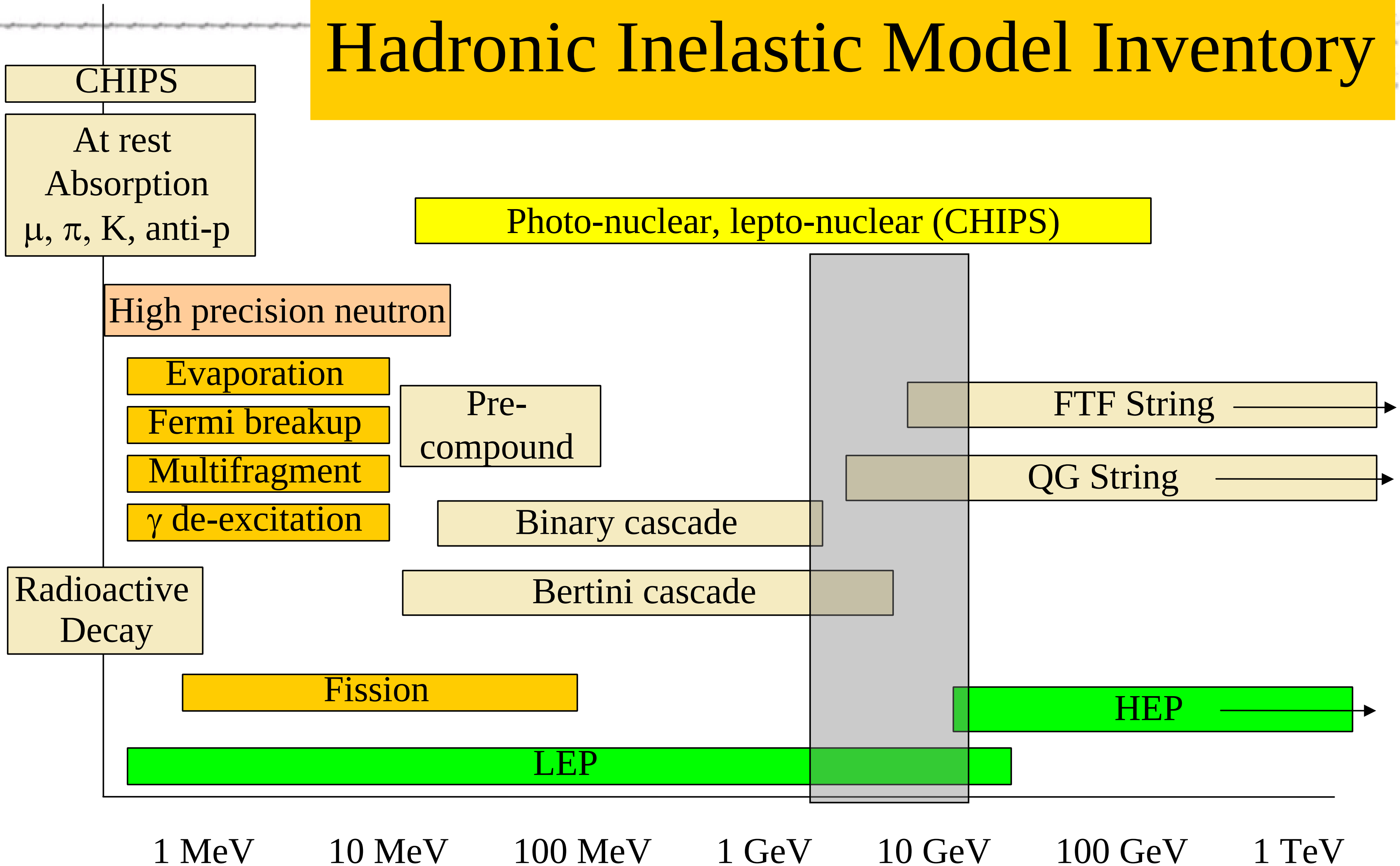

# Brief introduction to Physics Lists

4

Nuclear de-excitation
Evaporation etc.

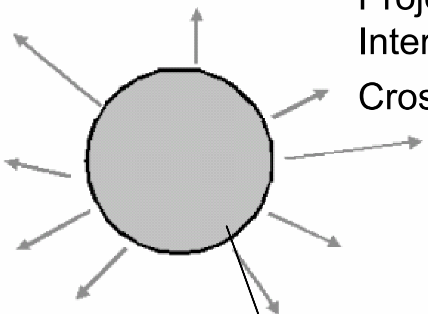

3

Bertini nucleon-nucelon cascade
step-like concentric nuclear potential in 3d
Projectile transported along straight-lines
Interaction according to mean free path

Cross-section and angles from experiment

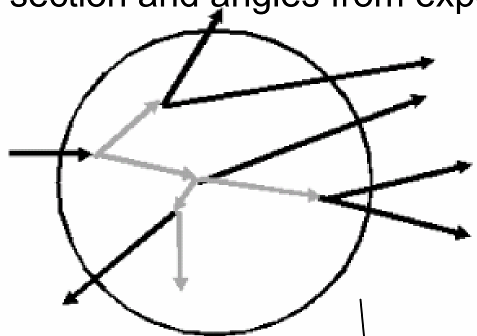

2

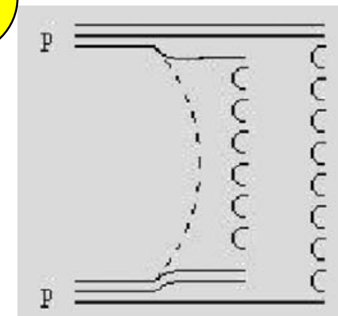


1

Particle nucleus
collision according
to cross-sections

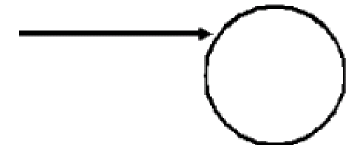

QGS: Quark-Gluon String

Nucleon is split in quark di-quark
Strings are formed
String hadronisation (adding q-qbar pair)
fragmentation of damaged nucleus
with pre-compound (P)
Nucleon/nucleon interaction+
Nuclear de-excitation

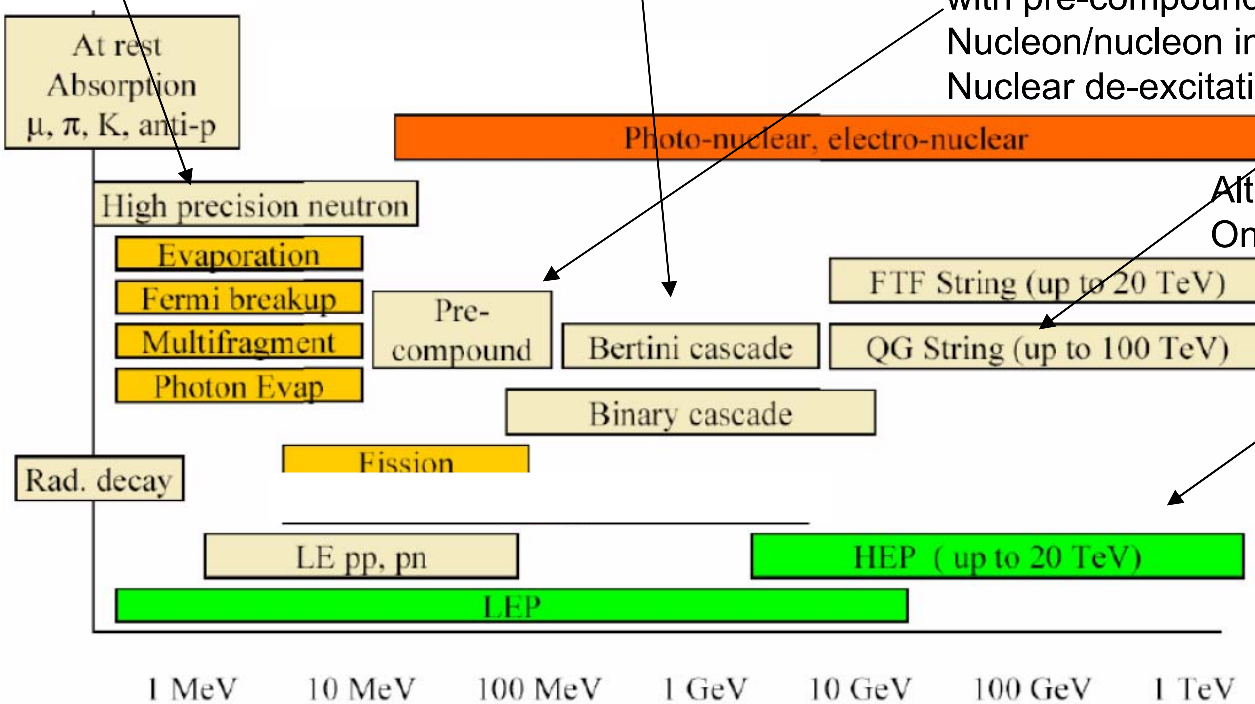


Fritiof:
Alternative string frag.
Only momentum exchanged

Parameterised
models
(as in old Gheisha)

QGSP-BERT

# Multiplicity of Secondary Particles at First Interaction


QGSP

QGSP-BERT

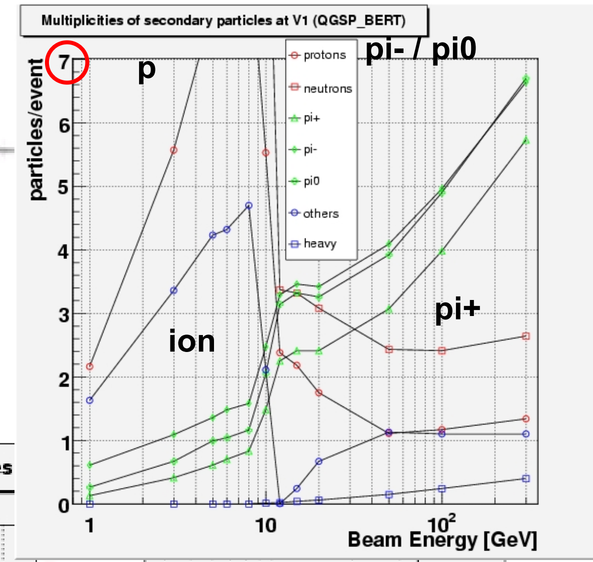


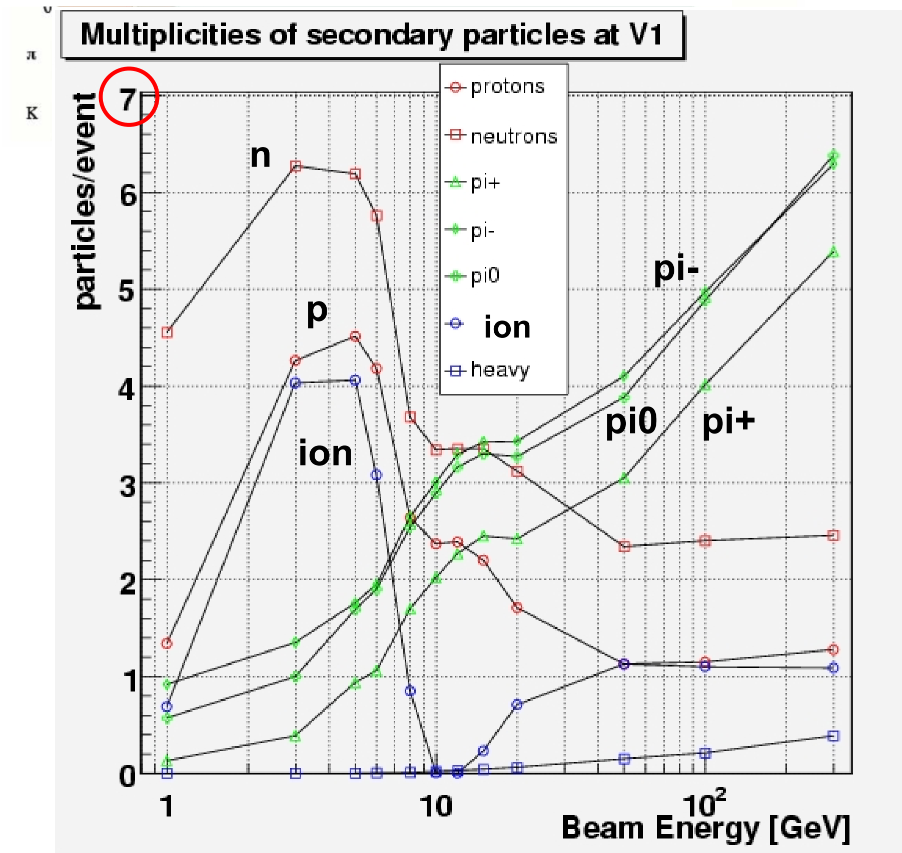


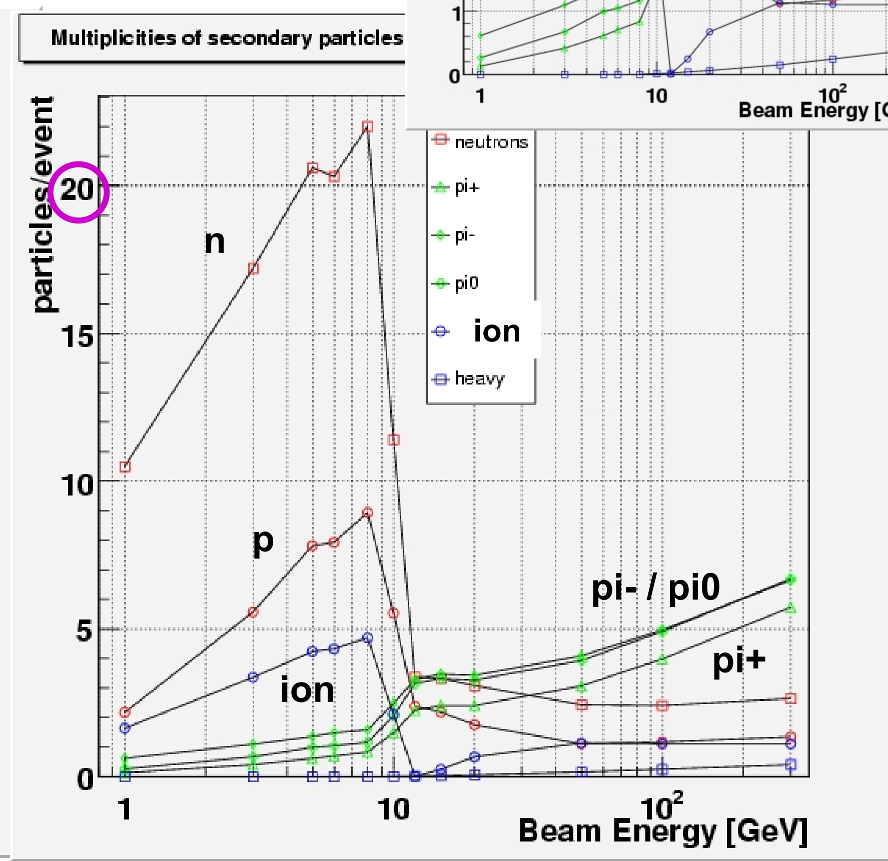


Too much neutrons / protons / ions ?

Pion production not smooth around 10-20GeV.

# Comparison of phys. lists

## Example of a model comparison study

G4 version 8.2
range cut 0.7 mm
pi- 30,100,300 GeV
Cu-LAr sampling calorimeter (25mm Cu : 8.5 mm LAr)
length = 10 $\lambda$, width = 150 cm
simplified geometry:

the calorimeter is divided in 4 longitudinal blocks (L1 – L4) 2.5 $\lambda$ each
and 3 concentric cylinders (R1 – R3) with R1<0.3 $\lambda$, 0.3 < R2 < 0.6 $\lambda$ and R3>0.6 $\lambda$

Always important to specify / check the range ($\propto$ E) cut
Rule of thumb: set range cut ~1/10 of minimum material thickness

# The results

| Observable | LHEP | QGSP | QGSC | QGSP_BIC | QGSP_BERT | QGSP_BERT_HP |
|---|---|---|---|---|---|---|
| $E_{vis}$ | $1113 \pm 2$ MeV | 1183 | 1160 | 1225 | 1277 | 1292 |
| $\sigma_E/E$ | 13.6% | 12.3% | 13.8% | 11.0% | 9.5% | 9.6% |
| $e/\pi$ | 1.30 | 1.22 | 1.24 | 1.18 | 1.13 | 1.12 |
| $f_{L1}$ | $67.8 \pm 0.5$ % | 66.3% | 67.3% | 65.3% | 62.1% | 61.6% |
| $f_{L2}$ | $26.3 \pm 0.3$ % | 26.9% | 26.3% | 27.5% | 29.5% | 29.4% |
| $f_{L3}$ | $5.1 \pm 0.1$ % | 5.8% | 5.6% | 5.9% | 7.1% | 7.4% |
| $f_{L4}$ | $0.8 \pm 0.04$ % | 1.0% | 0.9% | 1.2% | 1.4% | 1.5% |
| $f_{R1}$ | $72.8 \pm 0.3$ % | 76.1% | 76.2% | 72.7% | 67.5% | 66.7% |
| $f_{R2}$ | $23.7 \pm 0.1$ % | 21.1% | 21.0% | 22.6% | 25.8% | 25.6% |
| $f_{R3}$ | $3.6 \pm 0.04$ % | 2.8% | 2.8% | 4.7% | 6.7% | 7.7% |
| $\#EM$ | $25{,}931 \pm 120$ | 29,720 | 28,377 | 35,182 | 37,470 | 38,034 |

…

30 GeV pi-

let's look at this table step by step

# the choice of models

the two main opponents

| Observable | LHEP | QGSP | QGSC | QGSP_BIC | QGSP_BERT | QGSP_BERT_HP |
|---|---|---|---|---|---|---|

QGS + CHIPS

combine only theoretical models
with each other,
parameterization is used to fill the gaps

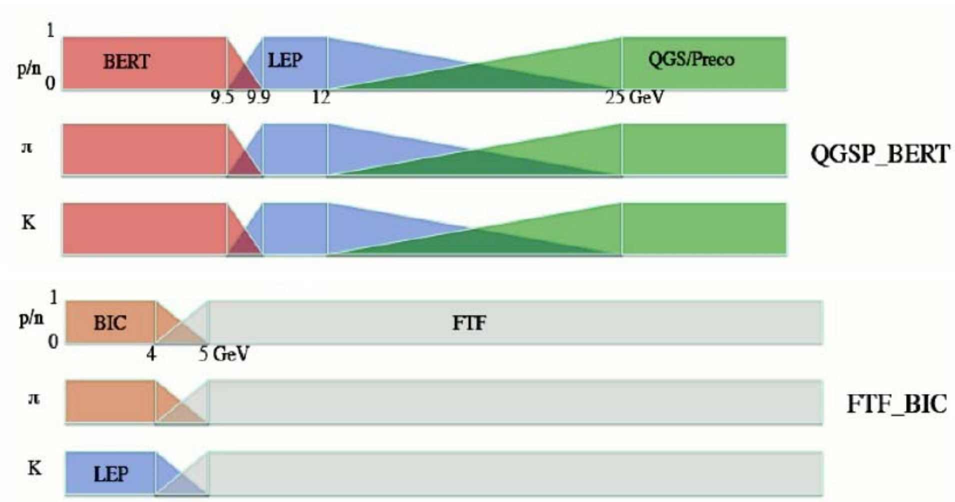


NOTE: new trend from G4 group, try to remove the mix between theoretical models and parameterization (LEP + HEP)

# Integral quantities

| Observable | LHEP | QGSP | QGSC | QGSP_BIC | QGSP_BERT | QGSP_BERT_HP |
|---|---|---|---|---|---|---|
| $E_{vis}$ | $1113 \pm 2$ MeV | 1183 | 1160 | 1225 | 1277 | 1292 |
| $\sigma_E/E$ | 13.6% | 12.3% | 13.8% | 11.0% | 9.5% | 9.6% |
| $e/\pi$ | 1.30 | 1.22 | 1.24 | 1.18 | 1.13 | 1.12 |

lowest E vis
worse E resolution
largest e/pi

largest E vis
best E resolution
lowest e/pi

← favorite by data

ATLAS End-cap hadronic calorimeter

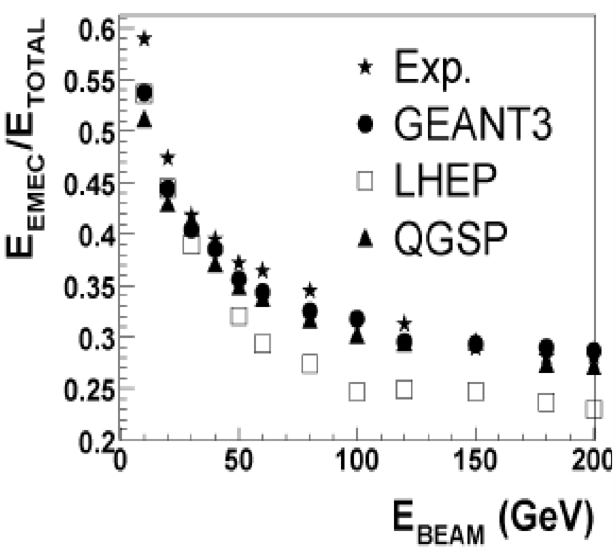


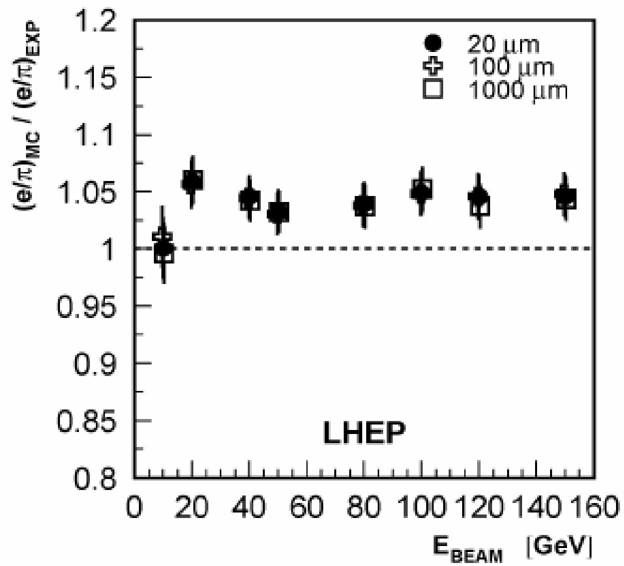


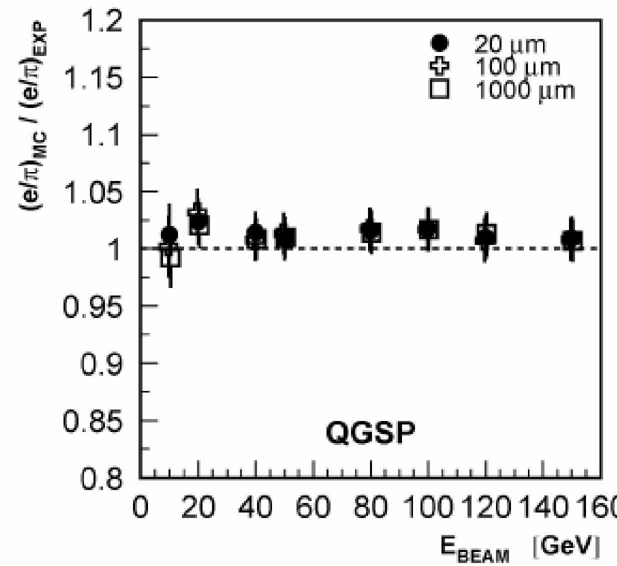

# longitudinal shower shape in data

CMS HCAL (brass/scintillator sampling)

LHEP predicts longest and wider showers
➔ better agreement to data

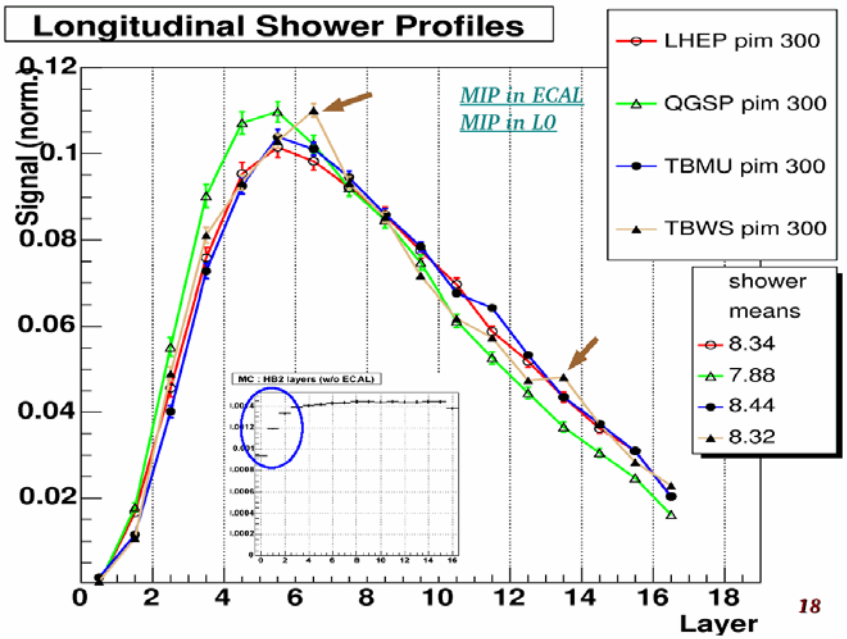


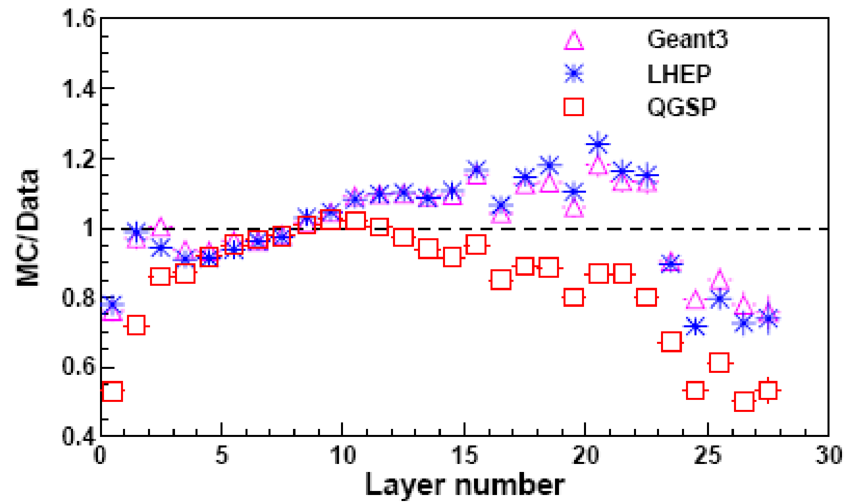


**Figure 9:** Ratio between simulations and data for longitudinal shower profile of 100 GeV $\pi$ in the HCAL standalone test-beam set-up.

# Shower shape

| Observable | LHEP | QGSP | QGSC | QGSP_BIC | QGSP_BERT | QGSP_BERT_HP |
|---|---|---|---|---|---|---|
| $f_{L1}$ | $67.8 \pm 0.5$ % | 66.3% | 67.3% | 65.3% | 62.1% | 61.6% |
| $f_{L2}$ | $26.3 \pm 0.3$ % | 26.9% | 26.3% | 27.5% | 29.5% | 29.4% |
| $f_{L3}$ | $5.1 \pm 0.1$ % | 5.8% | 5.6% | 5.9% | 7.1% | 7.4% |
| $f_{L4}$ | $0.8 \pm 0.04$ % | 1.0% | 0.9% | 1.2% | 1.4% | 1.5% |
| $f_{R1}$ | $72.8 \pm 0.3$ % | 76.1% | 76.2% | 72.7% | 67.5% | 66.7% |
| $f_{R2}$ | $23.7 \pm 0.1$ % | 21.1% | 21.0% | 22.6% | 25.8% | 25.6% |
| $f_{R3}$ | $3.6 \pm 0.04$ % | 2.8% | 2.8% | 4.7% | 6.7% | 7.7% |

same shower shape when exchanging pre-compound and CHIPS. BUT, they are the same for E<10 GeV

inter-nuclear cascade models make showers longer and wider
RIGHT direction!
but they change E res and e/pi
WRONG direction ➔ to be checked

Bertini stronger effect than Binary:
pi/k E<10 GeV Bertini
pi E<3 GeV Binary

Favorite
by data:
longer and wider showers

HP has small effect on shape

# shower composition

| Observable | LHEP | QGSP | QGSC | QGSP_BIC | QGSP_BERT | QGSP_BERT_HP |
|---|---|---|---|---|---|---|
| $\#EM$ | 25,931 $\pm$ 120 | 29,720 | 28,377 | 35,182 | 37,470 | 38,034 |
| $\#\pi$ | 48 $\pm$ 0.1 | 39 | 39 | 41 | 37 | 37 |
| $\pi^0/\pi$ | 38% | 38% | 38% | 37% | 32% | 32% |
| $\#p$ | 140 $\pm$ 0.7 | 129 | 147 | 121 | 151 | 144 |
| $\#n$ | 244 $\pm$ 1.1 | 247 | 272 | 445 | 807 | 647 |

LHEP has the smallest EM fraction

smallest fraction of pi0 due to Bertini instead of LEP for pi E<10GeV

electrons give the largest contribution to visible energy (followed by p, pi+/-, and ions. K and mu are negligible)

electron contribution to shower shape is shortest and narrowest

➔LHEP describes had. shower profiles well at high energies

➔too high EM component in QGS, maybe due to overproduction of pi0

LEP under-production of pi0 is compensated in high energy shower by over-production in HEP when used alone LEP does a bad job

from G4: we need to replace LEP with a better model for pions ➔ !!!

# there is more to G4 than physics lists

- hadronic cross sections: elastic (quasi- elastic) and inelastic contribute to longitudinal profile
- disadvantage in G4: hadron-nucleon cs for E>100 GeV is wrong

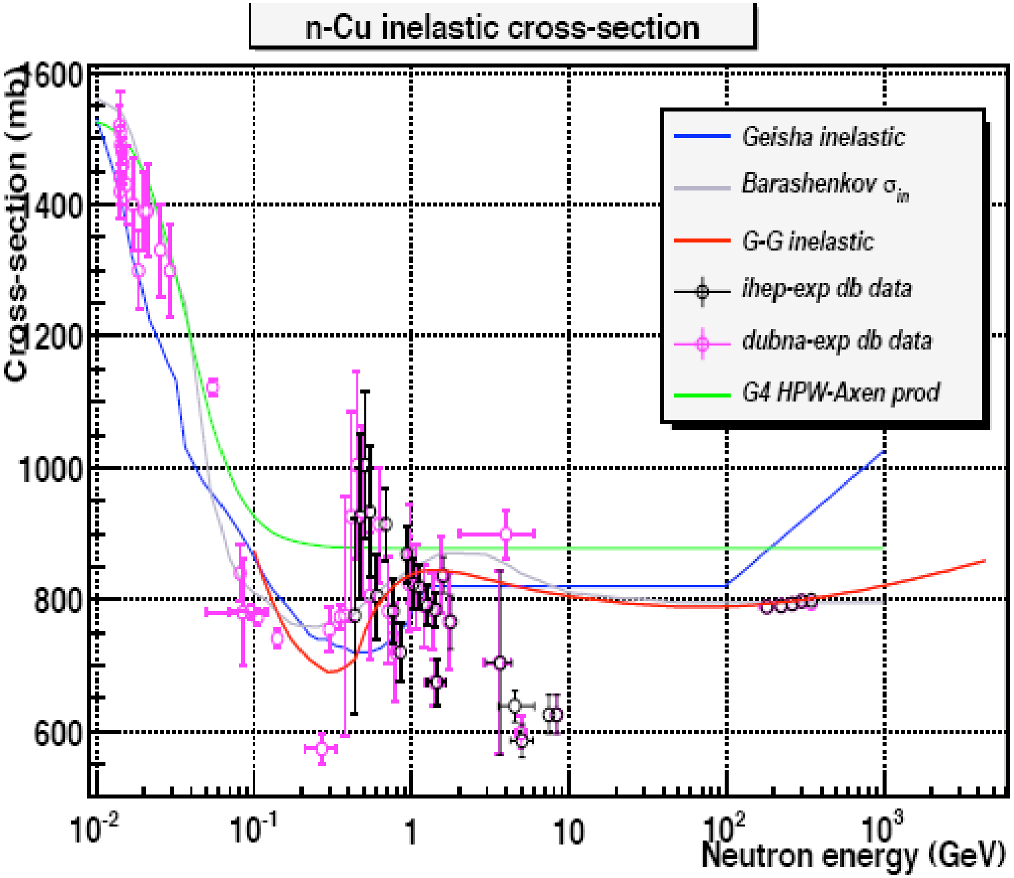


LHEP large relativistic rise

QGSP constant

new Glauber-Gribov model with small relativistic rise at E>100GeV better reproduces thin target data

# Elastic scattering

elastic scattering of hadrons directly affects shower development in matter

in scintillators E transfer from low E neutrons to recoil nuclei is dominated by neutron elastic scattering on protons in scintillator

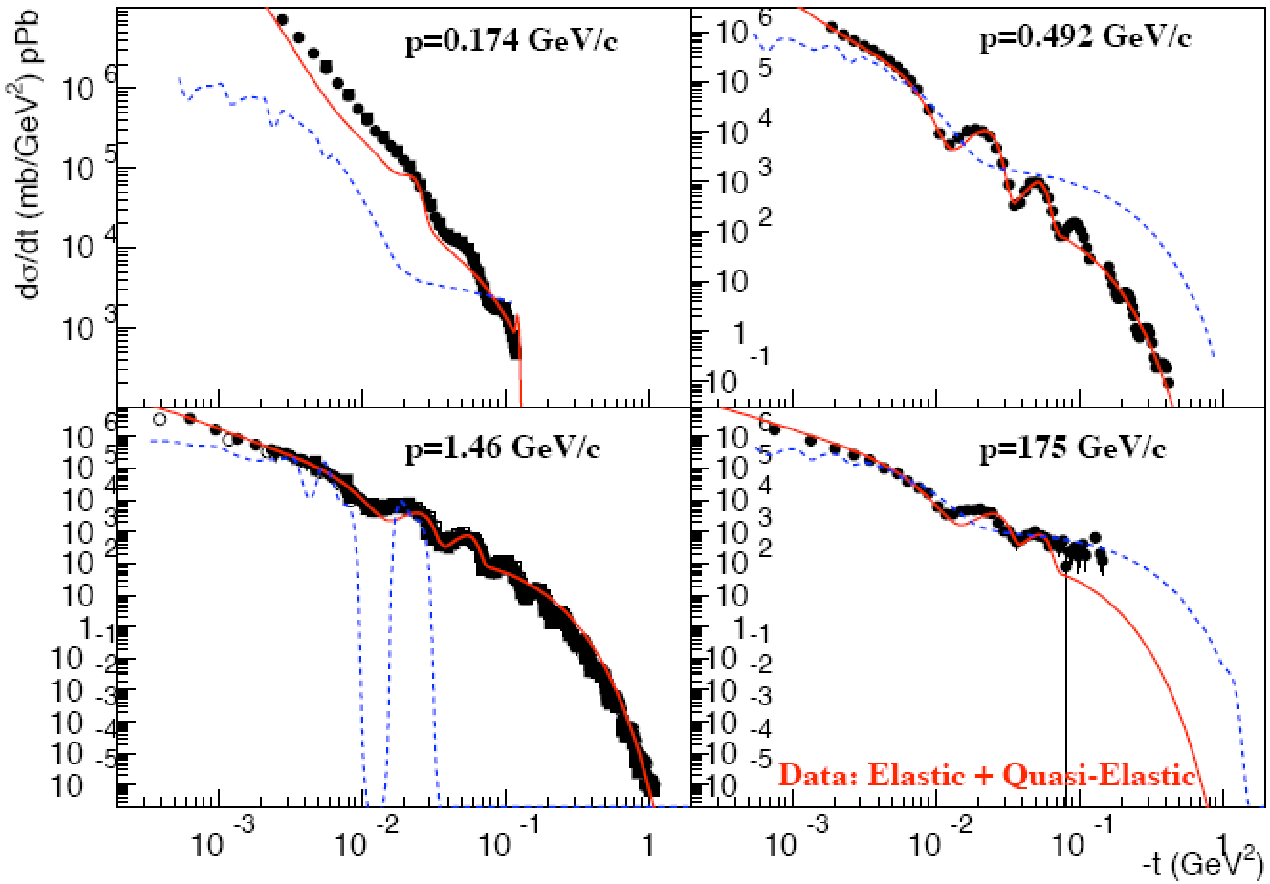


G4HadronElastic

G4QElastic

G4 8.2 includes G4QElastic in QGSC

QGSP still uses G4HadronElastic

can this be changed?

# Remarks on validation of physics lists

10 GeV energy range in GEANT has currently an “unphysical” step
➔ requires special validation work and change in the physics lists

no mixing of LHEP with theoretical cascade models suggested by G4

check cross sections used by various phys. lists before claiming wrong results

crosscheck first the general trends:

| | |
|---|---|
| LHEP / QGSP | better E res / shorter showers |
| QGSP/ QGSP_BERT | shower gets longer and wider |

try to disentangle physics and detector features
- remove effects from data
- minimize digitization impact on comparison

all studies from G4 group are based on ideal detector simulation compared to experimental data ➔ the more data available the better validation!

# There is not only GEANT

| Physics | MCNPX | GEANT4 | FLUKA | MARS | PHITS |
|---|---|---|---|---|---|
| **Particles** | 34 | 68 | 68 | 41 | 38 |
| **Charged particles** | CSDA | CSDA | CSDA | CSDA | CSDA |
| Energy loss | Bethe-Bloch | Bethe-Bloch | Bethe-Bloch | Bethe-Bloch | Bethe-Bloch |
| Scatter | Rossi | Lewis | Moliere improved | Moliere improved | Moliere |
| Straggling | Vavilov | Urban | Custom | Custom | Vavilov |
| XTR/Cheren. | No | Yes | No/yes | No | No |
| **Baryons** | | | | | |
| Neutron | | | | | |
| Low | Cont. (ENDF) | Cont. (ENDF) | Multigroup(72) | Cont. (ENDF) | Cont. (ENDF) |
| High | Models | Models | Models | Models | Models |
| Proton | | | | | |
| Low | Cont. (ENDF) | Models | Models | Models | Models |
| High | Models | Models | Models | Models | Models |
| Other | Model List:<br>Bertini<br>ISABEL<br>CEM<br>INCL<br>FLUKA89>3 GeV<br>LAQGSM (2.6.C) | Model list:<br>Hadron-nucleous<br>GHEISHA*<br>INUCL(Bertini)<br>BIC<br>CHIPS<br>QGS/FTF>8 GeV | Model list:<br>PEANUT(GINC)<br>+DPM+Glauber | Model list:<br>Custom<br>CEM<br>LAQGSM<br>DPMJET | Model list:<br>Bertini<br>JAM>3 GeV |

**Include intra-nuclear cascade models from FLUKA and MCNP**

Maybe integration of nuclear transport has less priority !?

# Energy deposited per particle type

Proton beam has larger proton fraction in shower, otherwise similar.

LAr has much less proton than Tile

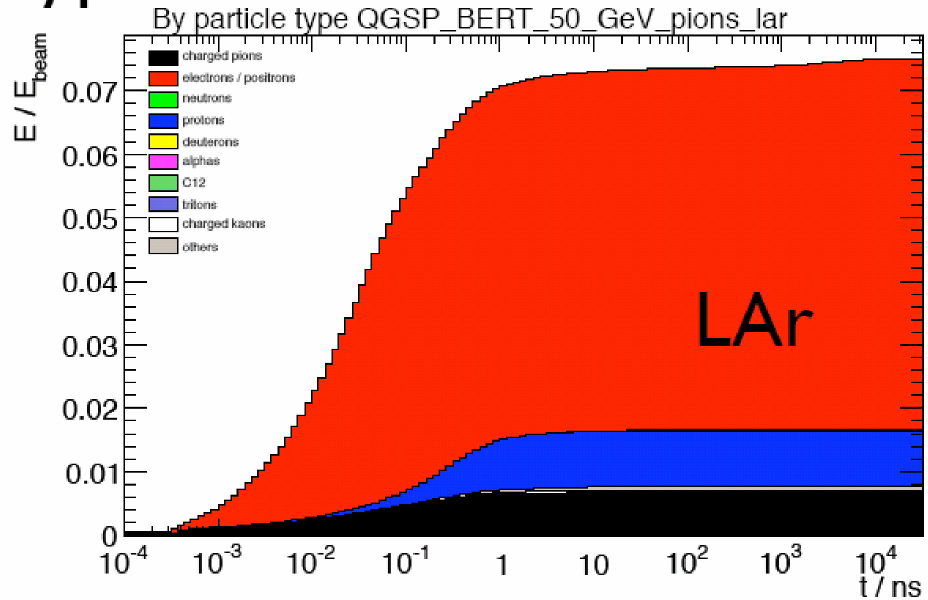


Energy deposited directly by neutrons in QGSP_BERT.

Protons seen depositing energy as late as 3–30 ns, while pions have deposited all their energy already after a few nanoseconds. Seen for the Bertini models.

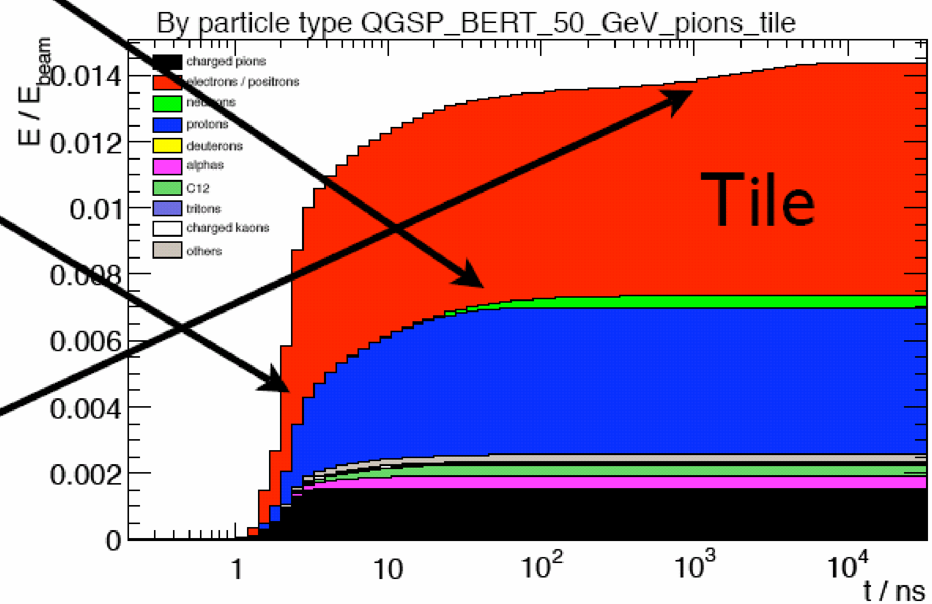


Very late deposition seen from electrons in QGSP_BERT.

# Origin of late protons

All plots for tile calorimeter
QGSP_BERT, 50 GeV pions

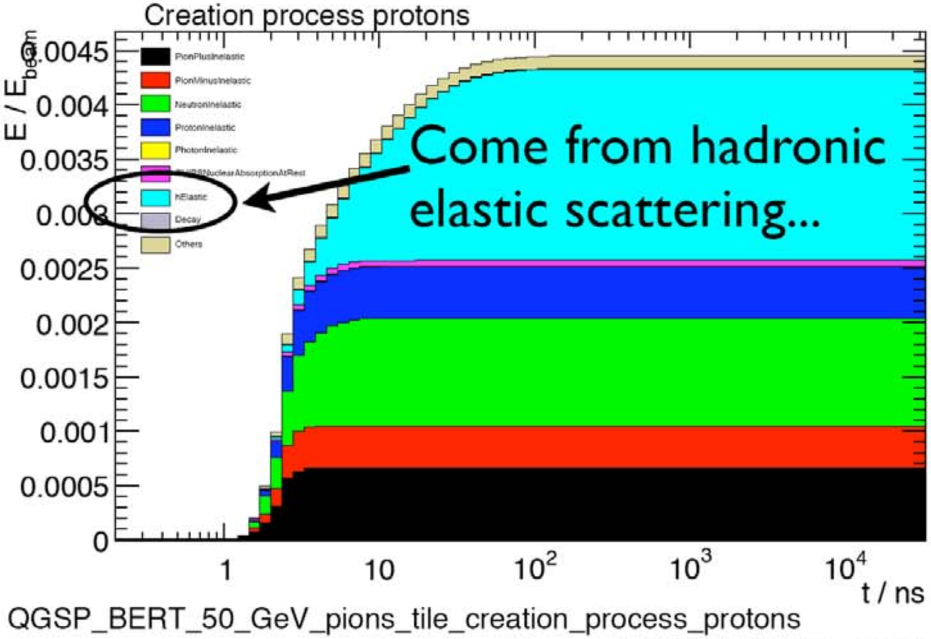


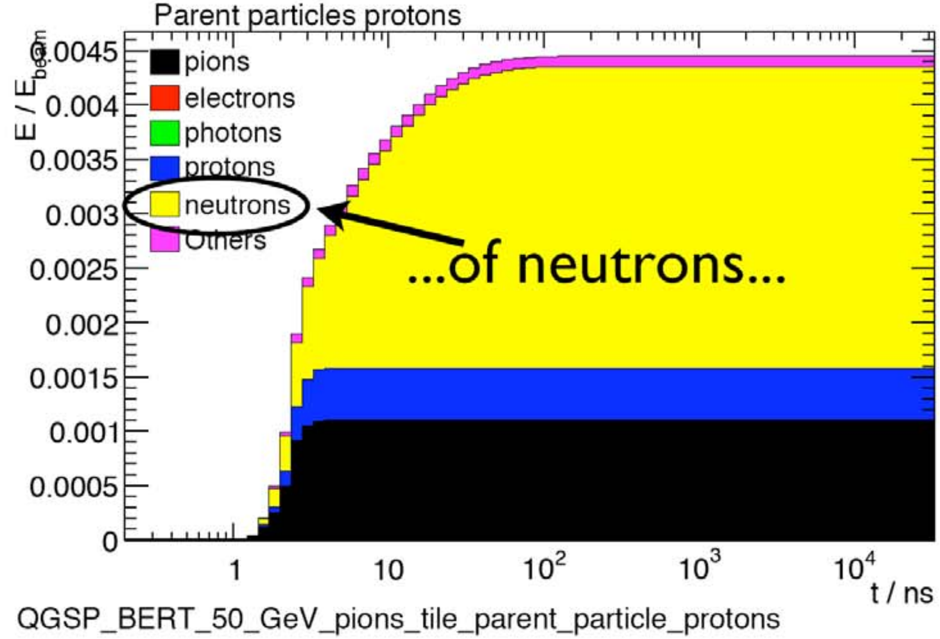


CTB Set-up

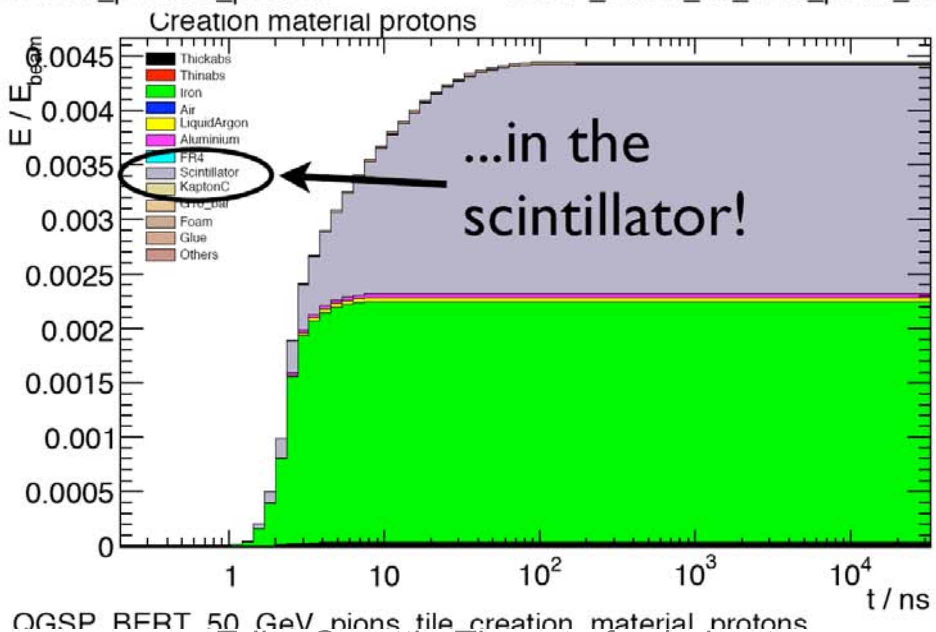

# Origin of very late electrons in tile

All plots for tile calorimete
QGSP_BERT, 50 GeV pions

Parent particles electrons

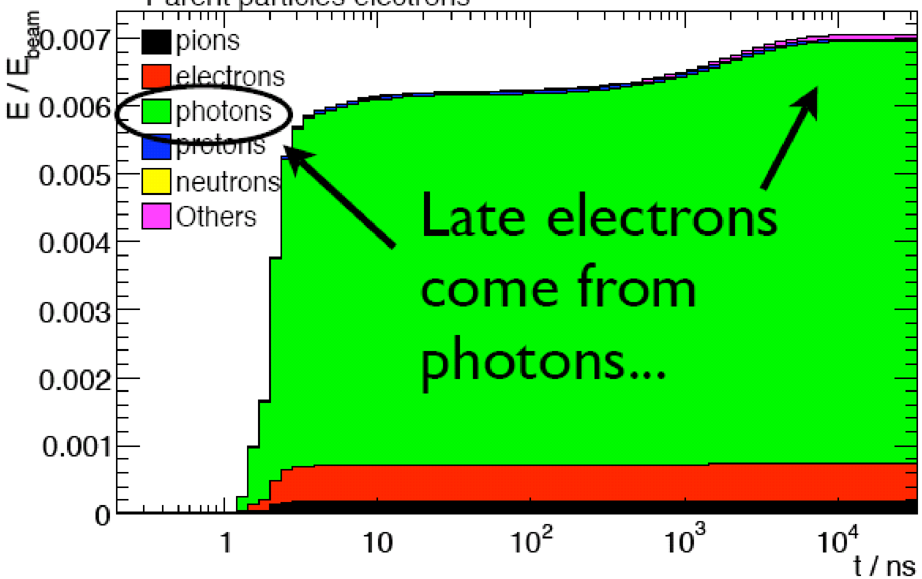


QGSP_BERT_50_GeV_pions_tile_parent_particle_electrons

Parent creation process electrons

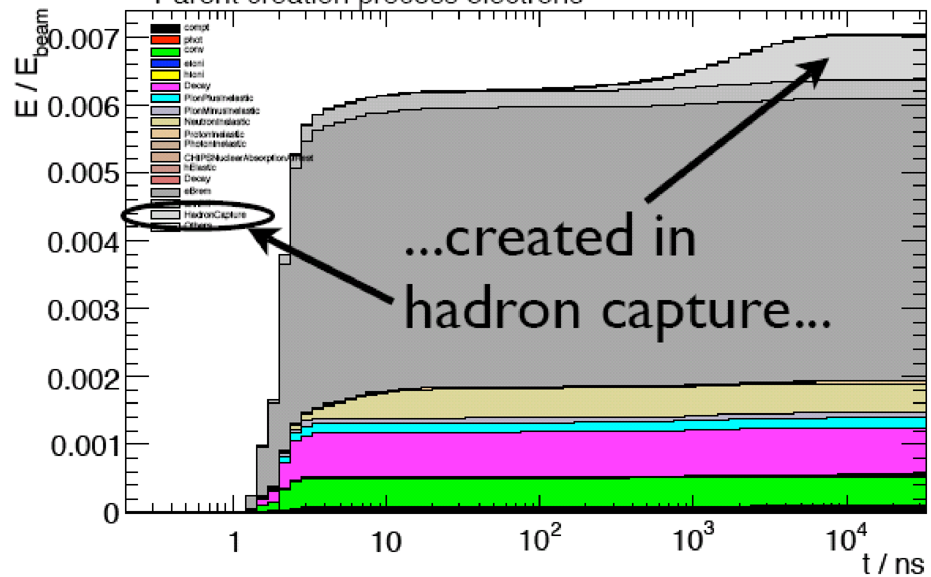


QGSP_BERT_50_GeV_pions_tile_parent_creation_process_electrons

Parent creation material electrons

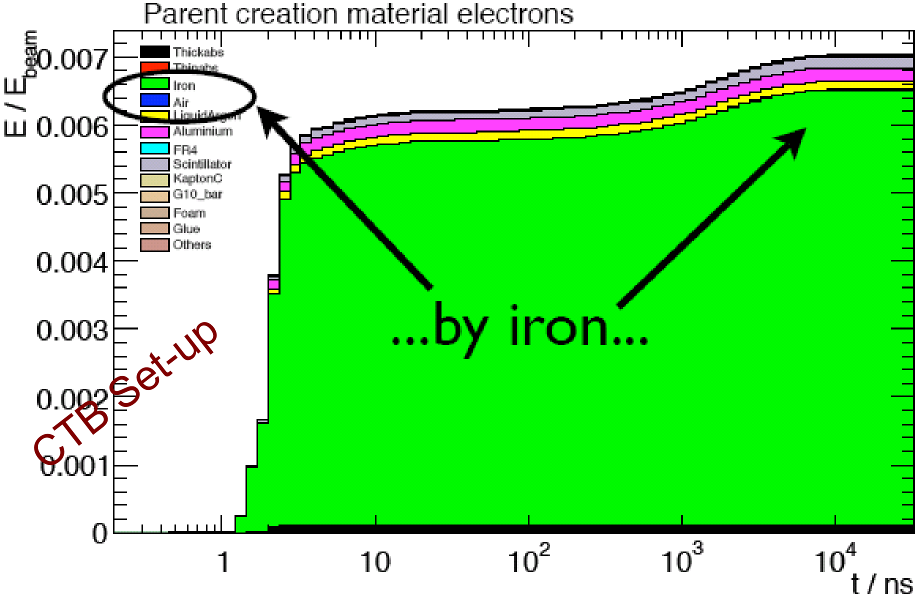


QGSP_BERT_50_GeV_pions_tile_parent_creation_material_electrons

Grandparent particles electrons

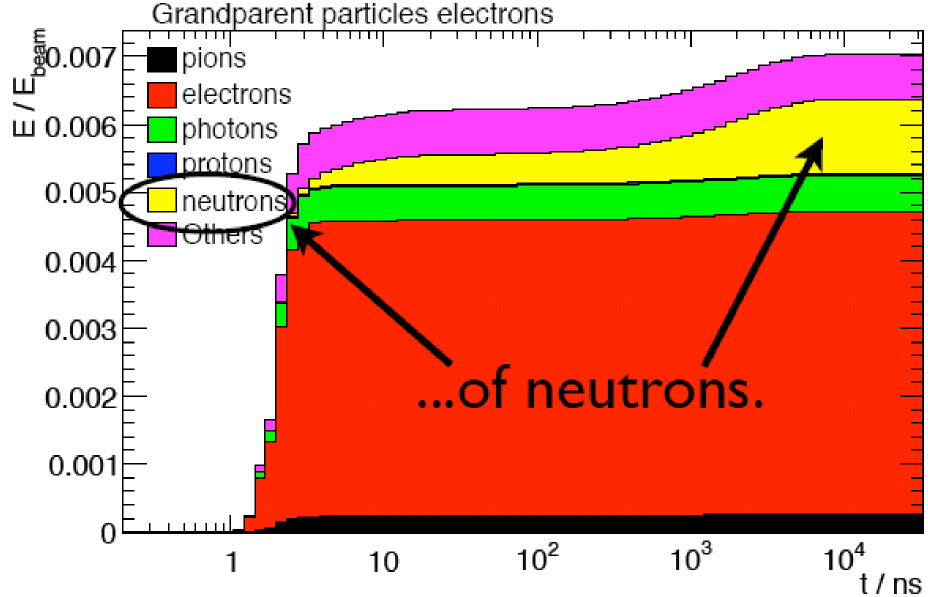


QGSP_BERT_50_GeV_pions_tile_grandparent_particle_electrons

CTB Set-up

# Conclusions

- We have investigated the timing structure of hadronic showers in the ATLAS combined testbeam geometry, and compared the QGSP, QGSP_BERT and QGSP_BERT_HP physics lists.
- Late (after the first few nanoseconds) depositions come mostly from protons freed by elastic scattering of neutrons in the scintillator of the tile calorimeter.
- With QGSP_BERT, we see a large fraction (~10 %) of very late depositions (after ~1 μs) that come from electrons from gammas emitted after neutron absorption in iron. More visible in QGSP_BERT than QGSP due to more neutrons produced to start with. This turn out to be an artifact of the inaccurate neutron absorption model in the non-HP physics lists (cross-sections are extrapolated from H and gamma energies are not accurately modeled), as confirmed by the effect disappearing when using QGSP_BERT_HP.

# A quick round of the most popular calorimeters

Cannot show them all → make a selection of one / technology

Homogeneous calorimeter: CMS ECAL ($PbWO_4$ crystals)

- → Fast, Best resolution relevant for $H \rightarrow \gamma\gamma$
- → Difficult to calibrate, expensive

Ionization chamber: ATLAS ECAL (LAr)

- → Stable, Linear, Easy to calibrate (!)
- → Moderate resolution

Sampling calorimeter: CALICE HCAL (scintillator tiles)

- → Fast, Cheap, high granularity possible relevant for PFLOW
- → Moderate resolution, Difficult to calibrate

A look more into the future:
- ultimate granularity: digital HCAL
- silicon micro-pixels r/o: digital ECAL

# Calibration and monitoring

Several steps to calibrate calorimeter response:

- Multi-channels calorimeters need to be equalize before summing energy
  ➔ use e, $\mu$ or injected charge as reference

- Energy sum in reference units has to be converted to GeV
  ➔ use MC or well known physics (i.e. $Z_0$)

Once the calorimeter is calibrated the response stability in time needs to be monitored:

- Variety of systems to monitor r/o electronics or whole calo cell

# Calibration and monitoring

In calorimeters with optical readout quantities which may vary in time are:

- amount of light generated in the active calorimeter layers
- if using wavelength shifters: the light collection and the conversion eff.
- light attenuation in active layers or WLS materials
- quantum efficiency of light detection
- gain of light detector

Depending on the monitoring method used one or more aspects are monitored but generally not all

- Charge injected in electronics monitors only readout circuit
- Laser light to the PMT monitors photodetector + r/o but not active material
- Movable $\beta$ or $\gamma$ sources cannot decouple problems in light generation or light transport

→ I will mix calorimeter technologies and their calibration & monitoring

# A quick round of the most popular calorimeters

Cannot show them all ➔ make a selection of one / technology

Homogeneous calorimeter: CMS ECAL ($PbWO_4$ crystals)

➔ Fast, Best resolution relevant for $H \rightarrow \gamma\gamma$

➔ Difficult to calibrate, expensive

Ionization chamber: ATLAS ECAL (LAr)

➔ Stable, Linear, Easy to calibrate (!)

➔ Moderate resolution

Sampling calorimeter: CALICE HCAL (scintillator tiles)

➔ Fast, Cheap, high granularity possible relevant for PFLOW

➔ Moderate resolution, Difficult to calibrate

A look more into the future:
- ultimate granularity: digital HCAL
- silicon micro-pixels r/o: digital ECAL

# CMS calorimeters

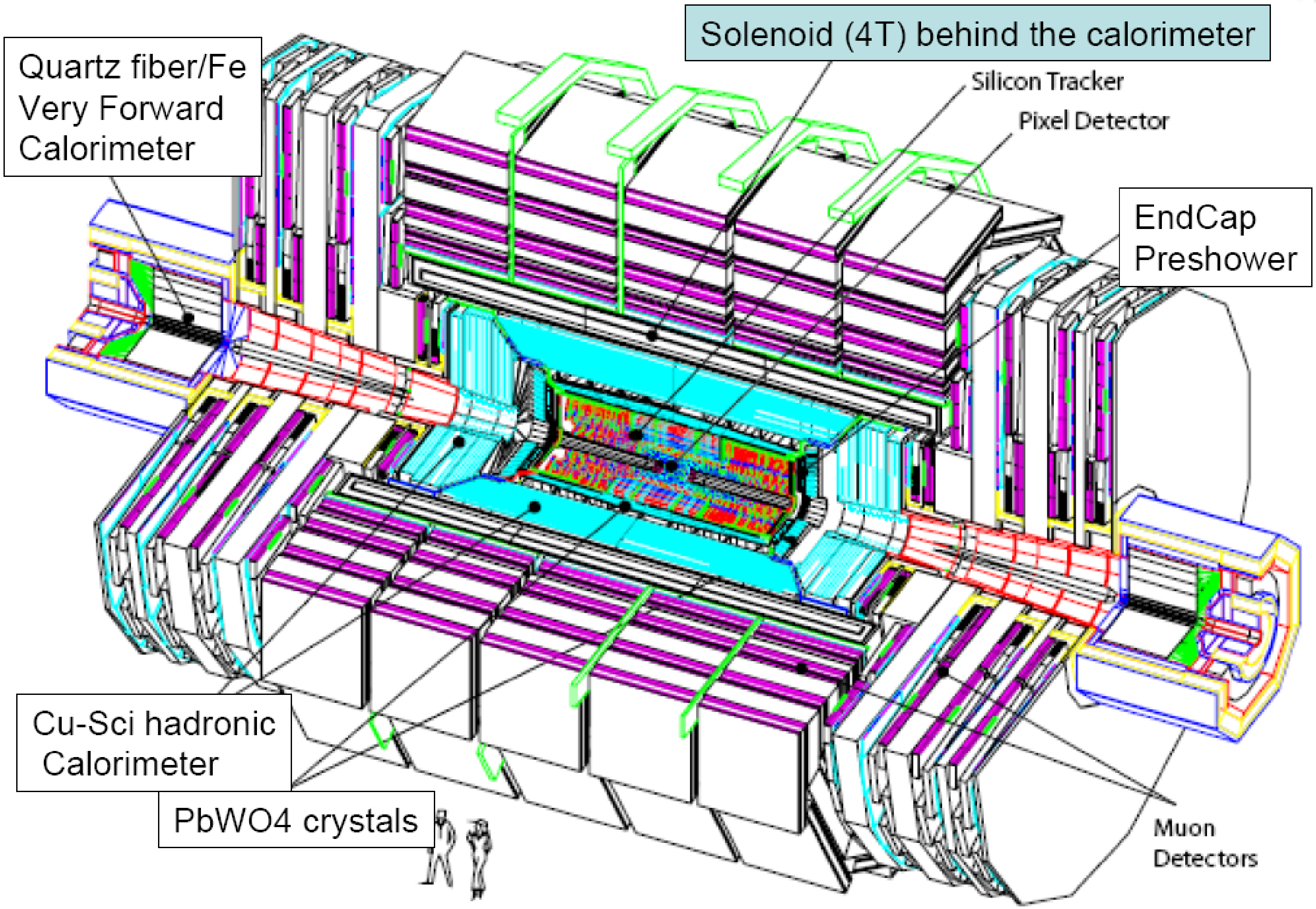

# Golden channel for Higgs discovery

CMS ECAL is designed for excellent performance in the golden Higgs decay channel: H → γγ (BR~0.002)

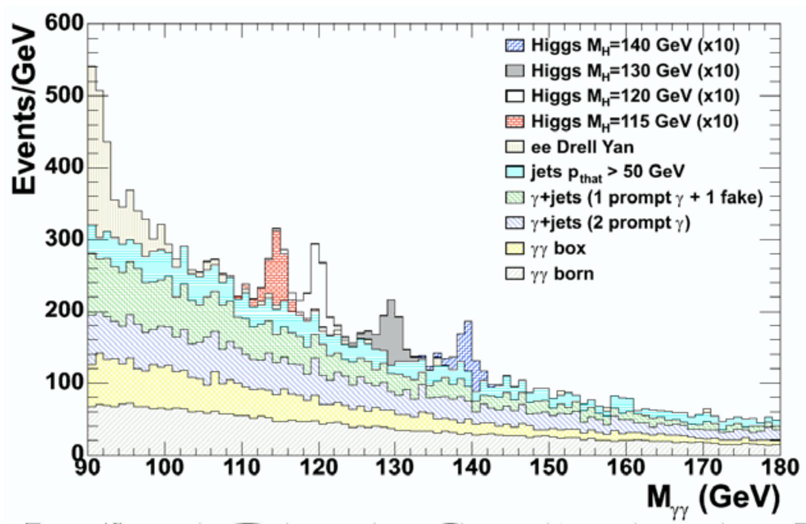


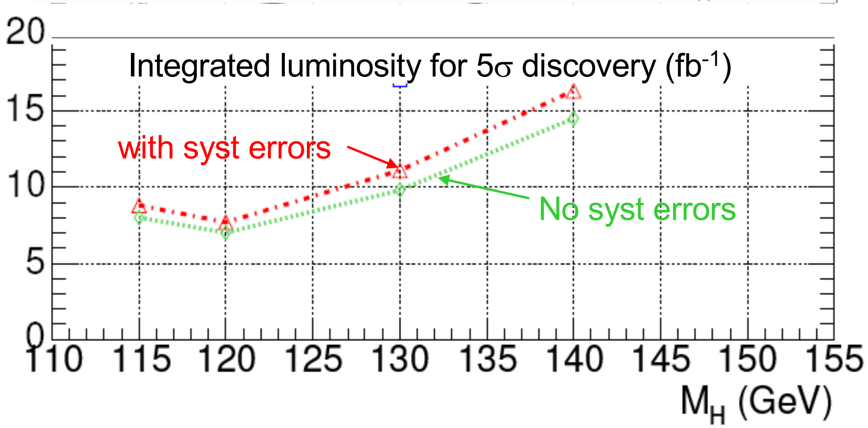


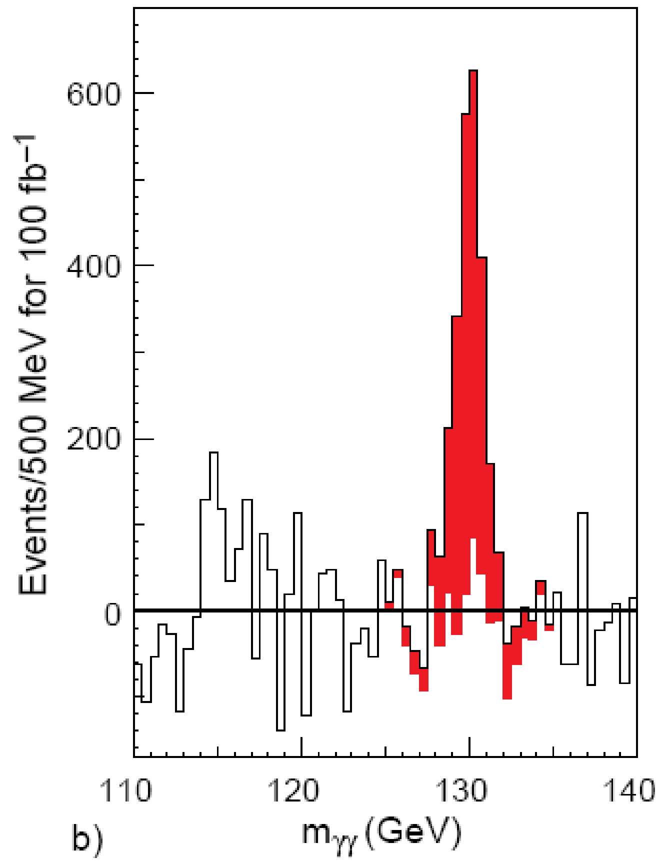


The expected background subtracted Higgs mass peak reconstructed from its two photon decays measured by the CMS PbWO4 crystal calorimeter

# CMS EM calorimeter

Inner radius = 1.29m
Inner length = 2x3.15 m

goal: $H \to \gamma\gamma$

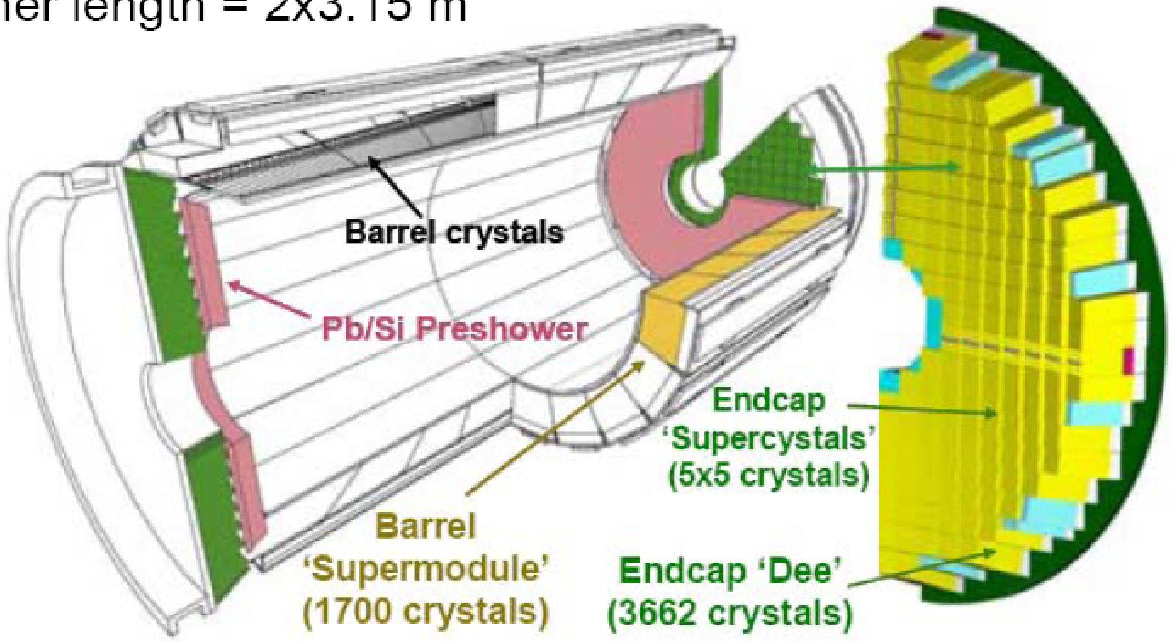


$PbWO_4$
$X_0$= 0.9 cm
$R_M$= 2.2 cm
Light yield:
~6pe/MeV
-2%/degree

<u>Barrel</u>: 1700*36 = 61200 crystals readout by 2 APD (5x5 mm)
<u>End-caps</u> 3662*4 =14648 crystals readout by vacuum photo-triodes
<u>Presampler</u>( $1.65<\eta<2.6$) 1.9 $X_0$ lead-X plane of Si strips- 0.9 $X_0$ lead-Y strips
138 000 channels: pitch 1.9 mm, length 63mm,thickness 320 $\mu$m

# CMS : em PbWO4 calorimeter

**Lead-Tungsten crystals**
light yield 9 p.e./MeV
**Dynamic range : 16 bits**
50 MeV-3 TeV
**Energy resolution: ~ 0.5%**
Barrel :$\sigma(E)/E$ = 200 MeV$\oplus$ 3%/$\sqrt{E}$ $\oplus$0.6 %
End-cap:$\sigma(E)/E$ = 200 MeV$\oplus$ 6%/$\sqrt{E}$ $\oplus$0.6 %
**Granularity: ~ 0.1 x 0.1 $\Delta\eta$ x $\Delta\phi$**
Barrel : 61 200 channels
End-cap: 16 000 channels

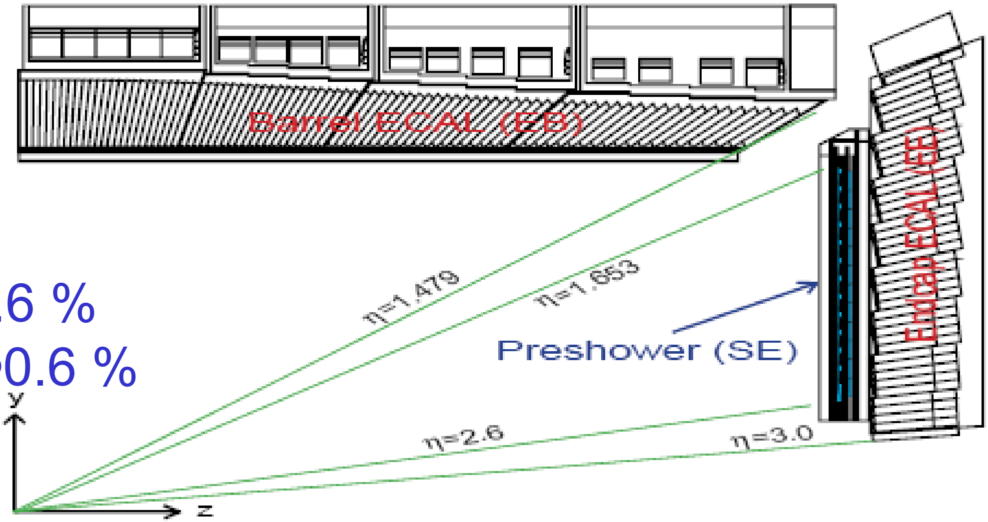


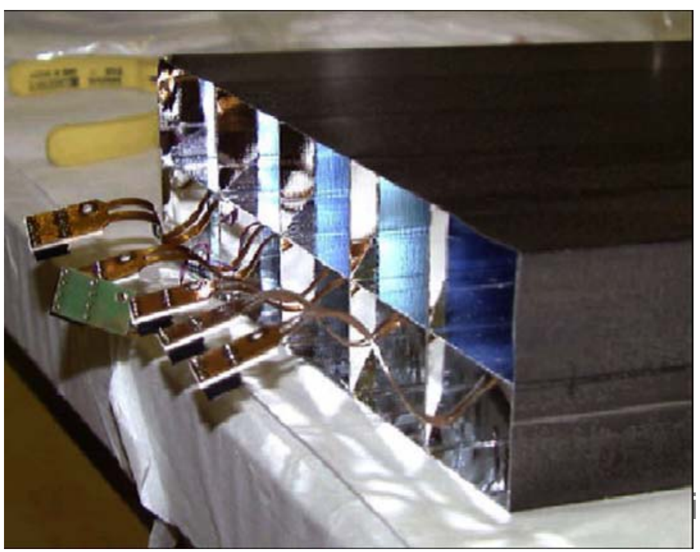

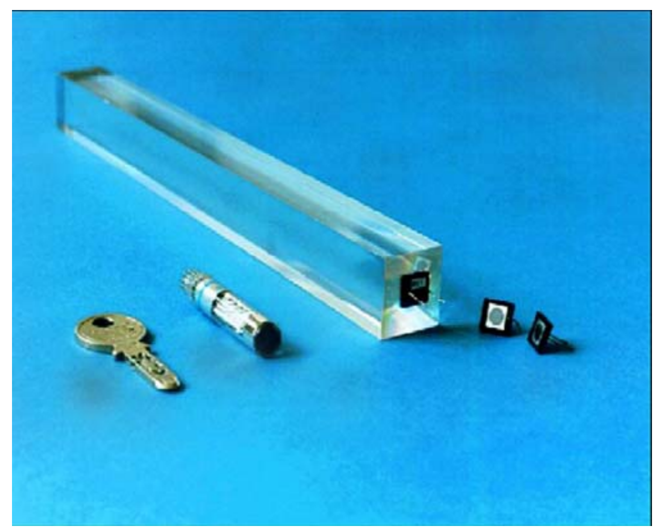

# Radiation hardness of PbWO4

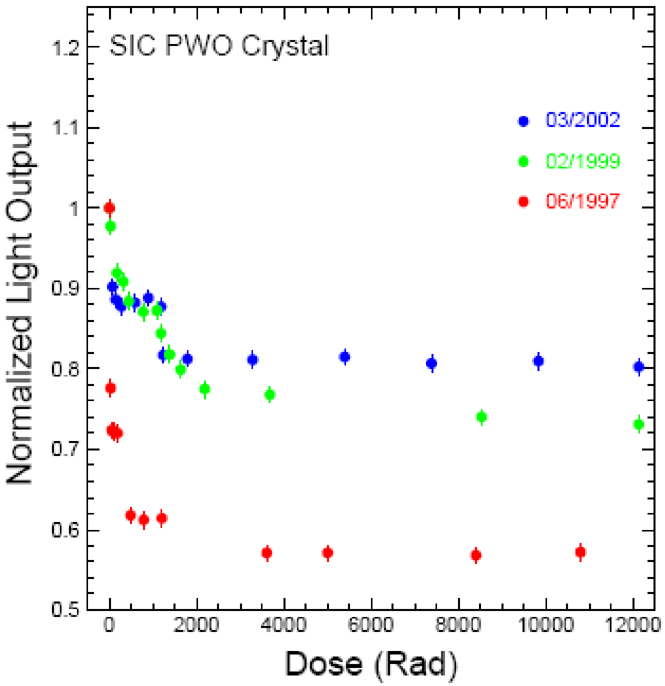


The progress of PbWO4 radiation hardness for full size (23 cm) CMS PbWO4 samples

Transmission Electron Microscopy pictures of a PbWO4 crystal of poor (left) radiation hardness, showing clearly the black spots of Ø 5–10 nm related to oxygen vacancies, as compared to that of a good one (right)

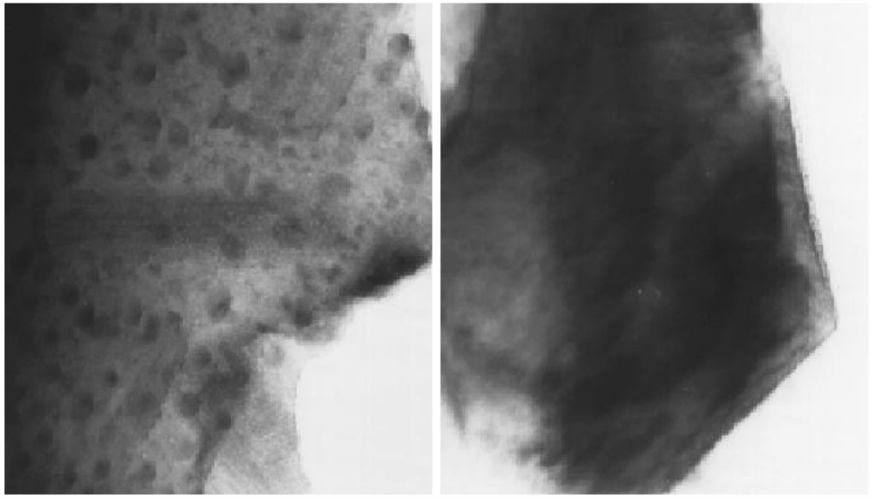

# CMS : em photodetector

**Avalanche photodiodes (APDs)**
Area : 25 mm$^2$ QE = 80%
Gain = 50 TC = -2%/K
Excess noise factor: 2.2
C= 30 pF
Bias~200-300 V

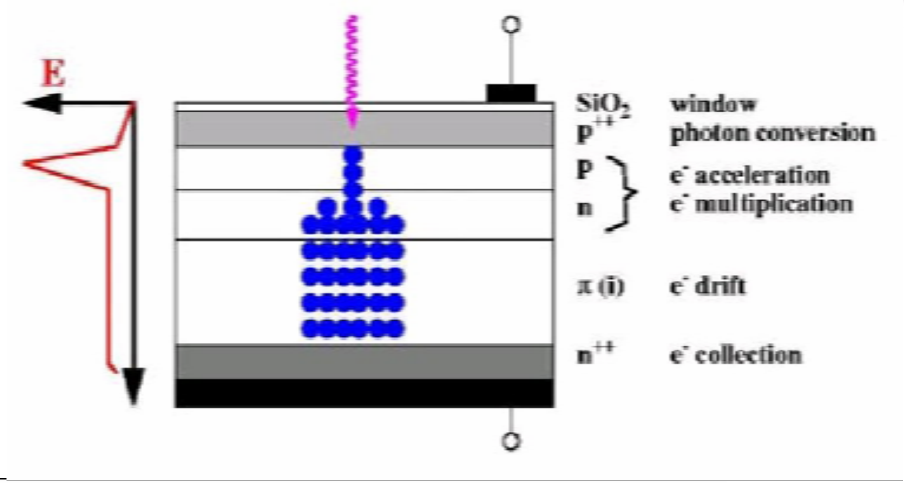


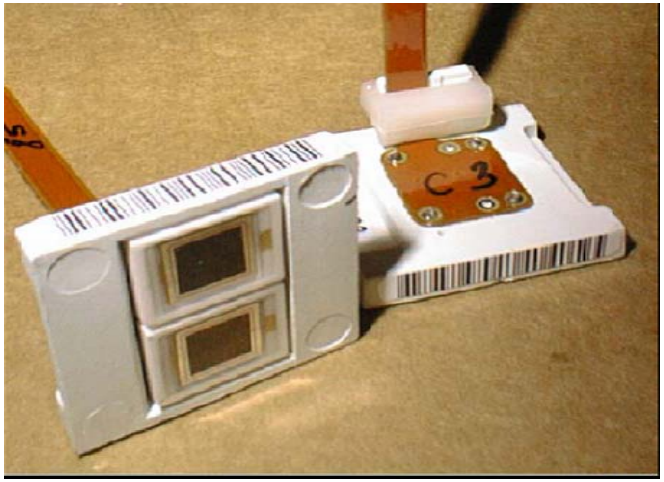

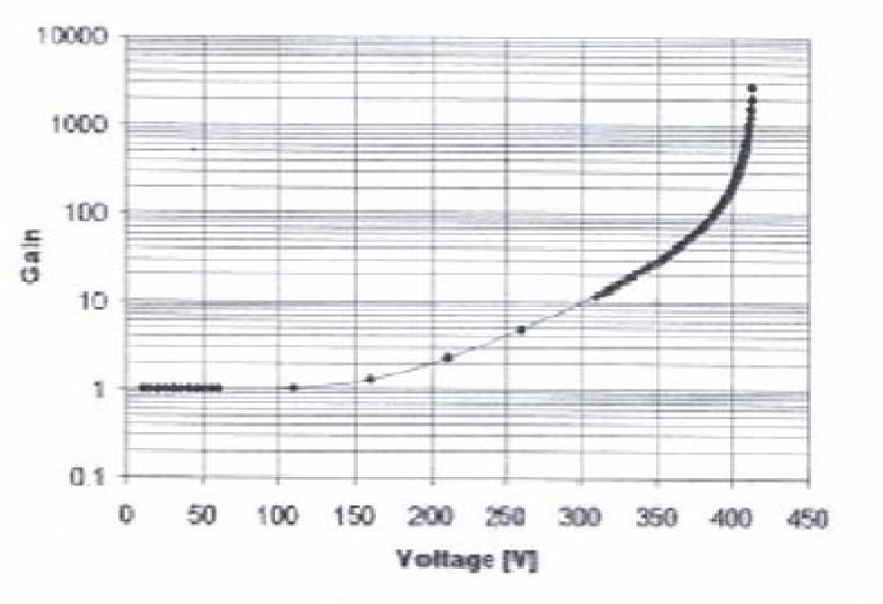

# CMS: ECAL Calibration

Optical system
Mimic physics

The laser monitoring system must track the change in the transparency precisely enough to maintain the constant term in the ECAL resolution of 0.55%.

This requires a measurement of the transparency with an accuracy of better than 0.2%.

The transparency in each crystal will have to be measured approximately every 30 minutes during LHC operation.

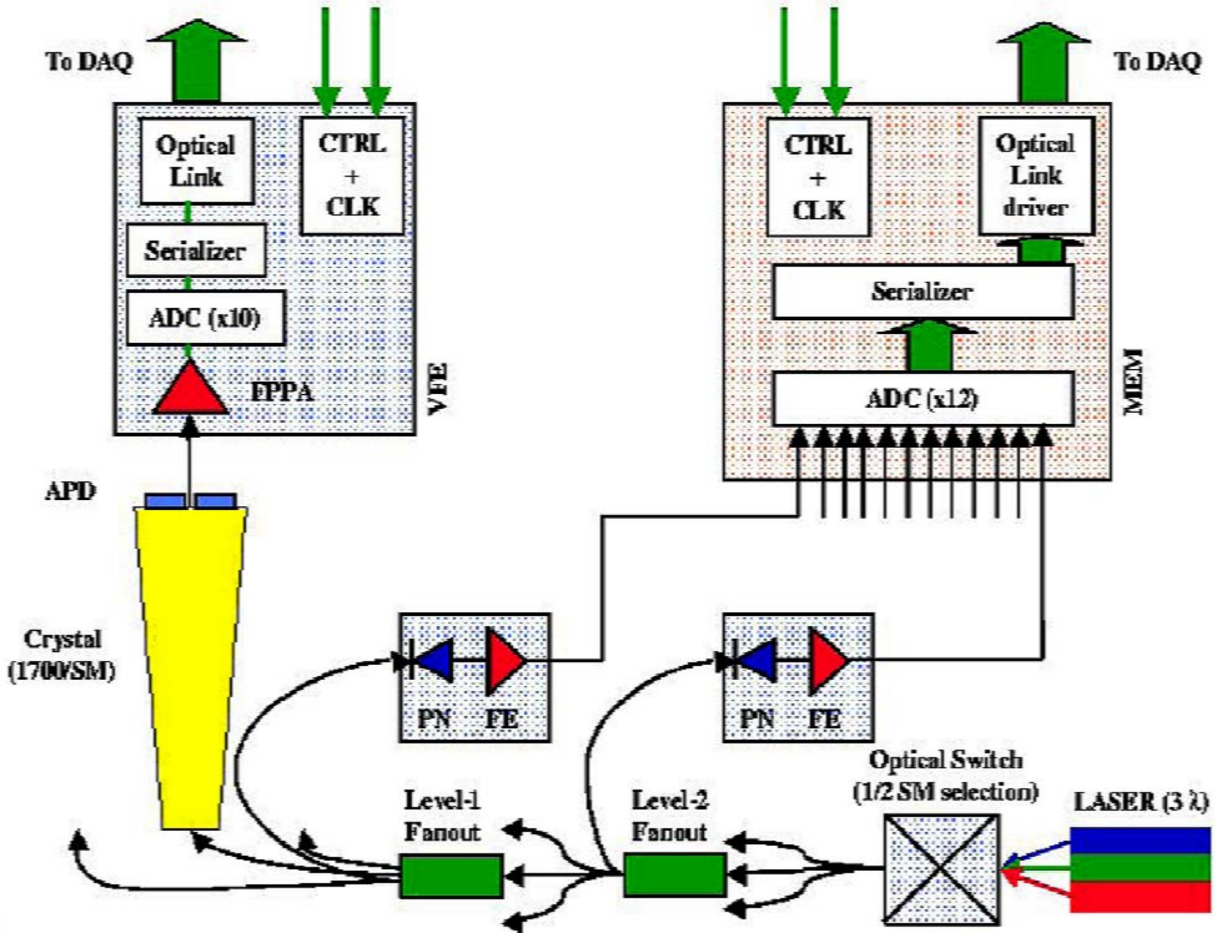


Blue laser peaked at the scintillation light wavelength 440 nm

# Calibration

convert individual channel response to particle energy for electrons, photons and hadrons

e.g. CMS ECAL:

to be determined

$$E_{\mathrm{e},\gamma} = G \times \mathcal{F} \times \sum_{i}^{\text{Cluster}} c_i \times A_i,$$

absolute energy scale

digitized signals

inter-calibration constants

cluster-algorithm dependent factor
(containment, position, particle type, momentum…)

# Inter-calibration @ Test Beam

$$E_{e,\gamma} = G \times \mathcal{F} \times \sum_i c_i \times A_i$$

e- beam @ 90 / 120 GeV on 9 SM

Fit X-Y coordinate of E deposition in single crystal to find maximal containment point

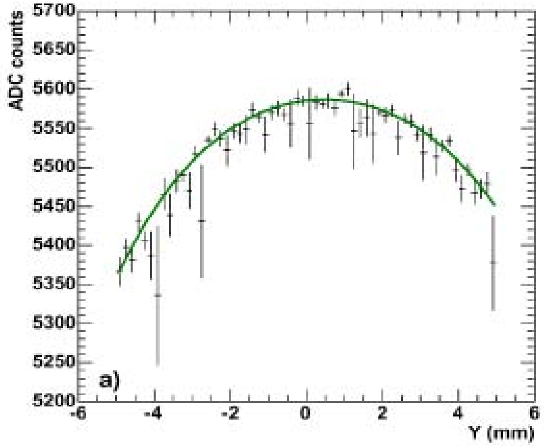


Apply impact point correction; keeping 6x6 mm² area around max; Gaussian fit of Energy distr.

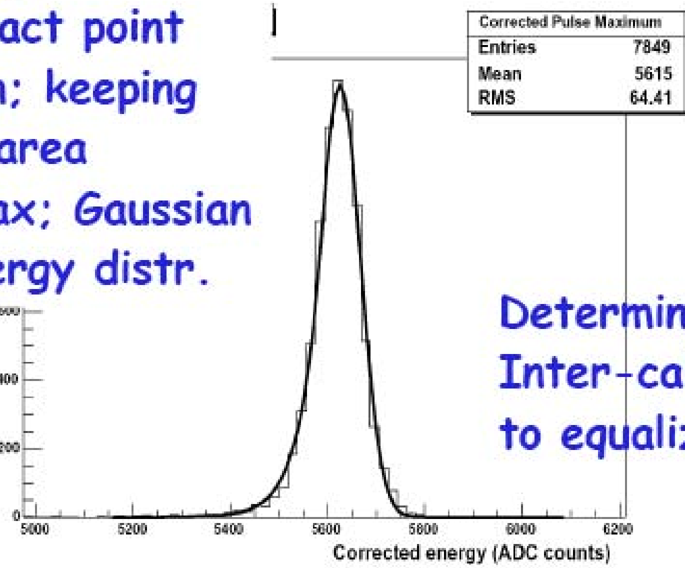


SM22 was exposed twice to the e- beam

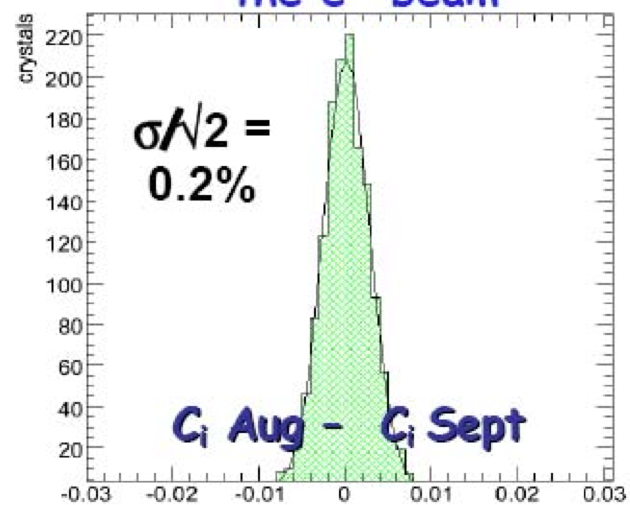


Determine relative Inter-calibration to equalize response

$$c_i = \frac{M_{ref}}{M_i}$$

precision achieved ~ 0.3 %

# Correction for impact position

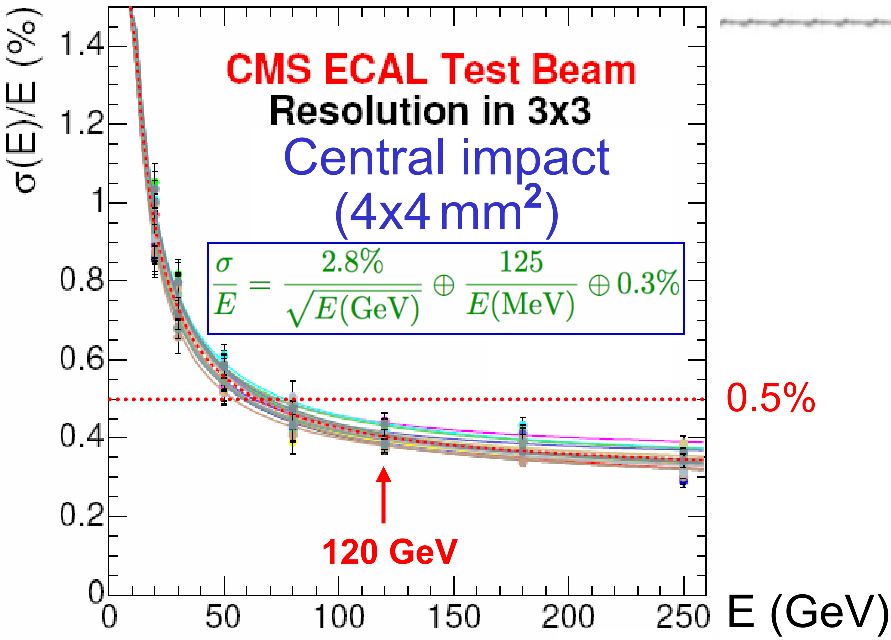


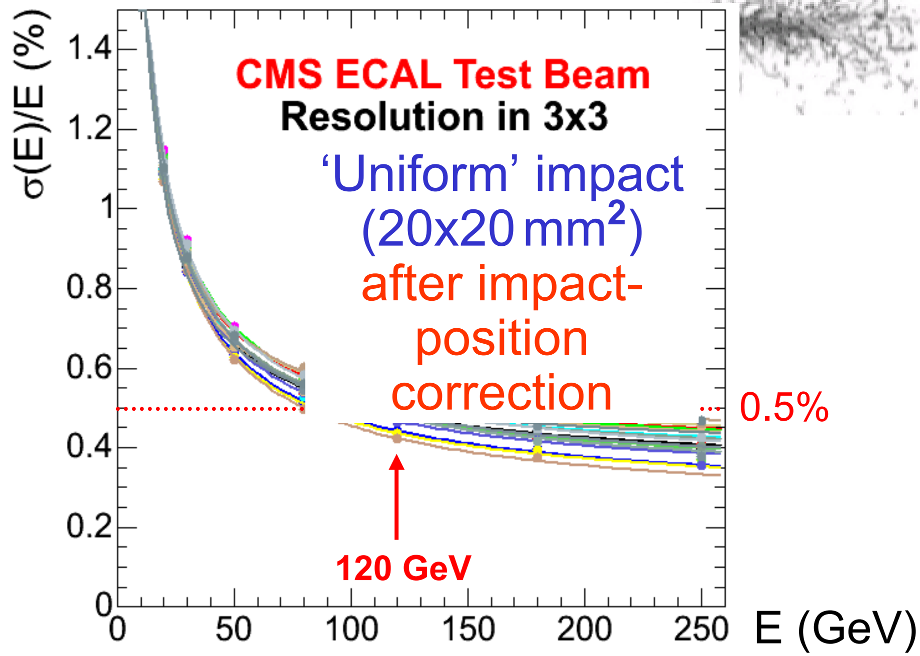


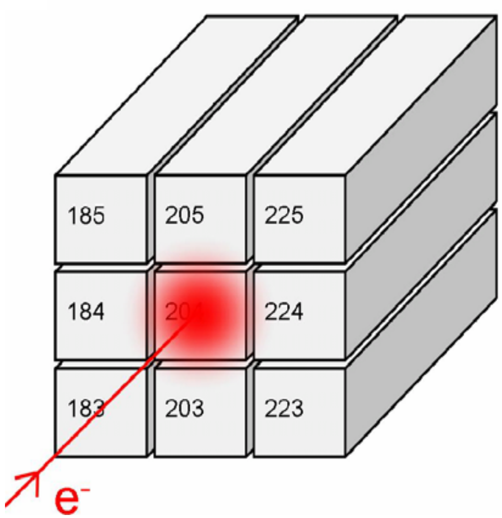


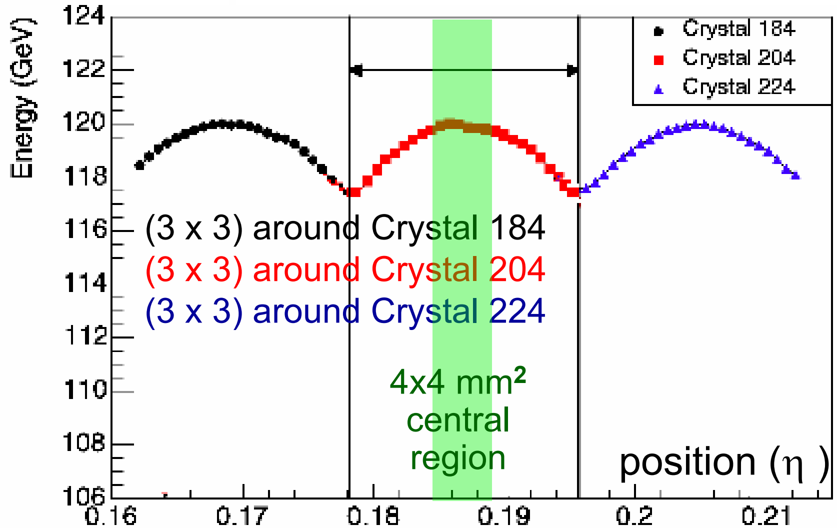


Response for Σ(3x3) varies by ~3% with impact position in central crystal

Correction made using information from crystals alone (works for $\gamma$)

Does **not** depend on **E**, $\eta$, $\phi$

# A quick round of the most popular calorimeters

Cannot show them all ➔ make a selection of one / technology

Homogeneous calorimeter: CMS ECAL ($PbWO_4$ crystals)

➔ Fast, Best resolution relevant for H➔$\gamma\gamma$

➔ Difficult to calibrate, expensive

Ionization chamber: ATLAS ECAL (LAr)

➔ Stable, Linear, Easy to calibrate (!)

➔ Moderate resolution

Sampling calorimeter: CALICE HCAL (scintillator tiles)

➔ Fast, Cheap, high granularity possible relevant for PFLOW

➔ Moderate resolution, Difficult to calibrate

A look more into the future: - ultimate granularity: digital HCAL

- silicon micro-pixels r/o: digital ECAL

# ATLAS calorimeters

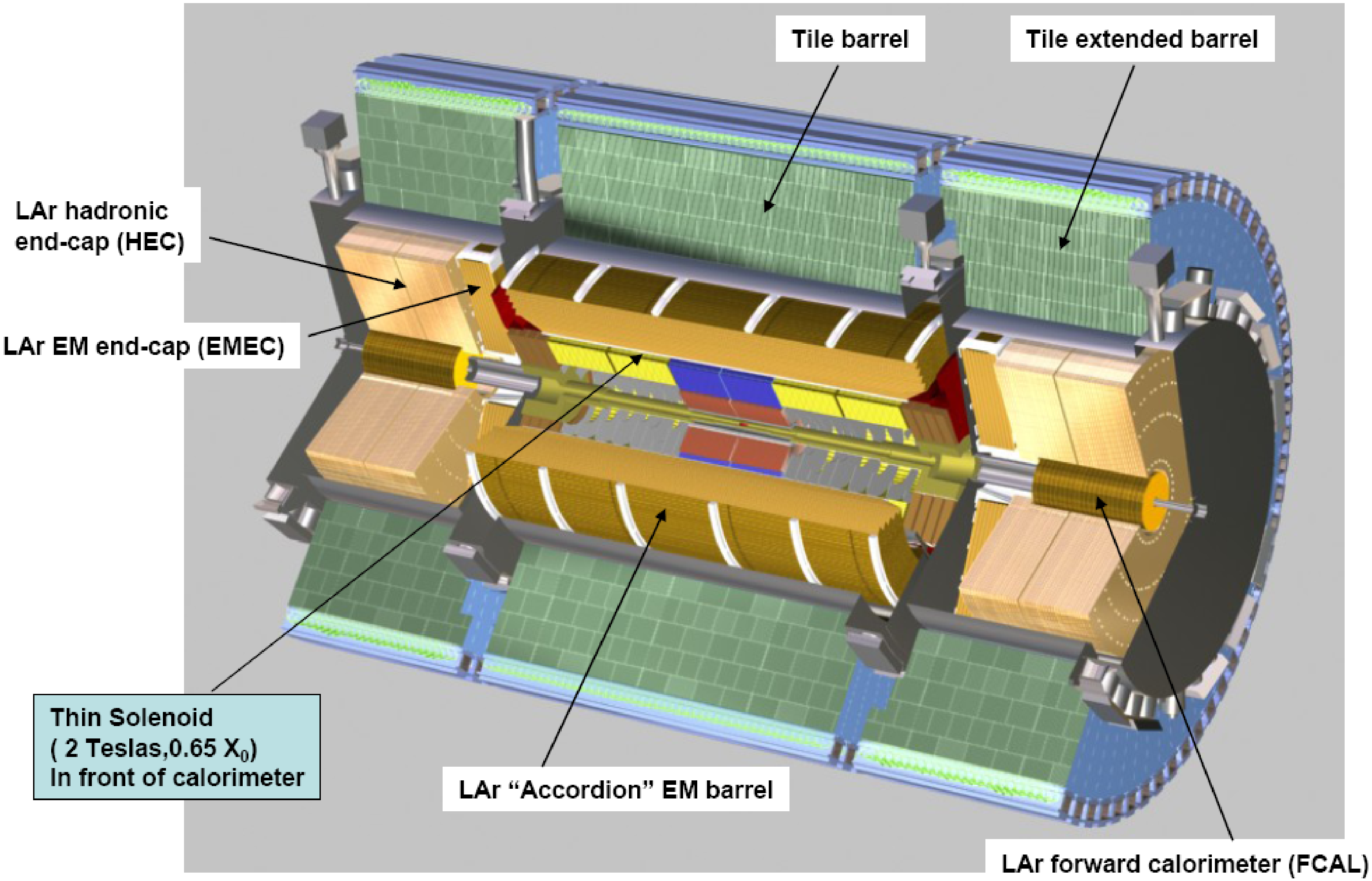

# Driving physics requirements

EM Calorimeters

Benchmark channels H →γγ, H →ZZ → eeee need high resolution O(100 GeV) range, coverage to low $E_T$

Z'→ee to few TeV range

b-physics (decay of H and t): e down to GeV range

Design goals for |η| | < 2.5

$\sigma(E)/E = 10\%/\sqrt{E} \oplus 200\text{-}400\ \mathrm{MeV}/E \oplus 0.7\ \%$

noise term given by: Electronics + Pileup noise

Constant term < 1% ➔ E res for H ~1%

Linearity better than 0.1%

Hadron and forward Calorimeters

Benchmark channels: Higgs with W →jet jet, Z/W/top need good jet-jet mass resolution

Higgs fusion, forward physics: good forward jet tagging

$E_T^{MISS}$: jet resolution, linearity

Design goals: $50\% / \sqrt{E} \oplus 3\%$ for |η| | < 3

$50\% / \sqrt{E} \oplus 10\%$ for 3 < |η| < 5

➔ mainly driven by res. for t mass in di-jet ~1%

# Why Liquid Argon calorimeter

Liquid argon calorimeter: stability and uniformity of the ionisation signal

Physics requirements

- Excellent energy resolution: to reconstruct energy of $e^-$, $\gamma$ and jets
- Large dynamic range: from 50 MeV to 3 TeV
- Charge not totally integrated: fast response (< 50 ns)
- Good radiation tolerance: high fluences during 10 years

Energy resolution :

$$\frac{\sigma_E}{E} = \frac{10\%}{\sqrt{E}} \oplus \frac{300\,\mathrm{MeV}}{E} \oplus 0.7\%$$

expected constant term

| Non-uniformity sources | % |
|---|---|
| Absorber non-uniformity | 0.2 |
| Liquid gap non-uniformity | 0.15 |
| Residual $\Phi$-modulation | 0.2 |
| **Electronics read-out** | **0.25** |
| + other effects … | |
| Total | < 0.7 |

Main contribution!

Linked to our ability to calibrate the 200000 channels with a good accuracy

# ATLAS : LAr e.m. calorimeter

pointing “tower” geometry

- granularity 0.03 x 0.03 $\Delta\eta$ x $\Delta\phi$
- 3 segments in depth
- no cracks in azimuth
- presampler to correct for energy losses in the material in front

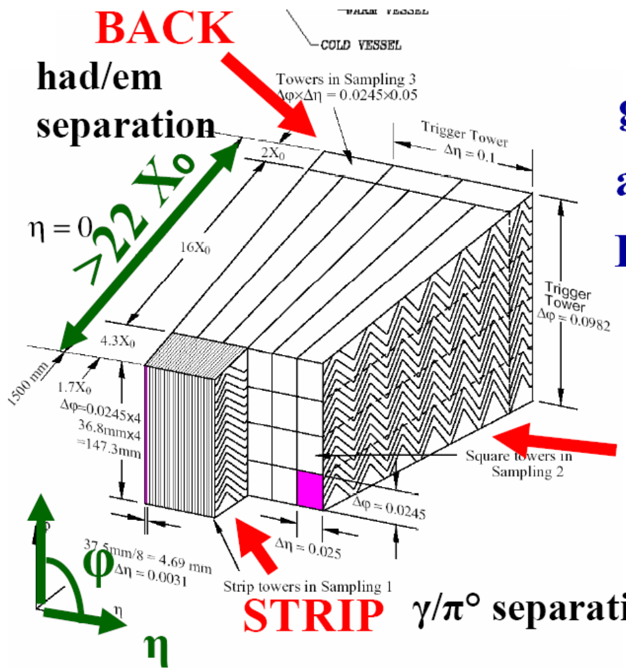


**gap thickness 2.1 mm**

**absorbers 1.5-1.1 mm**

**HV 2kV**

**MIDDLE**

**main energy deposition**

$\gamma/\pi^0$ separation

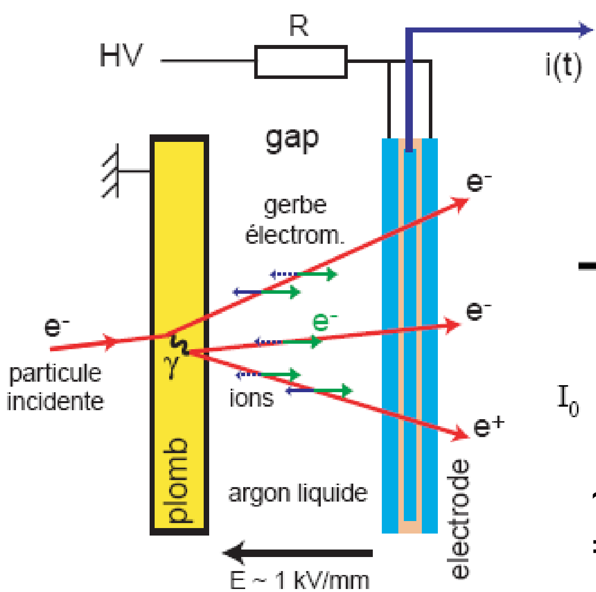


2.1 mm ~ 450 ns

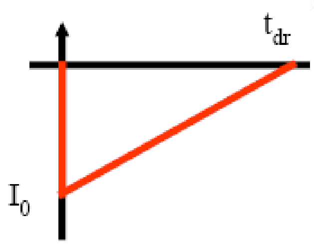


**Ionization signal**

~500ns long
=20 bunch xings

➔ reduced to 45ns peaking time by shaping

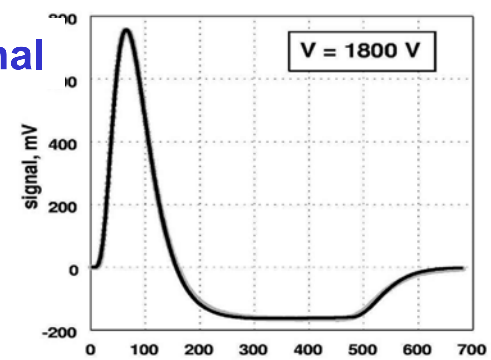


**Signal after shaping**

# Cell reconstruction step

Convert measured current [μA] to ADC amplitude

use channel-to-channel calibration pulser system

➔ Correct for calibration ↔ physics pulse height differences for same injection current

Intended LAr electronics calibration chain:

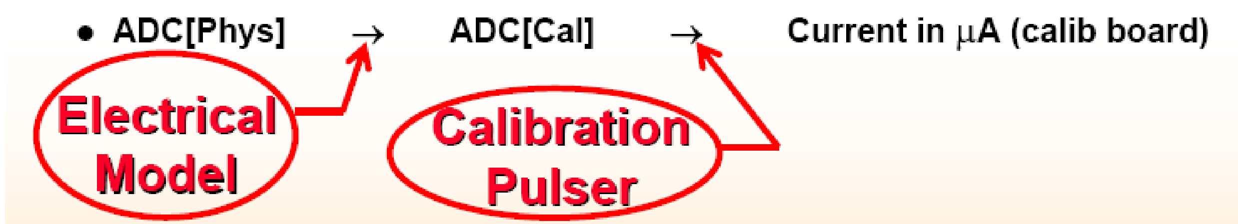


Still need: μA →MeV (from testbeam, MC, ...)

Alternative, if channel response uniform enough, can convert directly

ADC[Phys] →MeV (from testbeam)

Note: T dependence on signal generation 2%/K ➔ not relevant since T stability expected ~0.3K

# The Calibration board in the electronics chain

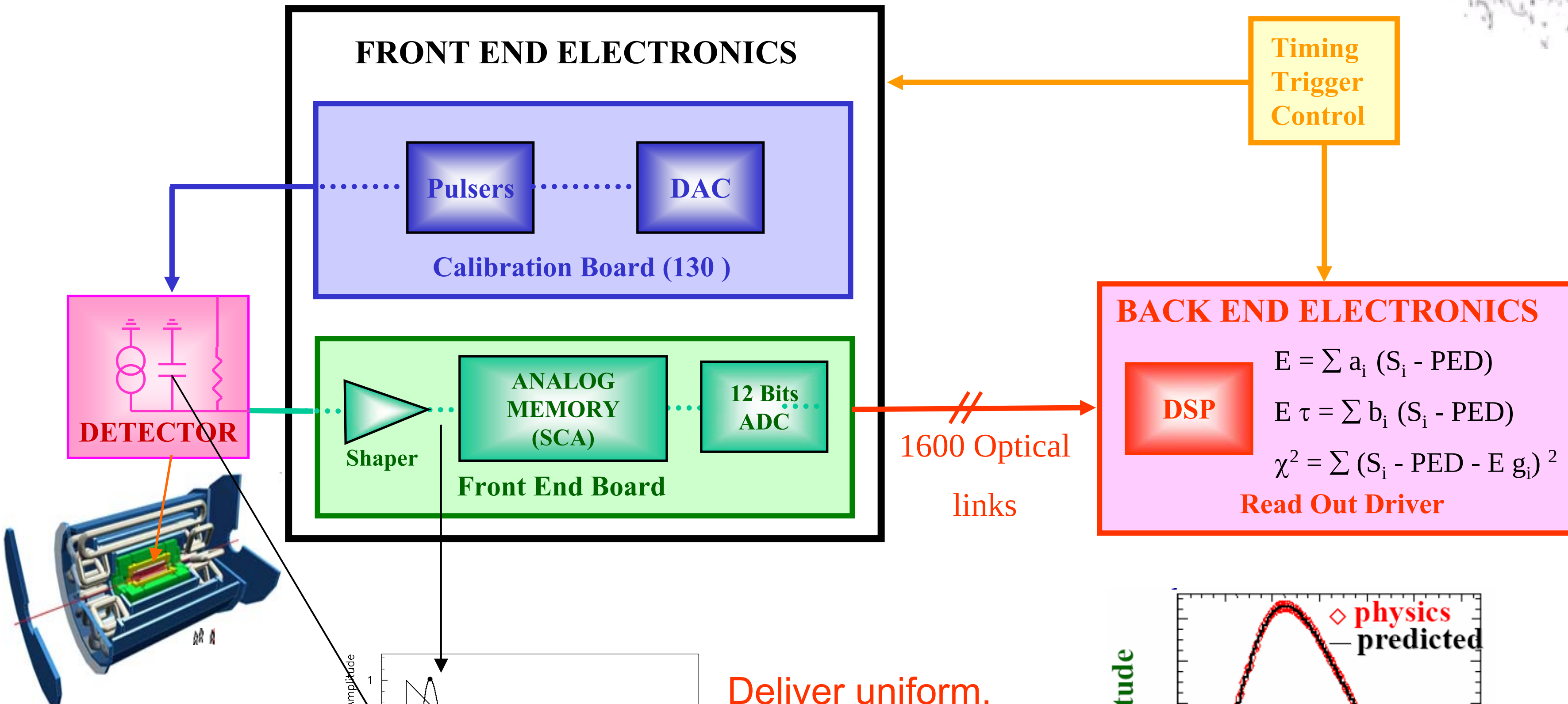


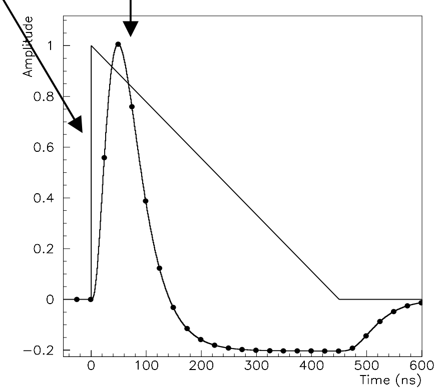


Deliver uniform, stable and linear signal with a shape similar to that of the calorimeter ionization current

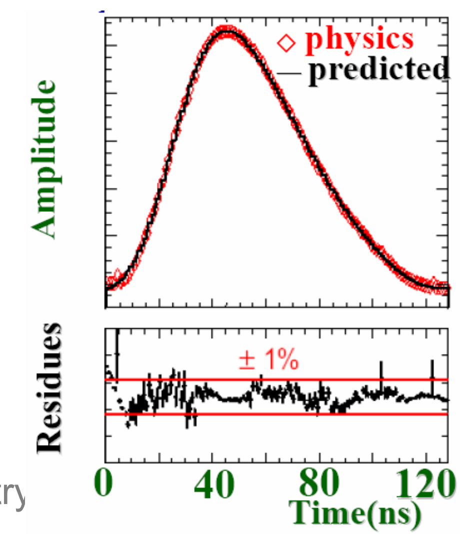

# LAr detectors: calibration pulser system

Very stable design: Accuracy / channel uniformity: O(0.5%)

- **EM**
  - Inject on summing boards
- **HEC**
  - Inject at calo pads
- **FCAL**
  - Inject on FEB backplane

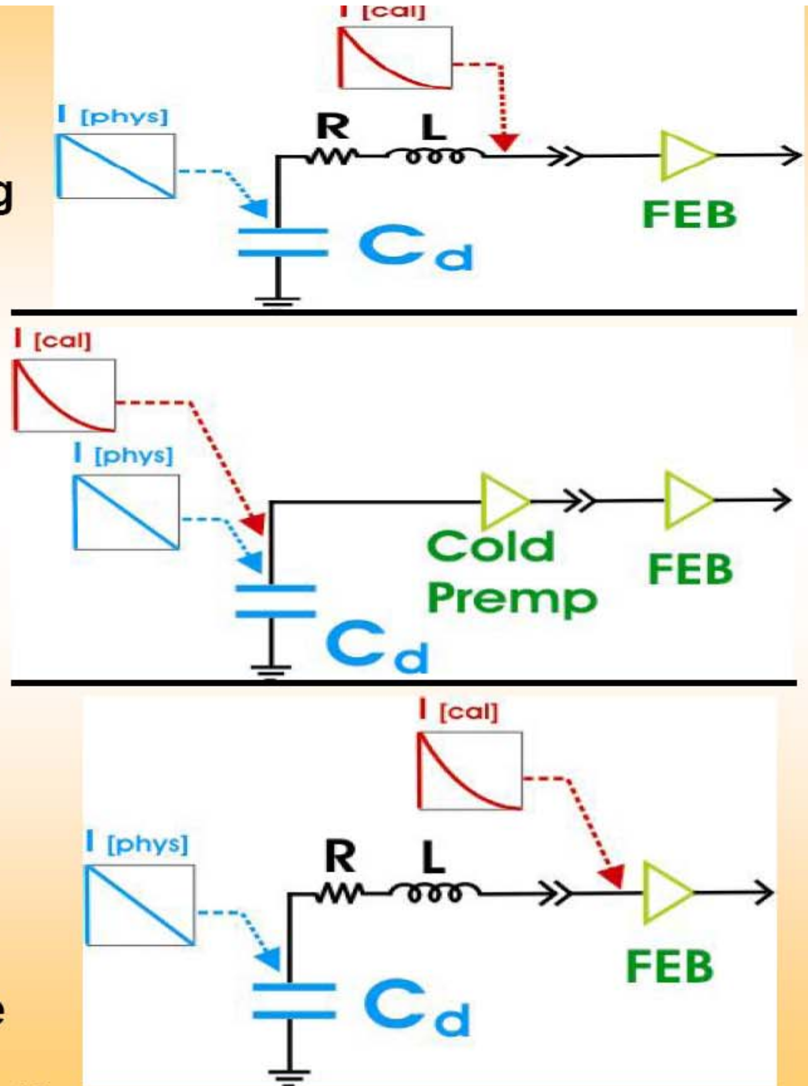


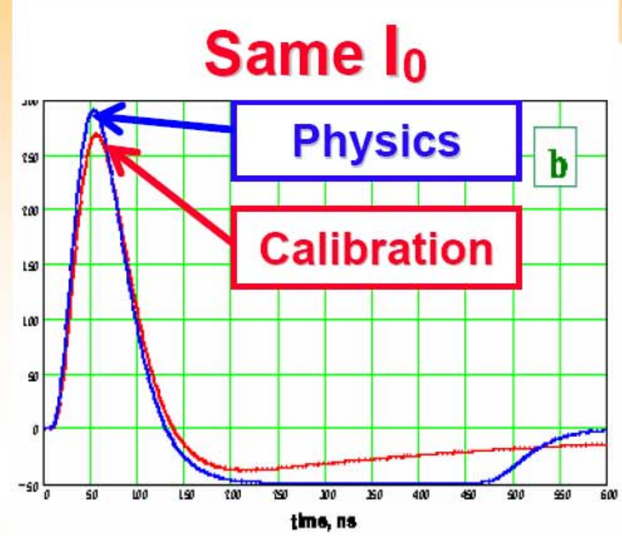


- **To use calibration system:**
  - Understanding ADC[phys]/ADC[cal] for fixed $I_0$ is key

# Test beam results of the ATLAS EM LAr

## ENERGY RECONSTRUCTION

2nd step: Cluster reconstruction

3rd step: Corrections

$$E=\alpha * E_{PS} + E_{strip} + E_{middle} + \beta * E_{back}$$

- compensates for dead material
- corrects for longitudinal leakages ( $\beta \Rightarrow 0$ for $E < 40$ GeV )

($\alpha$ and $\beta$ obtained by minimizing the energy resolution at each $\eta$)

**Design goals (SM Higgs mainly, $E_{Tmiss}$):**

- sampling term $a \sim 10\ \%\ \sqrt{\text{GeV}}$
- constant term $b \sim 0.5\ \%$ in $\Delta\eta \times \Delta\varphi = 0.2 \times 0.4$ rad

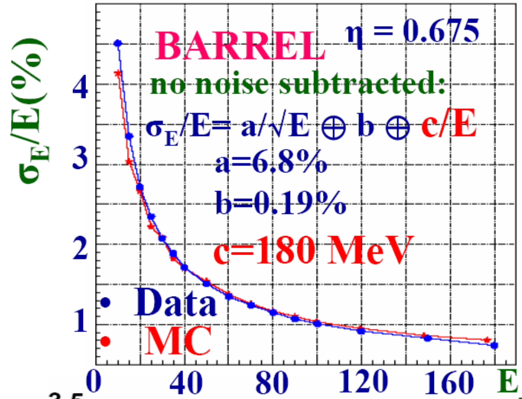


e⁻ impact point:
$\eta = 0.48 \pm 0.01$
$\Delta\varphi = 0.02$ rad
a=8.95%
b=0.33%
noise subtracted

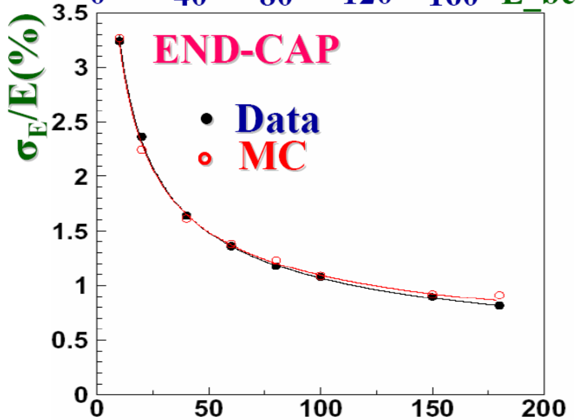


E_beam(GeV)

e⁻ impact point:
$\eta = 1.9 \pm 0.01$
$\Delta\varphi = \pm 0.01$ rad
$a = (10.35 \pm 0.05)\ \%$
$b = (\ 0.27 \pm 0.02)\ \%$
noise and beam spread subtracted

- within requirements
- good agreement with MC
- energy scale from 'first principles' corrected at 5%

# EMEC LAr commissioning at test beam

$$E_{\mathrm{reco}} = E_{\mathrm{em}}^{\mathrm{EMEC}} = \alpha_{\mathrm{em}}^{\mathrm{EMEC}} I_{\mathrm{vis}}^{\mathrm{EMEC}}$$

$$\sigma\left(E_{\mathrm{reco}}\right) = \sigma'\left(E_{\mathrm{reco}}\right) \oplus \sigma_{\mathrm{noise}}$$

$$\frac{\sigma'\left(E_{\mathrm{reco}}\right)}{\left\langle E_{\mathrm{reco}}\right\rangle} = \frac{a}{\sqrt{E_{\mathrm{reco}}}} \oplus b$$

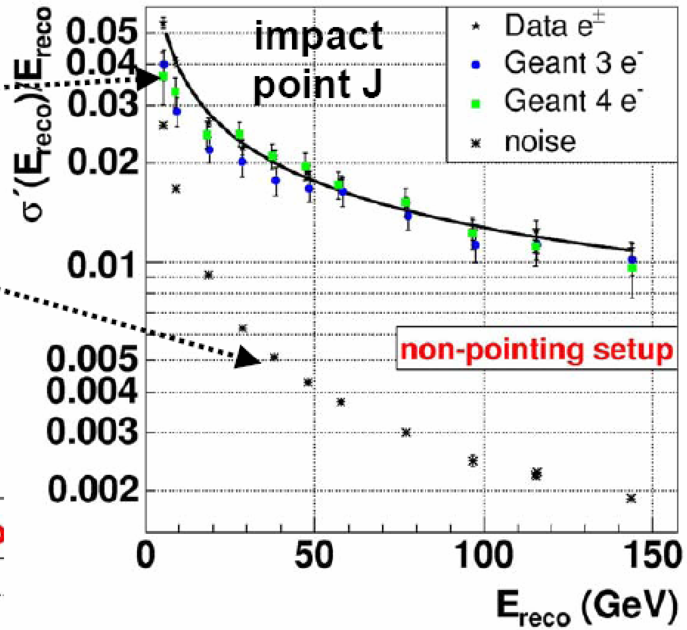


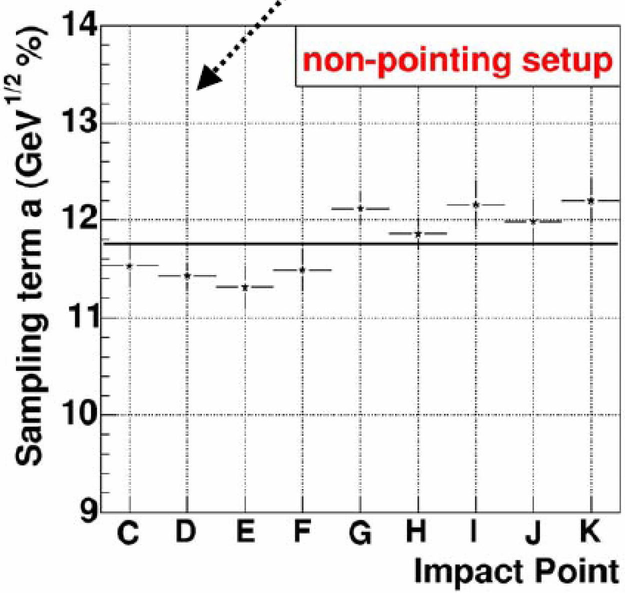


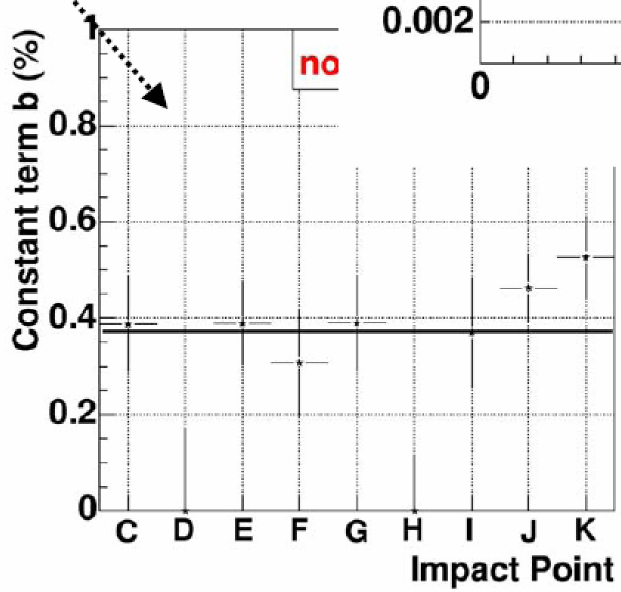


Note: non-pointing setup!!

possibly some $\eta$ dependence, due to $\eta$ variation of sampling fraction and weak $\eta$ dependence of electric field

**ATLAS**

**Start data taking with well pre-calibrated calorimeter ( < 1%)**

- *Electronic calibration system*
- *Mechanics uniform by construction*

10% tested with beams: Uniformity of response ~0.45%

**Long range $Z \rightarrow e\,e$ or $W \rightarrow e\,\nu$ decays**

***50k** $Z \rightarrow e\,e$ **events (0.1 $fb^{-1}$ ) global constant term <0.7%***

**CMS**

**Start-up intercalibration for ECAL:**

- Cosmic inter-calibration — *all barrel supermodules ≤ 2 %*
- **1/4 of ECAL SMs** testbeam inter-calibration **~ 0.3 %**

**Intercalibration and absolute calibration in situ:**

- $\phi$-symmetry in min. bias ev. — *fast equalisation at 1.5 to 2%*
- $W \rightarrow e\,\nu$ from E/p — *inter-calibration*
- $Z \rightarrow e\,e$ invariant mass — *absolute calibration*

**From W alone intercalibration < 0.5% with 5 $fb^{-1}$**

**MC studies show that faster calibration is possible by $\pi^0$ mass reconstruction**

Cannot show them all ➔ make a selection of one / technology

Homogeneous calorimeter: CMS ECAL ($PbWO_4$ crystals)

➔ Fast, Best resolution relevant for $H \rightarrow \gamma\gamma$

➔ Difficult to calibrate, expensive

Ionization chamber: ATLAS ECAL (LAr)

➔ Stable, Linear, Easy to calibrate (!)

➔ Moderate resolution

Sampling calorimeter: CALICE HCAL (scintillator tiles)

➔ Fast, Cheap, high granularity possible relevant for PFLOW

➔ Moderate resolution, Difficult to calibrate

A look more into the future:

- ultimate granularity: digital HCAL
- silicon micro-pixels r/o: digital ECAL

# ILC: hadronic calorimeter

Iron/plastic(tiles) sandwich

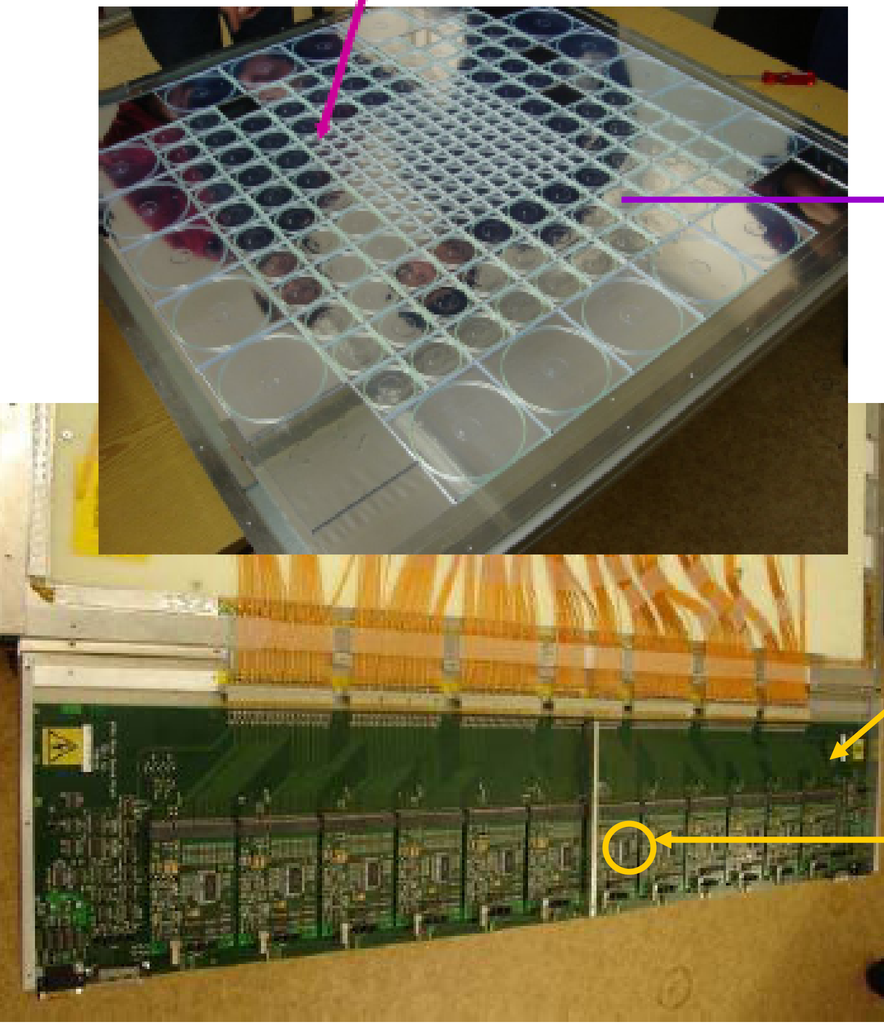

Single tile readout with WLS fiber + SiPM:

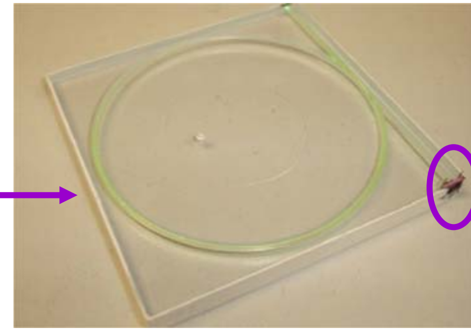

pixel device operated in Geiger mode

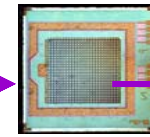

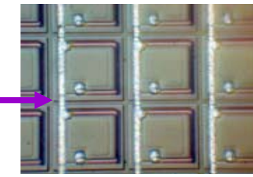

Read out 216 tiles/module
38 sampling layers
~8000 channels

VFE: control board for 12 ASICs / layer connect to SiPMs

ASIC: amplification + shaping + multiplexing (18 ch.)

# A calorimeter for test beam experiments

38 layers of sampling structure
High longitudinal and lateral segmentation
segmentation

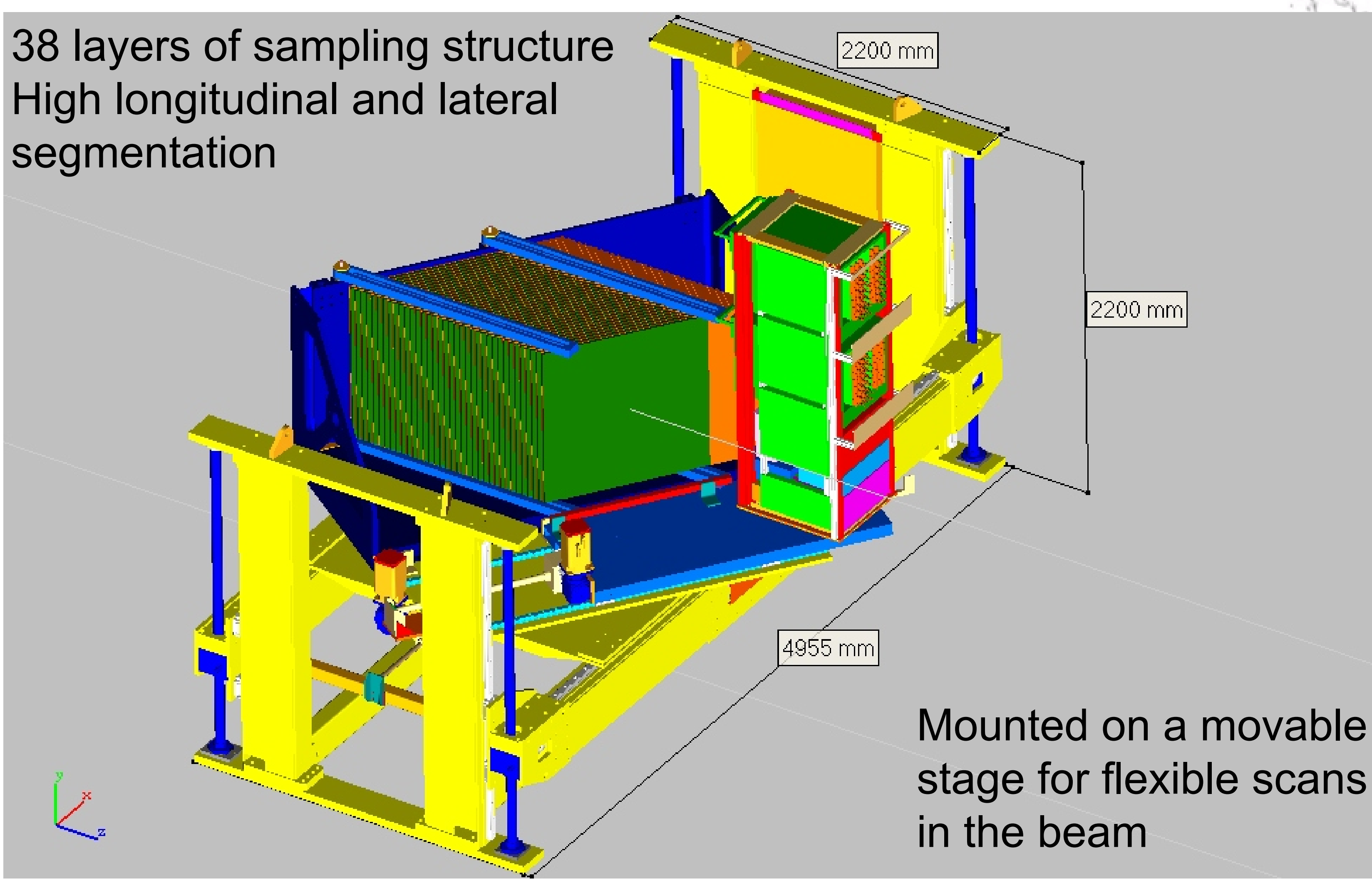


Mounted on a movable stage for flexible scans in the beam

# Calibration strategy

Non trivial equalization of scintillator tiles response based on:

- Detection of mip from $\mu$ or $\pi$ stabs
- Redundant monitoring system combining low/high intensity UV LED light on each tile + temperature readout of each layer

Use EM scale to convert response in MIP to GeV

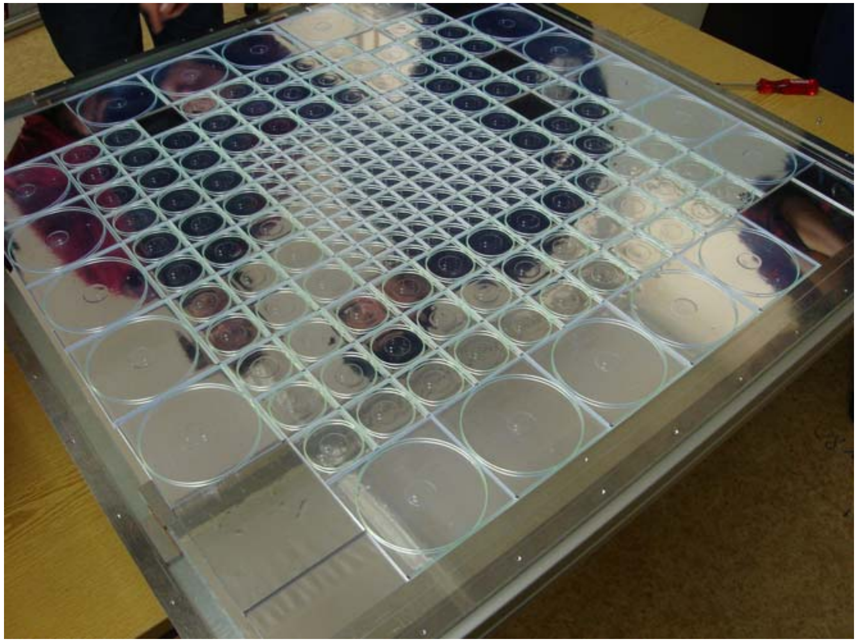

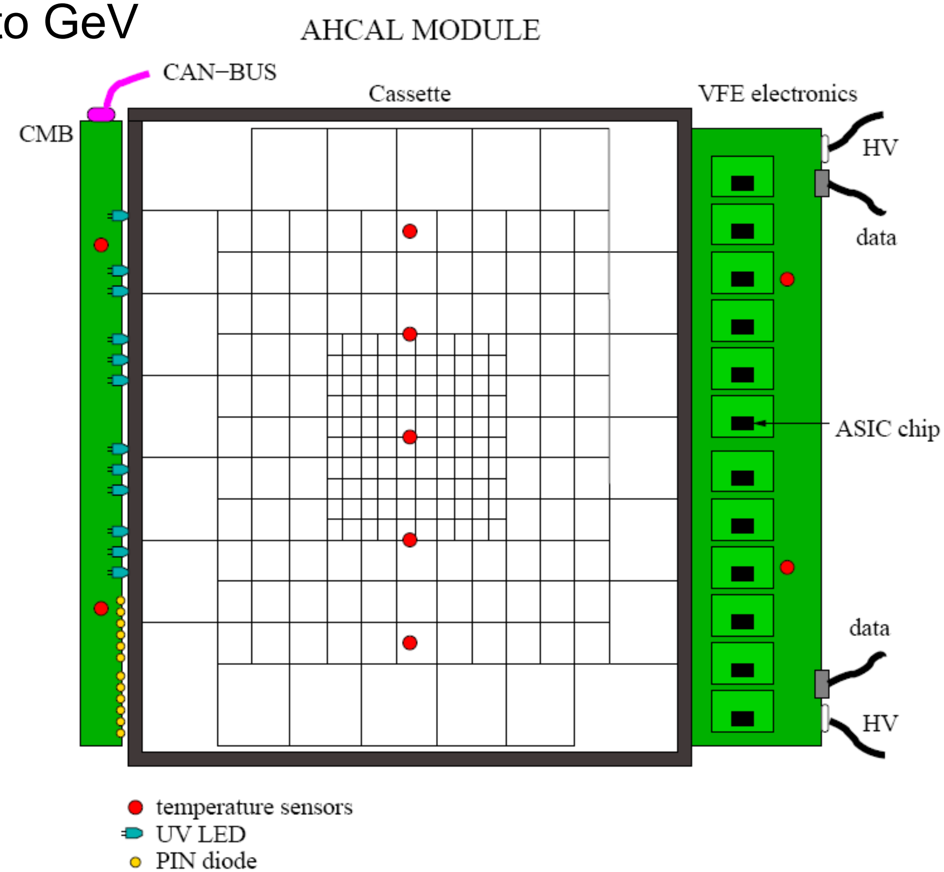

# Tile response equalization with MIP

Using muon signal

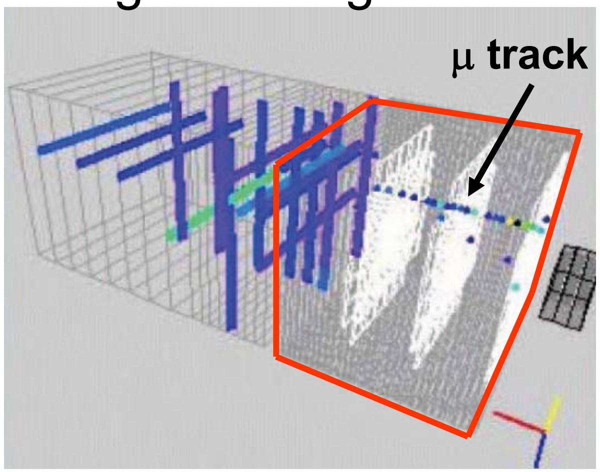

$\mu$ **track in HCAL**

**Single pixel signal from SiPM**

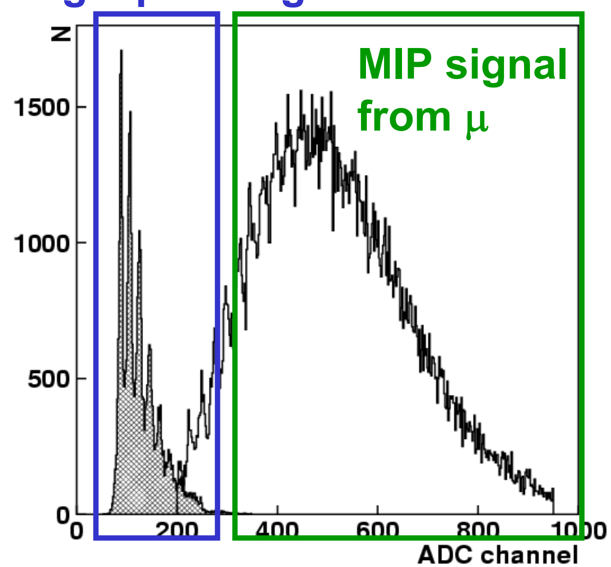


Using pion shower
select MIP stabs using the high granularity of the HCAL

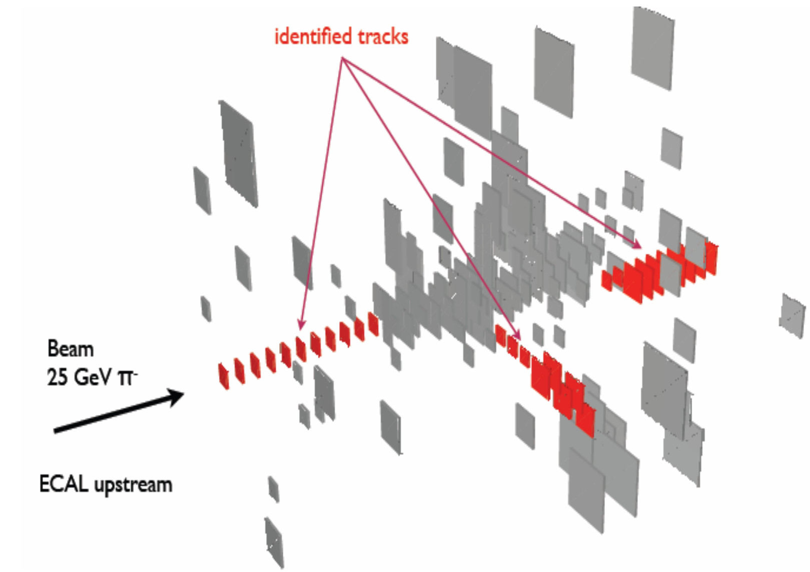


Luminosity requirement for in-situ calibration with MIP stabs from jets (ILC detector)

| | Luminosity at 91 GeV | Luminosity at 500 GeV |
|---|---|---|
| layer-module to 3% to layer 20 | 1 $pb^{-1}$ | 1.8 $fb^{-1}$ |
| layer-module to 3% to layer 48 | 10 $pb^{-1}$ | 20 $fb^{-1}$ |
| HBU to 3% to layer 20 | 20 $pb^{-1}$ | 36 $fb^{-1}$ |

more statistics obtained from $Z_0 \rightarrow \mu\mu$ events

# Importance of monitoring/calibration system in a SiPM based calorimeter

SiPM response is non-linear

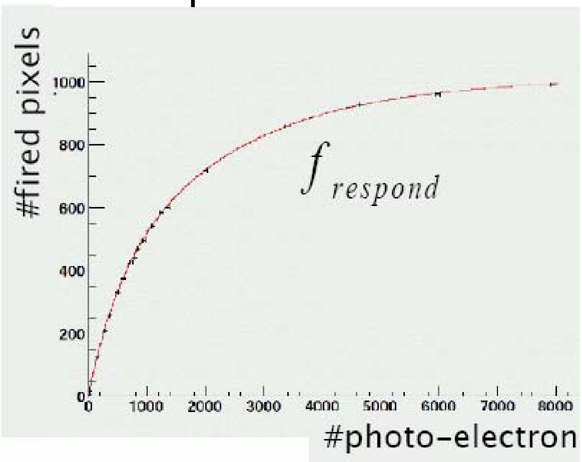


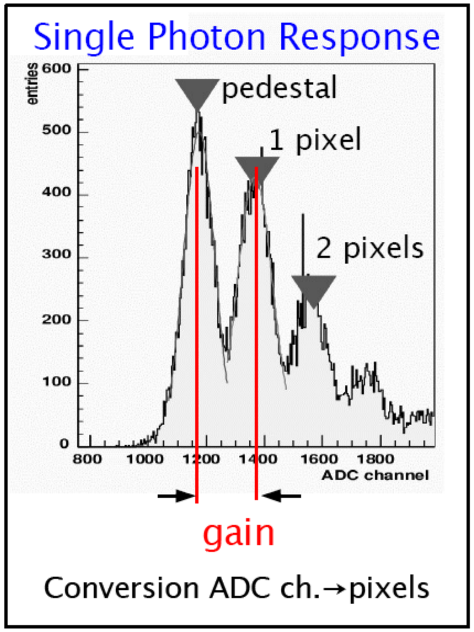


Calibration system should deliver:

- -Low intensity light for SiPM Gain calibration
- -High intensity of light for saturation monitoring
- -Medium intensity light for monitoring T,V variations

AHCAL layer = 216 tiles

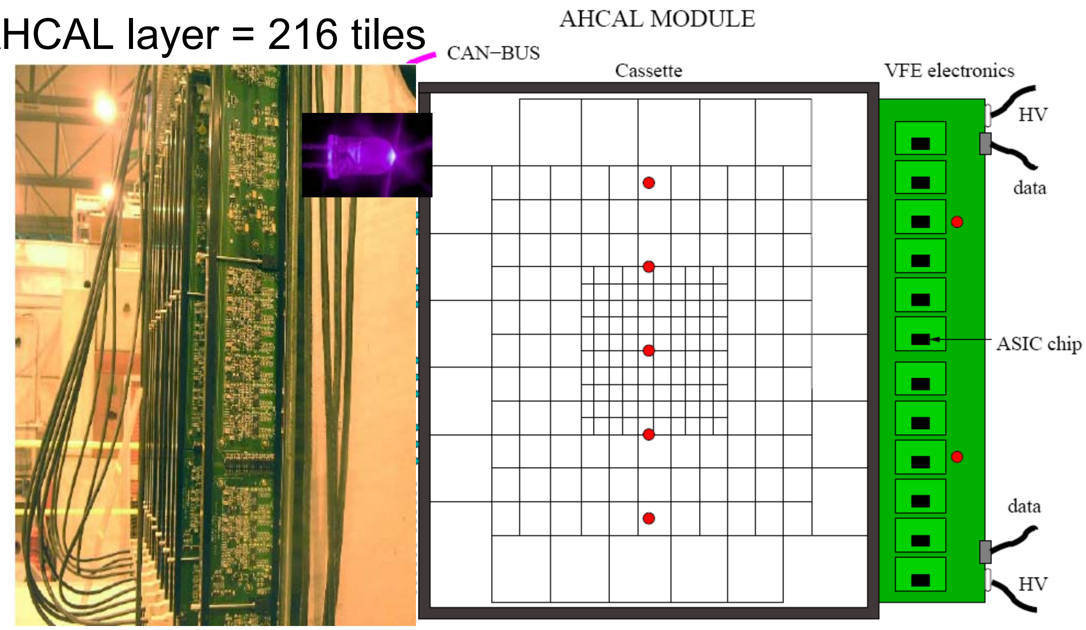


Light intensity for 8000 channels within factor 2
>94% calibration efficiency on full calorimeter

# The power of high granularity

**REAL DATA!**

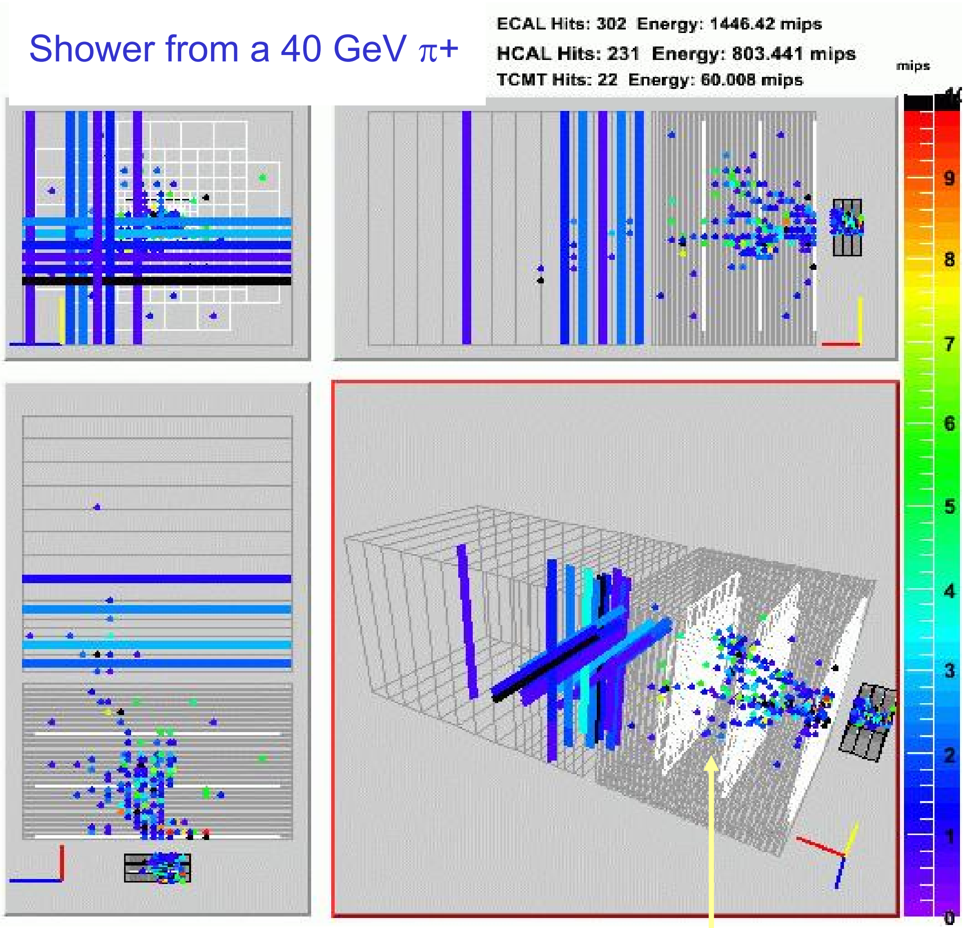


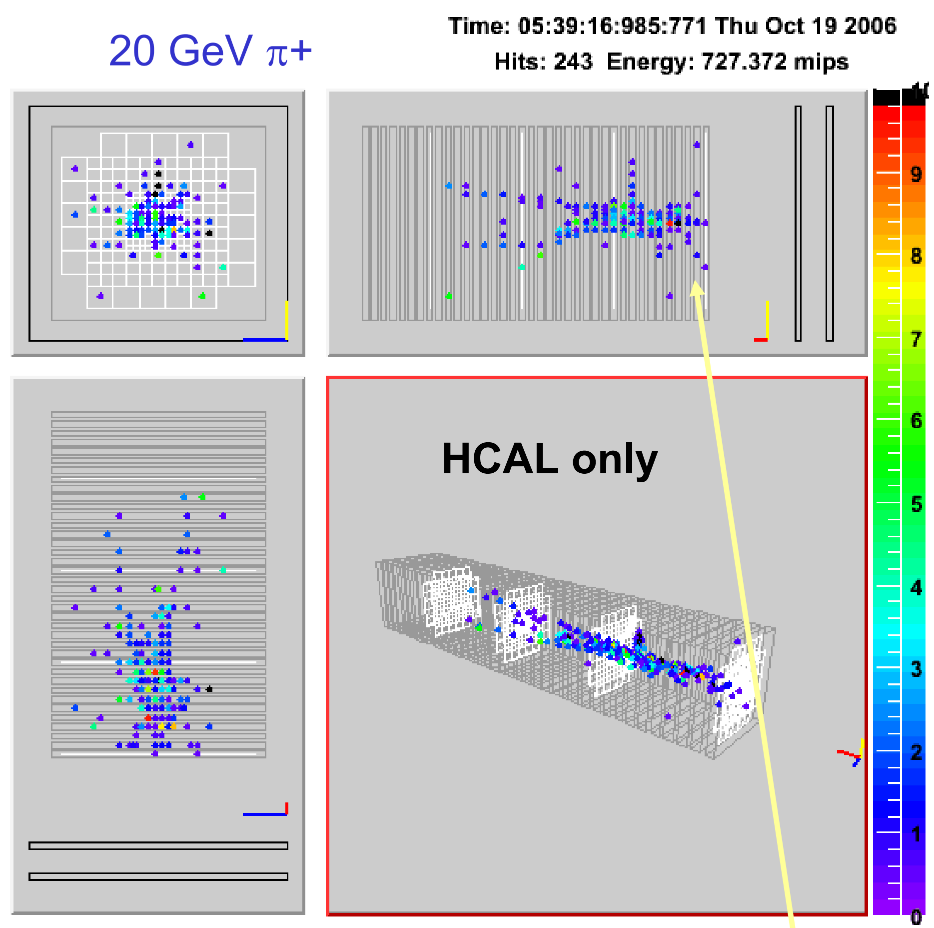


**Clear structure visible in hadronic shower**

**Back-scattered particle**

# The power of high granularity

**REAL DATA!**

**HCAL**

**40GeV/c pion with CALICE online analysis software**

Imaging calorimetry

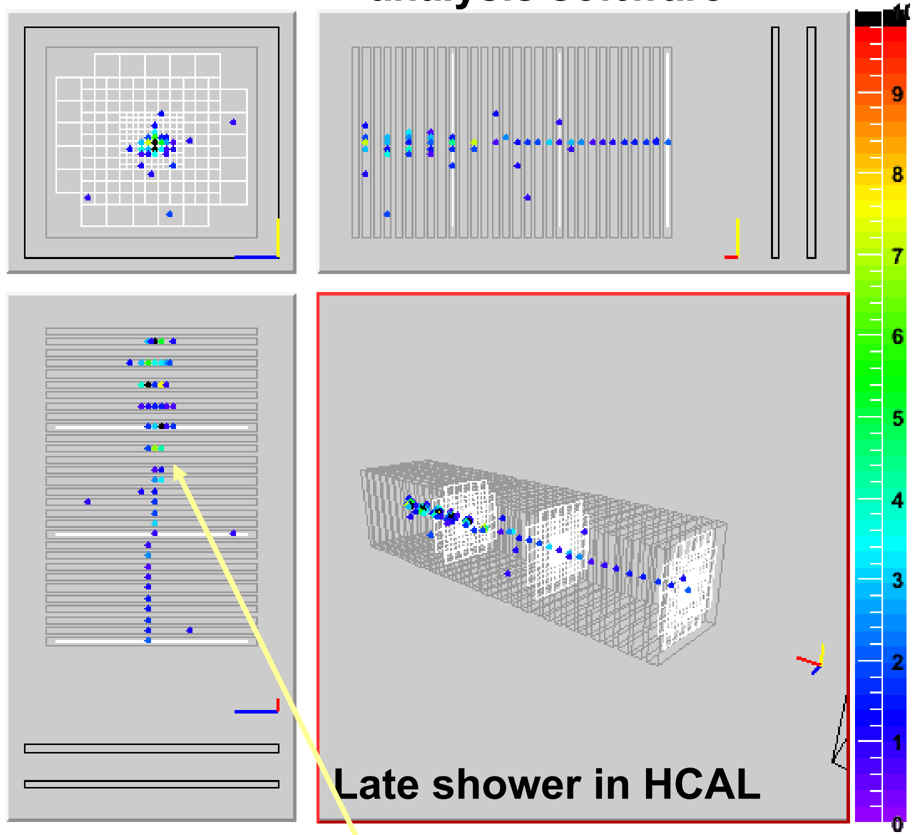


**Clear determination of the first interaction**

# A calorimeter for Particle Flow

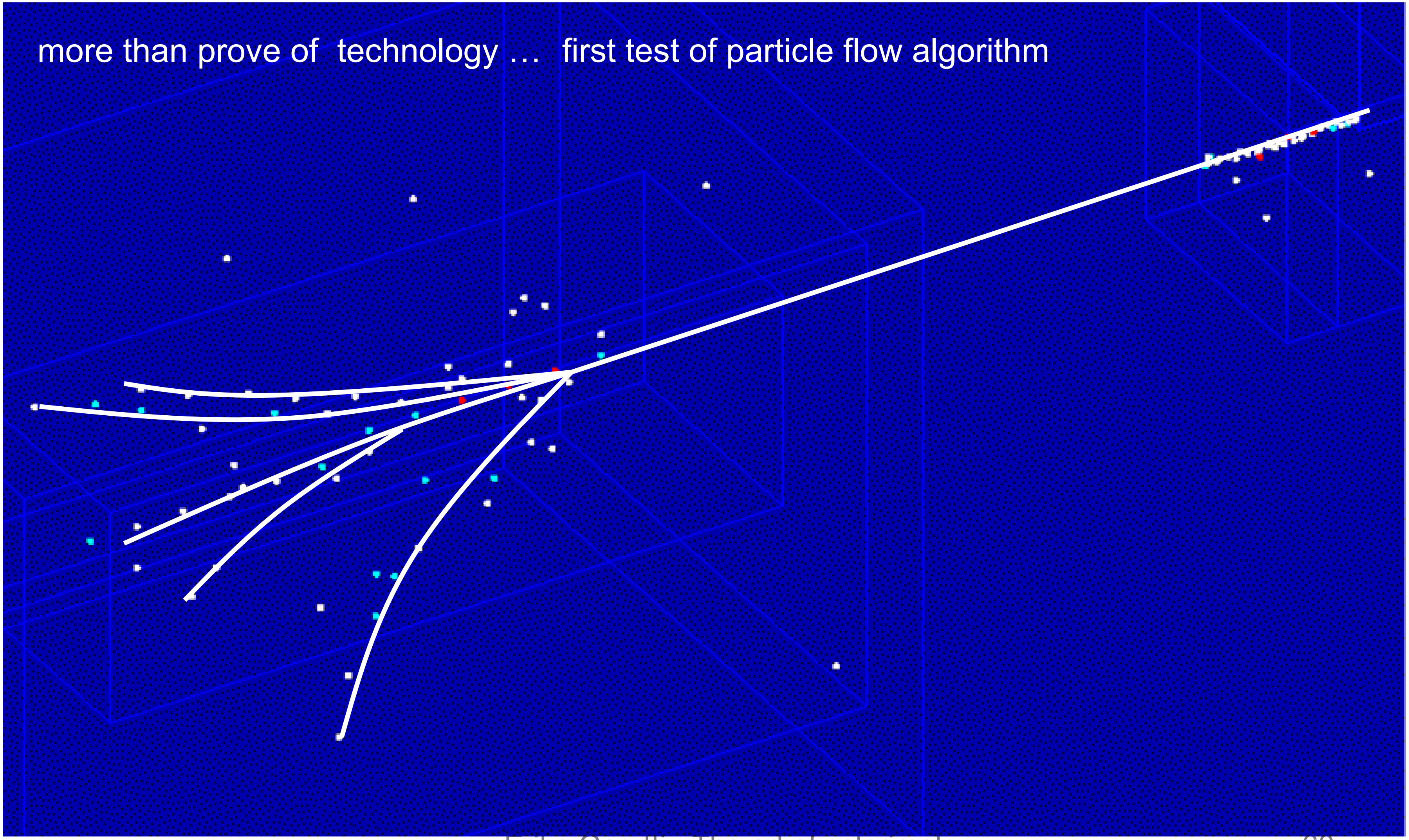

# Analog .vs. Digital

photon analysis

$$E_\gamma \neq \sum N_i$$

ECAL: Analog readout required

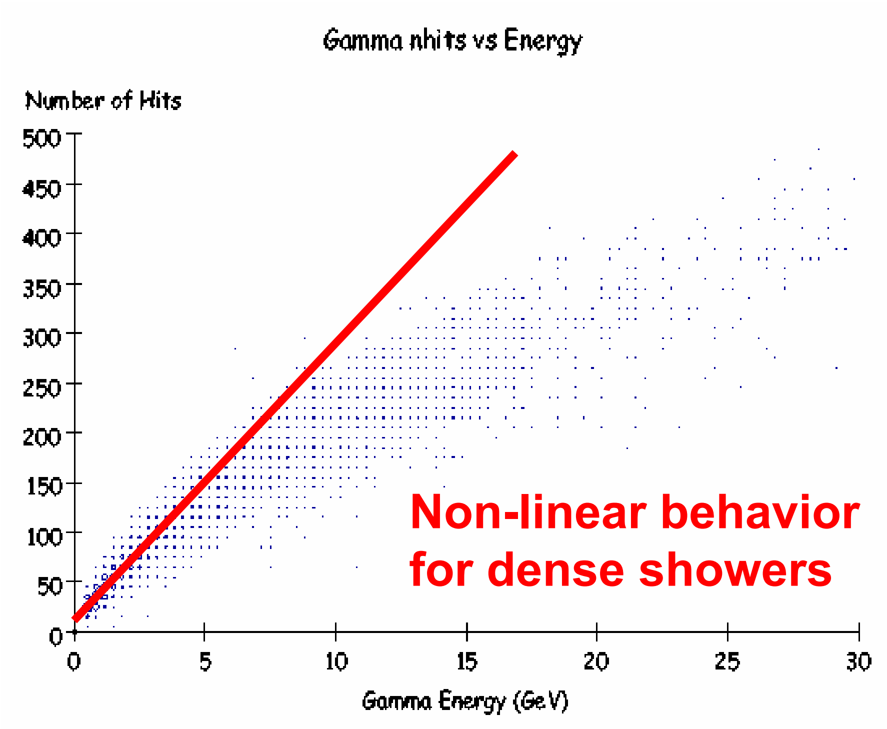


hadron analysis

$$E_h \propto \sum N_i$$

HCAL: either Analog or Digital readout

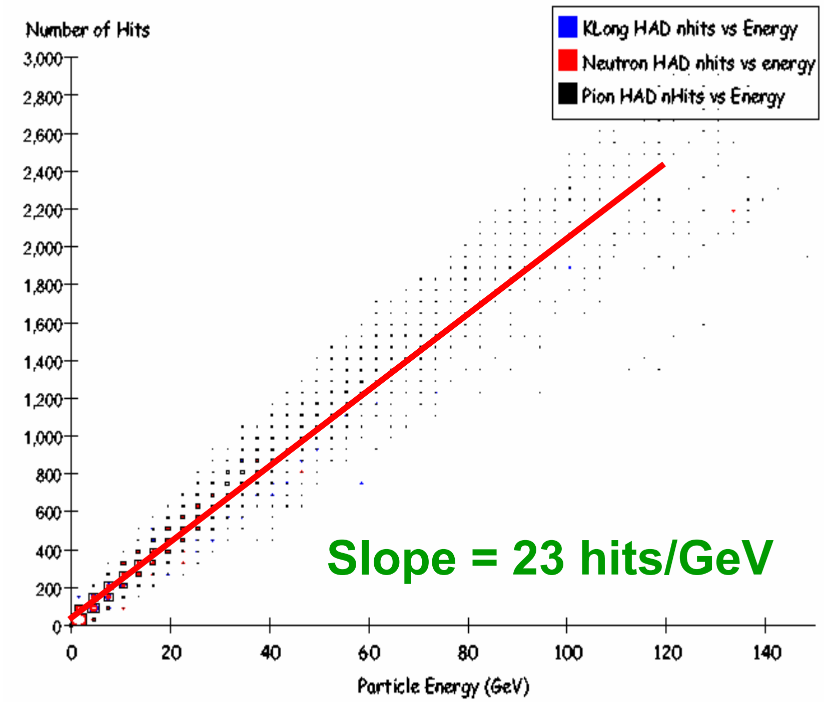


Calorimeter cell size 1x1cm$^2$

# The Digital HCAL

Sandwich structure of steel and gas chambers

3 layers of gas amplification with GEM foils

onboard readout

Pad readout

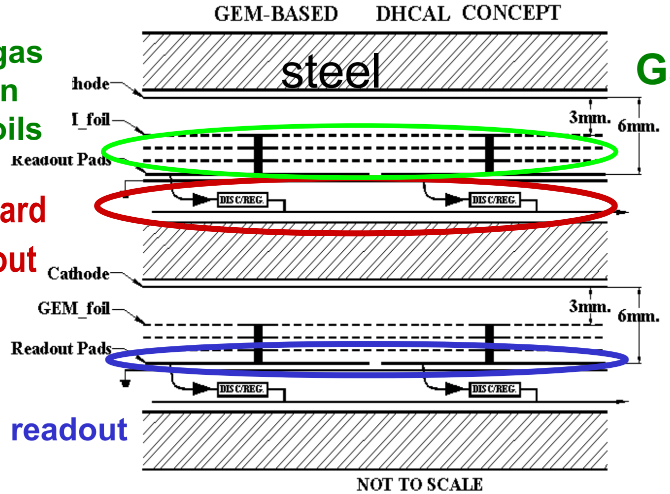


Gas Electron Multiplier foil

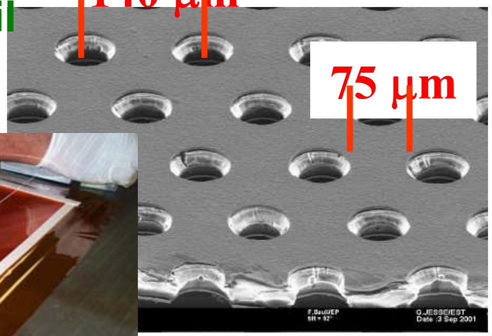


mechanic challenge !

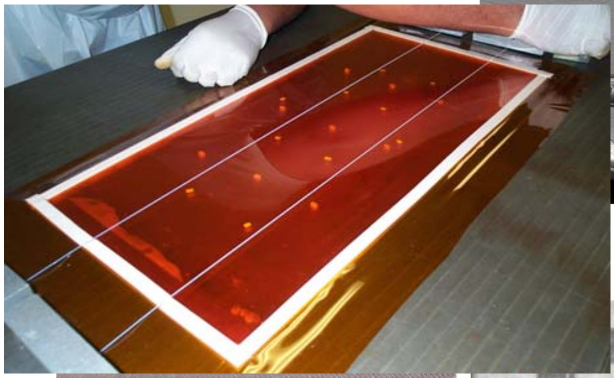

Micro mesh gaseous structure

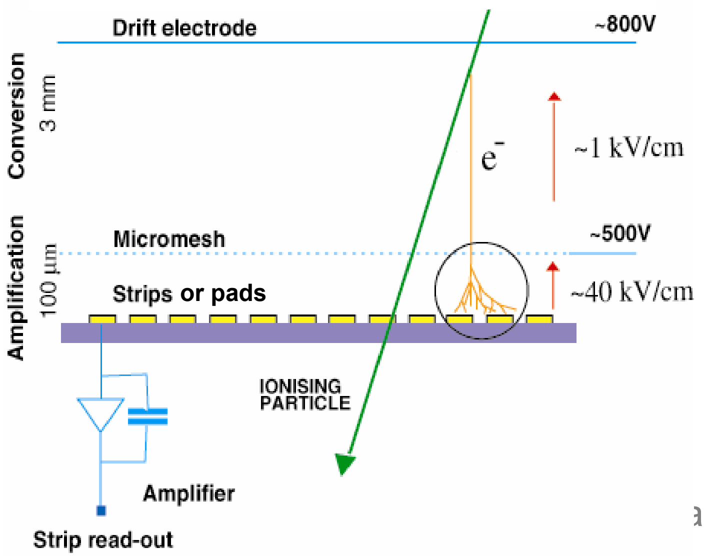


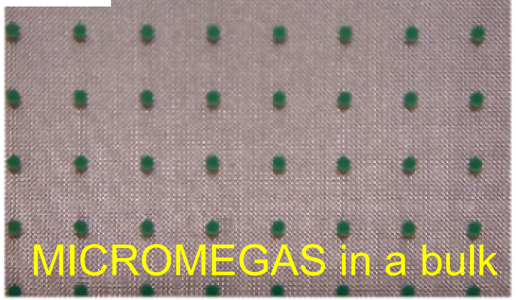


80 μm

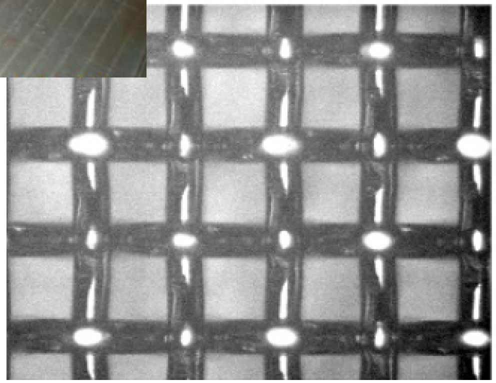

Pillars: 400u Ø, 100u height

Ampl. gap 25-150μm → narrow avalanches

excellent spatial and time resolution

# Digital HCAL with RPC

from J. Repond, CALICE meeting

first test prototype of Digital HCAL with Resistive Plate Chamber readout tested at Fermilab TB in summer 2007:

Equipped 9 chambers 20 x 20 cm$^2$
with 4 chips ASIC each
256 channels/chamber $\rightarrow$ **2300 channels total**
**System can be extended to 1 m$^2$**

**2-$\pi$ event (upstream shower?)**

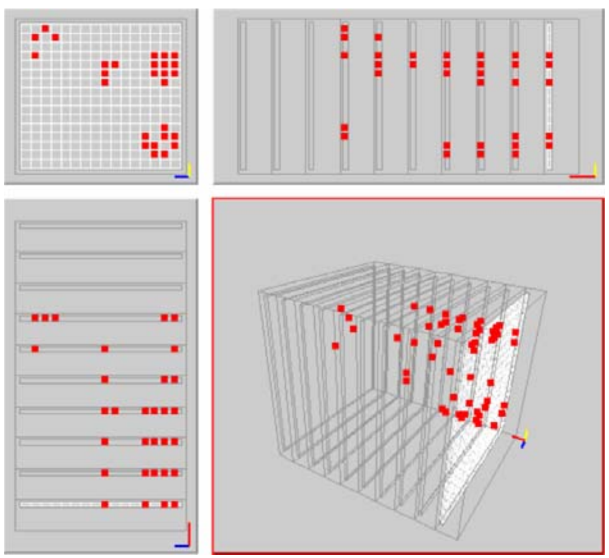

**8 GeV $\pi^+$ event (early shower)**

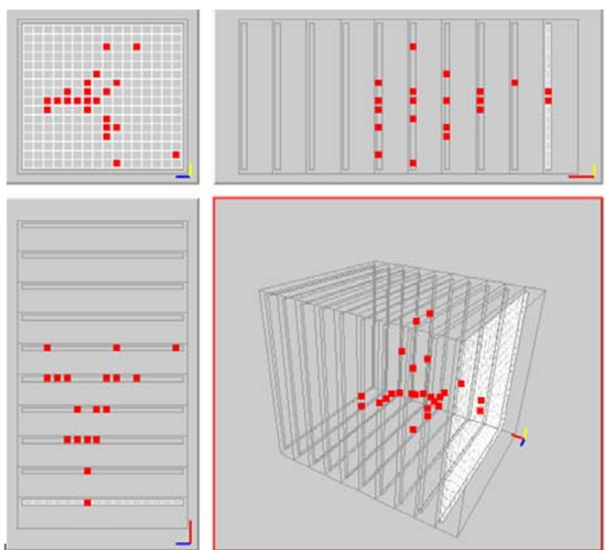

digital readout scheme

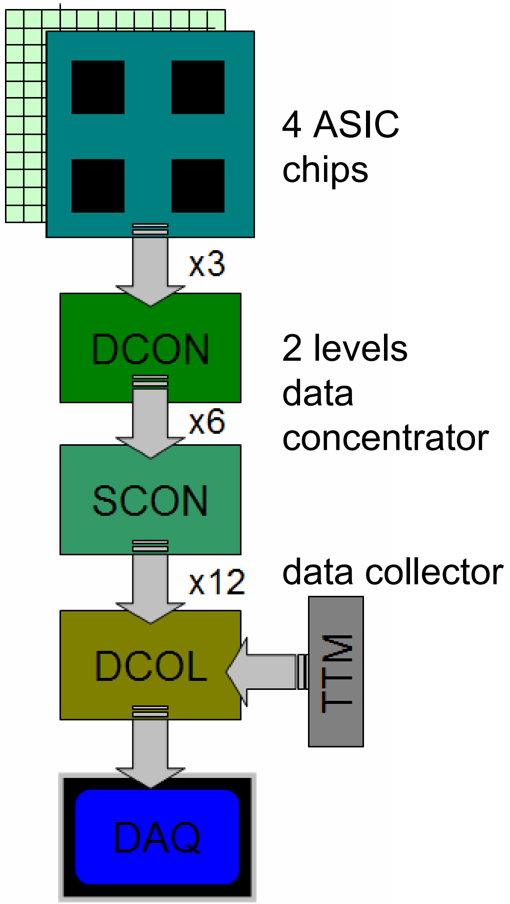

# Assembly of a 1 $m^3$ prototype

**Semidigital RPCs**

Biggest challenge: integrate electronics in 6mm PCB ➔ special chip design

ASIC - HARDROC ( Ω LAL)

- 3 thresholds, masks, optimized power pulsing
- controlled in a fully automatic way using a robotic system used for CMS trackers

- 1 $cm^2$ readout pads
- 3 mm of Ar/i$C_4H_{10}$ : 95/5
- Analog readout prototypes for characterization (GASSIPLEX chips), 6x16, 12x32 $cm^2$
- Digital readout prototypes with embedded electronics (HARDROC/DIRAC chips), 8x32, 32x48 $cm^2$

2 ASU = 48 ASICs = 3072 channels = 1/3 $m^2$

# Highest granularity ECAL

CALICE:
Si-W with analog readout

30 layers W-Si
1 cm² Si-PADs (next version with 0.5x0.5 cm² Si-PADs)
~10000 channels

➔ Imaging calorimeter!!

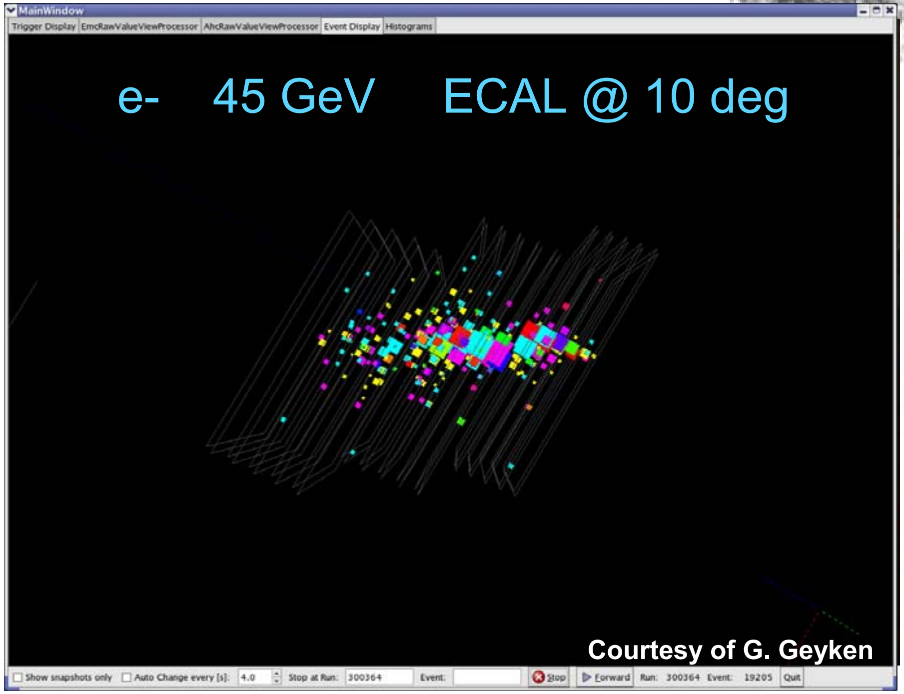


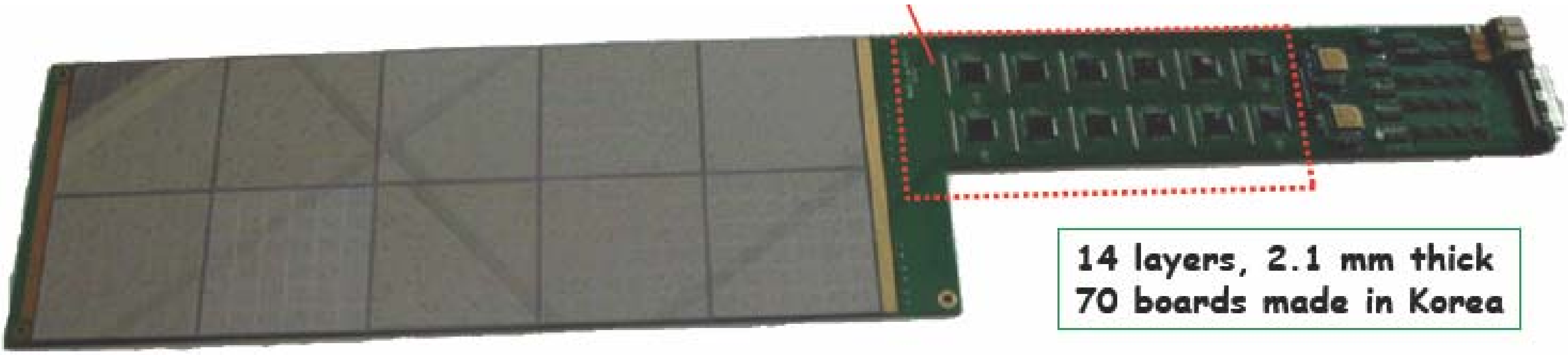

# Analog .vs. Digital

photon analysis

$$E_\gamma \neq \sum N_i$$

ECAL: Analog readout required

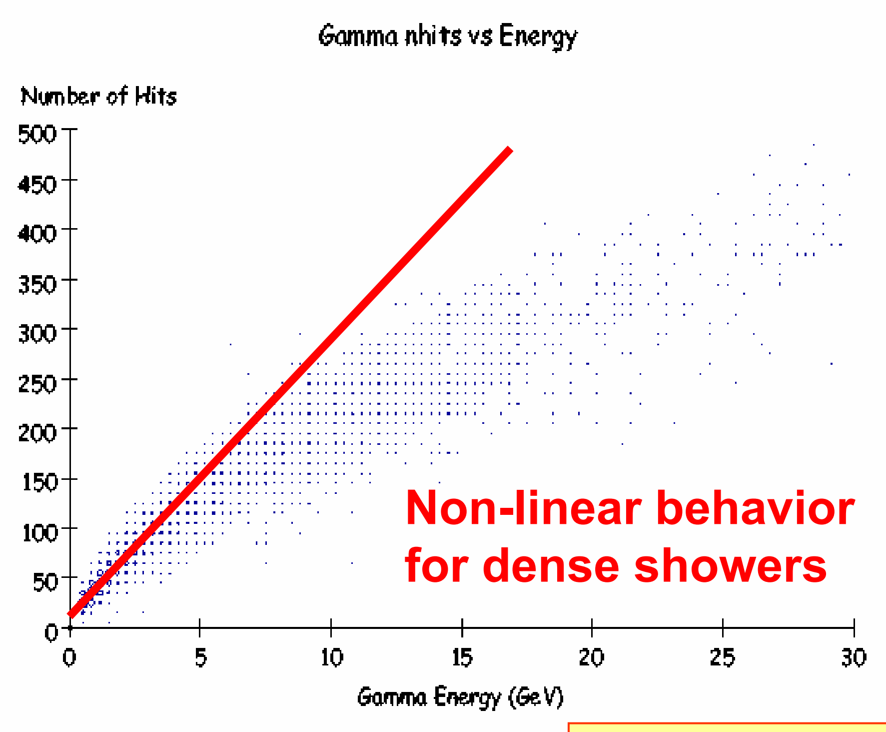


hadron analysis

$$E_h \propto \sum N_i$$

HCAL: either Analog or Digital readout

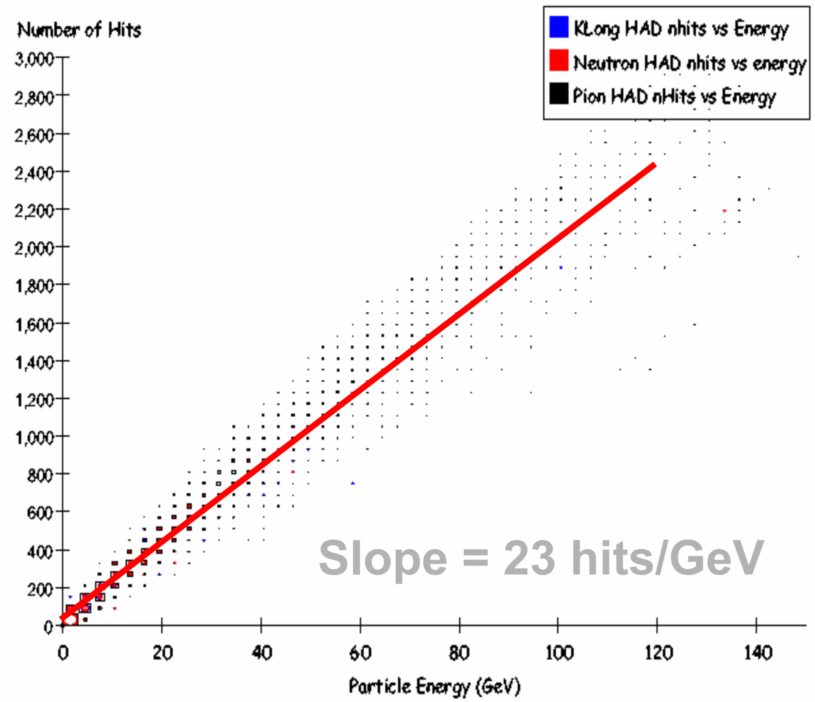


Calorimeter cell size 1x1cm$^2$

# Digital ECAL

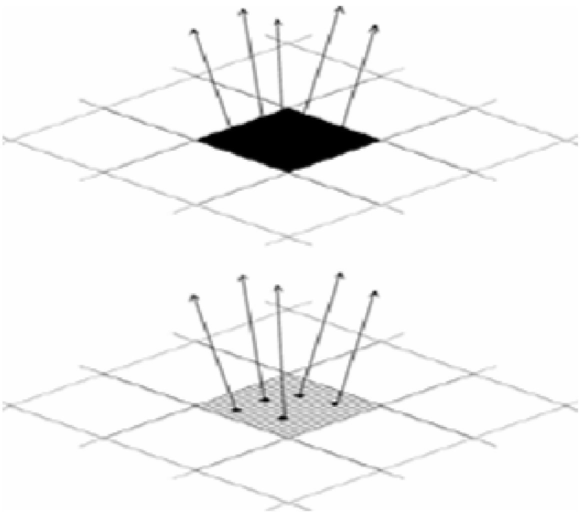

Next R&D steps:

- Swap ~0.5x0.5 $cm^2$ Si pads with smaller pixels
- "Small" = at most one particle/pixel
- 1-bit ADC/pixel, i.e. Digital !

How small should a pixel be?

- EM shower core density at 500GeV is ~100/$mm^2$
- Pixels must be<100×100$\mu m^2$
- Baseline: 50×50$\mu m^2$
- Gives ~$10^{12}$ pixels for ECAL – "Tera-pixel APS"
- Mandatory to integrate electronics on sensor

➔MAPS (Monolithic Active Pixel Sensors)
  - developed for vertex detectors

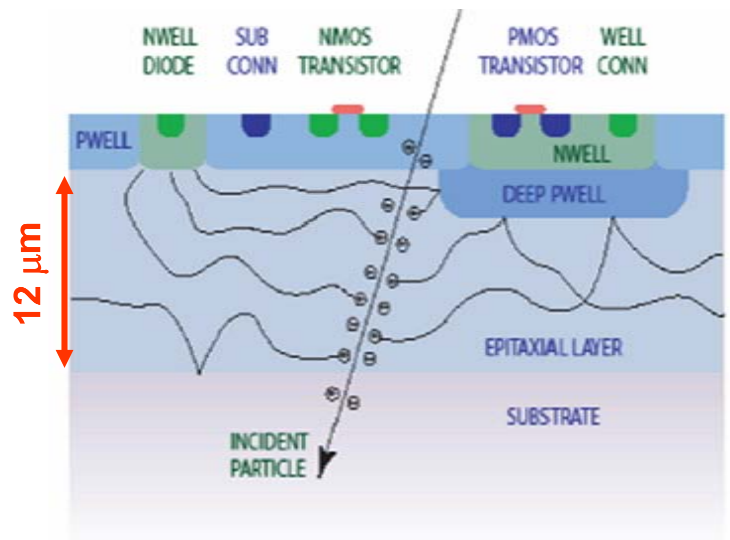

# Pixel Occupancy

MAPS concept requires binary readout...

➔ need at most 1 hit per pixel or else lose information

## Si-W ECAL, 100GeV electrons

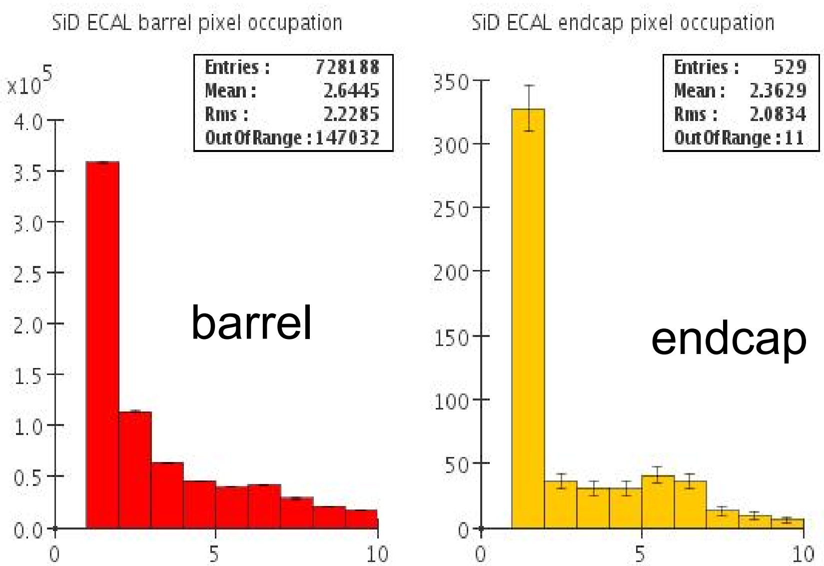


## MAPS ECAL, 100GeV electrons

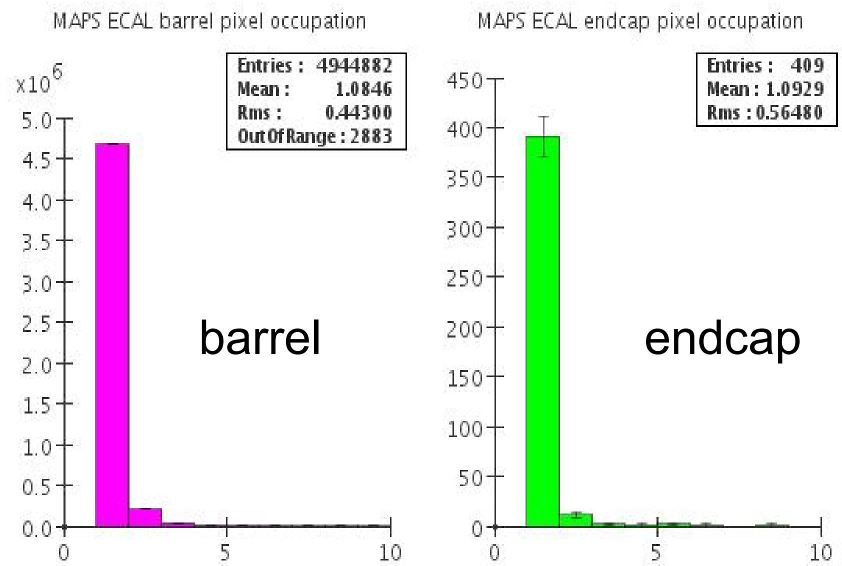


Select optimal pixel pitch from simulation studies

# MIP Signal

Estimate MIP threshold

**SiD Baseline, 16mm$^2$ area cells**

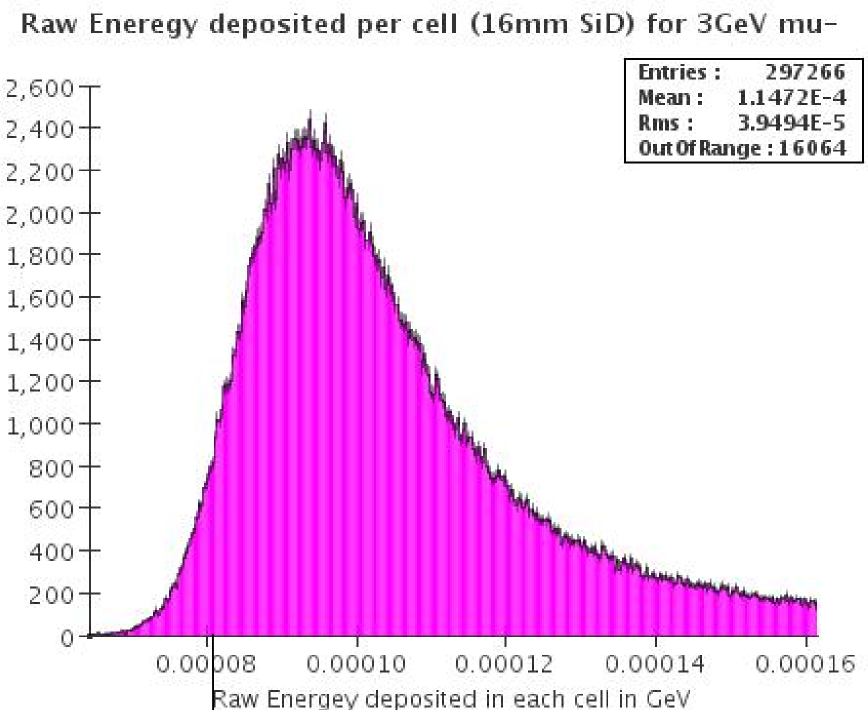


threshold of 0.5MIP = 47keV

**MAPS 50x50 micron pixels**

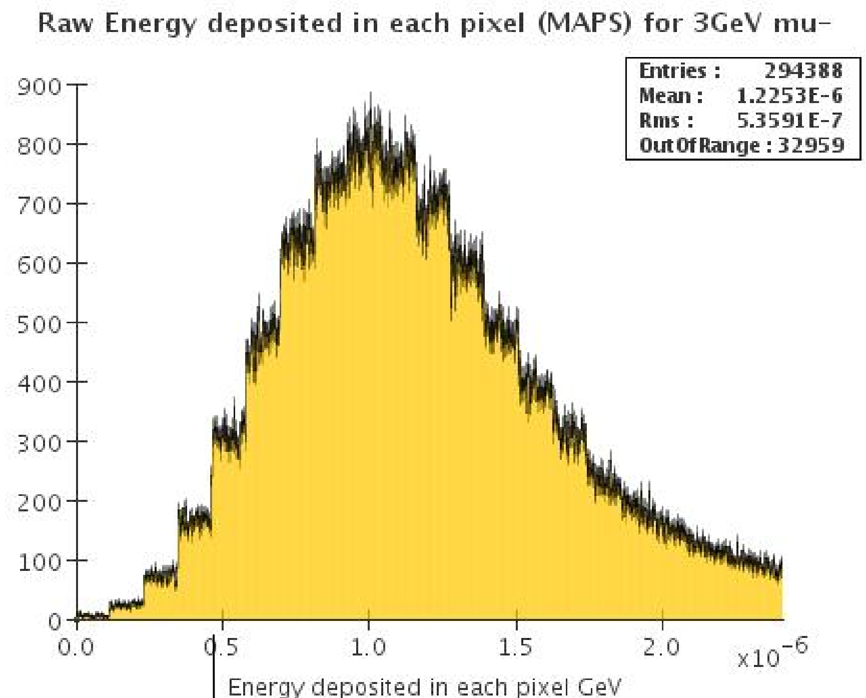


threshold of 0.5MIP = 0.5keV

(compare to 430 keV for scintillator tiles in HCAL)

# MAPS calorimeter

CALICE proposed pixel design: includes an amplifier and a comparator with programmable threshold. The charge collection is performed by 4 diodes, which are positioned symmetrically around the center

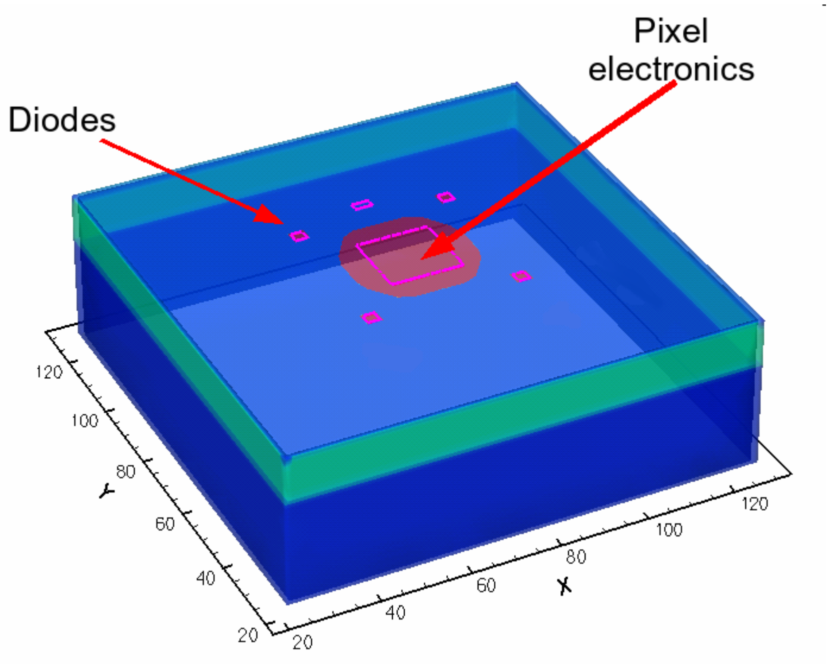


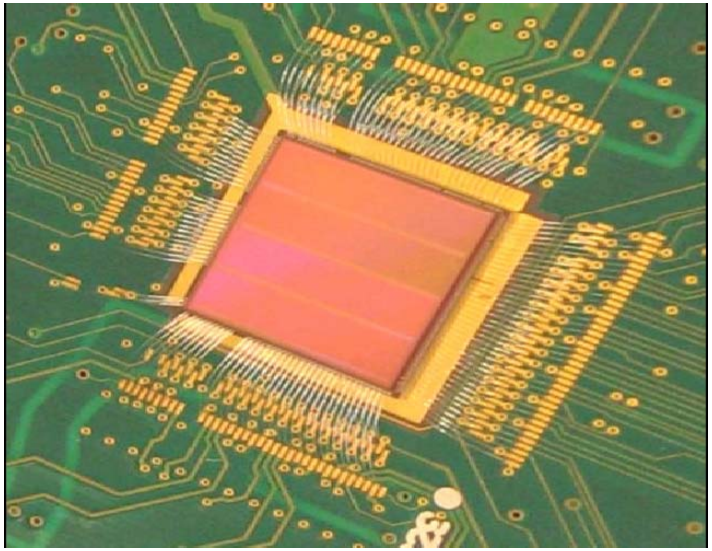

8.2 million transistors
28224 pixels; 50 μm
Pixel: 4 diodes, Q-preamp, mask+trim
Sensitive area 79.4mm$^2$

# Analog vs digital ECAL

great improvement in imaging capability

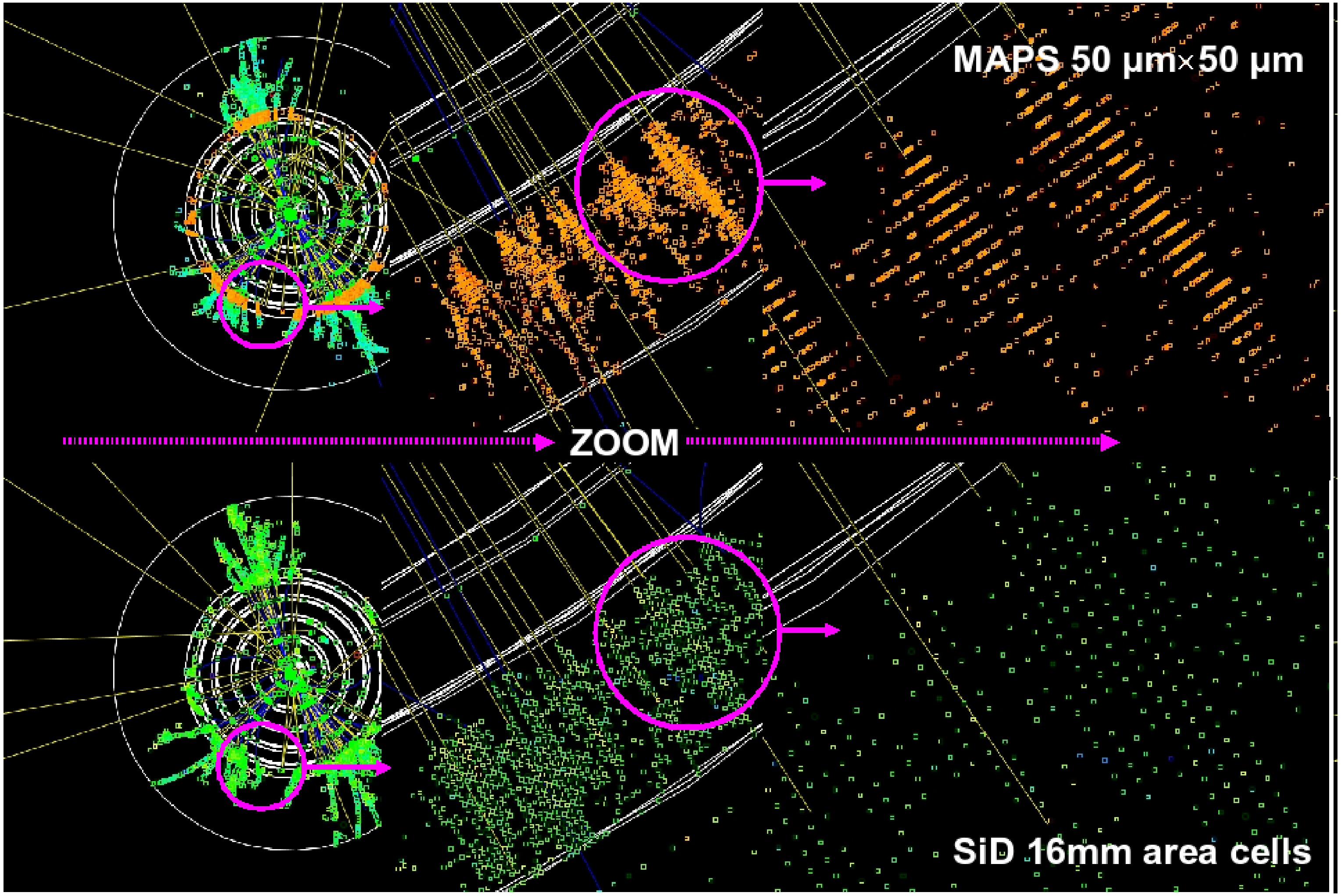

# Calorimeters at non-collider experiments

| | |
|---|---|
| 1) Calorimeters in space: | PAMELA |
| 2) Calorimeters for neutrino physics: | Cuoricino/Cuore |

# Pamela's scientific objectives

- ✓ Study antiparticles in cosmic rays
- ✓ Search for antimatter
- ✓ Search for dark matter ($e^+$ and pbar spectra)
- ✓ Study cosmic-ray propagation
- ✓ Study solar physics and solar modulation
- ✓ Study the electron spectrum (local sources?)


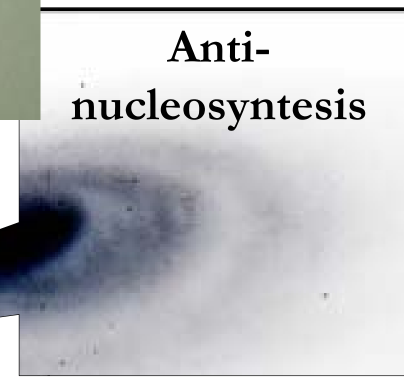


The first historical measurements of the $\bar{p}/p$ - ratio and various Ideas of theoretical Interpretations

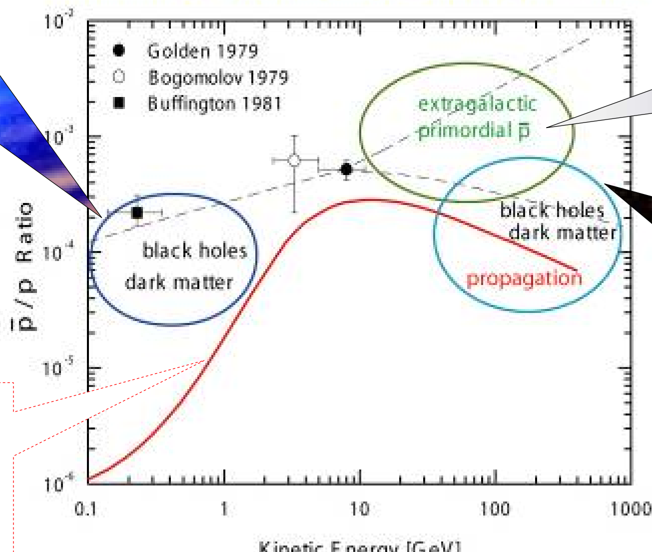


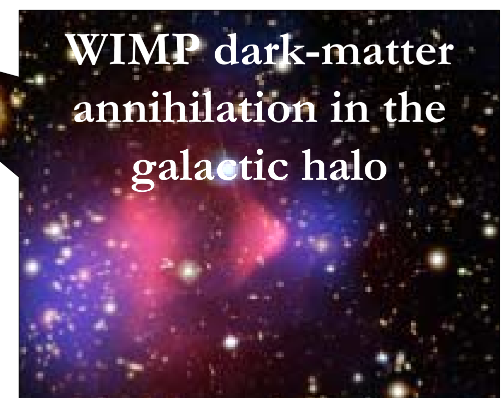


**Background:**
**CR interaction with ISM**
**CR + ISM → p-bar + …**

# PAMELA milestones

Launch from Baikonur: June 15$^{th}$ 2006, 0800 UTC.
Power On: June 21$^{st}$ 2006, 0300 UTC.
Detectors operated as expected after launch

PAMELA in continuous data-taking mode since commissioning phase ended on July 11$^{th}$ 2006

As of now:

- 1128 days in orbit
- Trigger rate ~ 25 Hz
- Data taking ~73% live-time
- >13 TByte of raw data downlinked
- >$10^9$ triggers recorded and under analysis

| | Energy range |
|---|---|
| Antiprotons | 80 MeV - 190 GeV |
| Positrons | 50 MeV – 300 GeV |

# PAMELA detectors

Main requirements → high-sensitivity antiparticle identification and precise momentum measurement

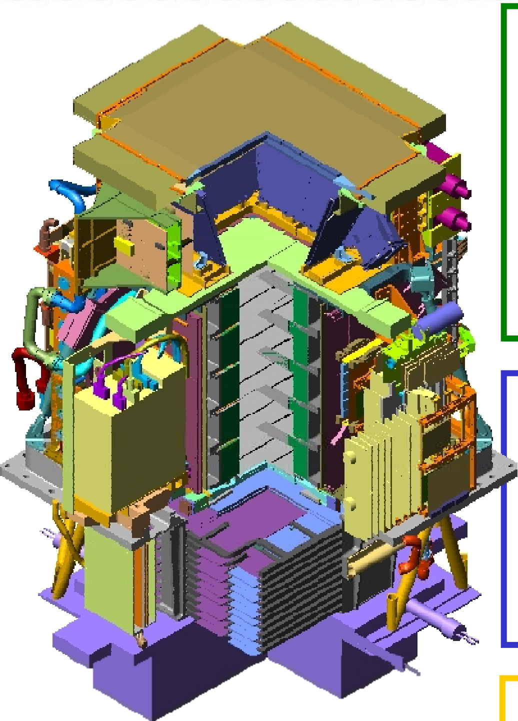

**GF: 21.5 cm² sr**
**Mass: 470 kg**
**Size: 130x70x70 cm³**
**Power Budget: 360W**

**Time-Of-Flight**
**plastic scintillators + PMT:**
- Trigger
- Albedo rejection;
- Mass identification up to 1 GeV;
- Charge identification from dE/dX.

**Electromagnetic calorimeter**
**W/Si sampling (16.3 X0, 0.6 λI)**
- Discrimination e+ / p, anti-p / e⁻ (shower topology)
- Direct E measurement for e⁻

**Neutron detector**
**³He Tubes:**
- High-energy e/h discrimination

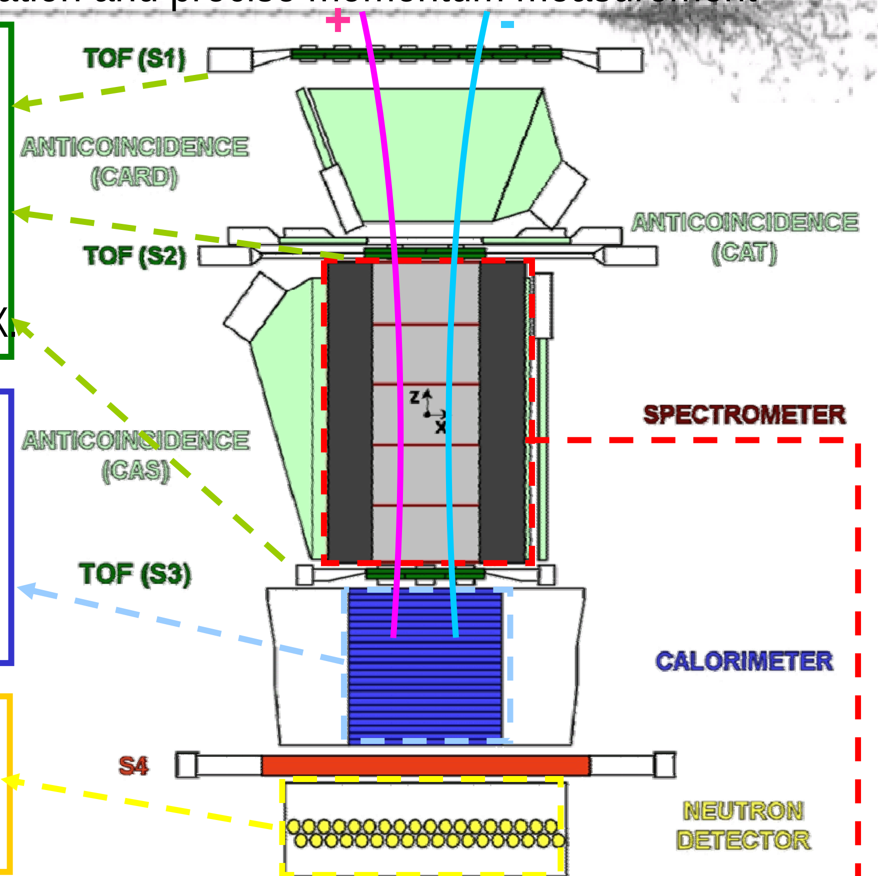


**Spectrometer**
**microstrip silicon tracking system + permanent magnet**
It provides:
- *Magnetic rigidity* → R = pc/Ze
- *Charge sign*
- *Charge value from dE/dx*

# Principle of operation

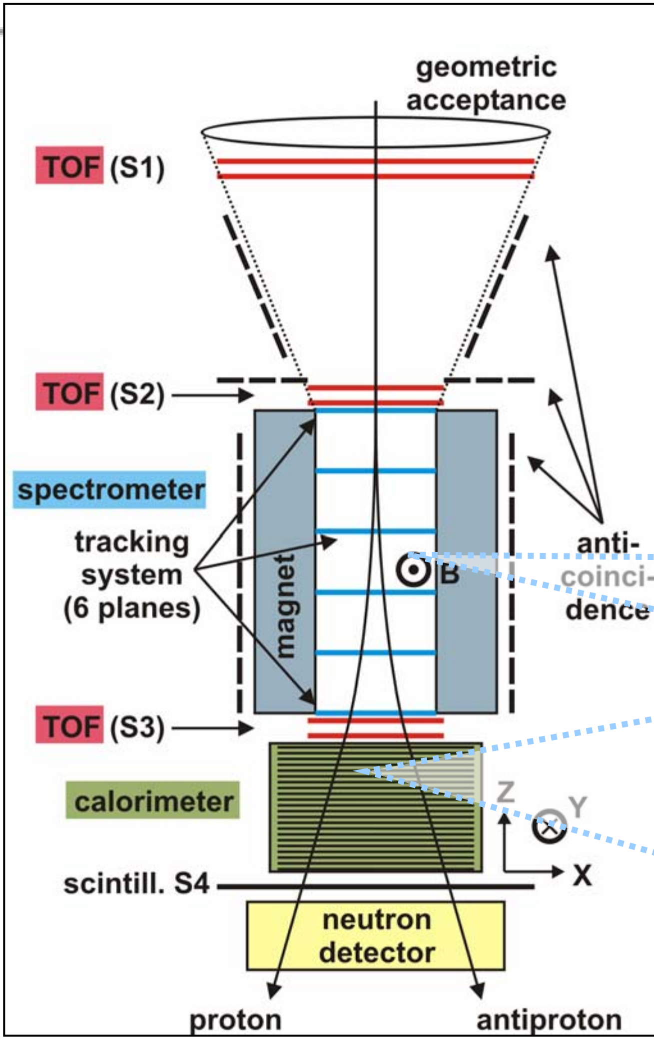


## Z measurement

$$-\frac{dE}{dx} = Kz^2\frac{Z}{A}\frac{1}{\beta^2}\left[\frac{1}{2}\ln\frac{2m_ec^2\beta^2\gamma^2T_{\max}}{I^2} - \beta^2 - \frac{\delta(\beta\gamma)}{2}\right]$$

Bethe Bloch
ionization energy-loss of heavy (M>>me) charged particles

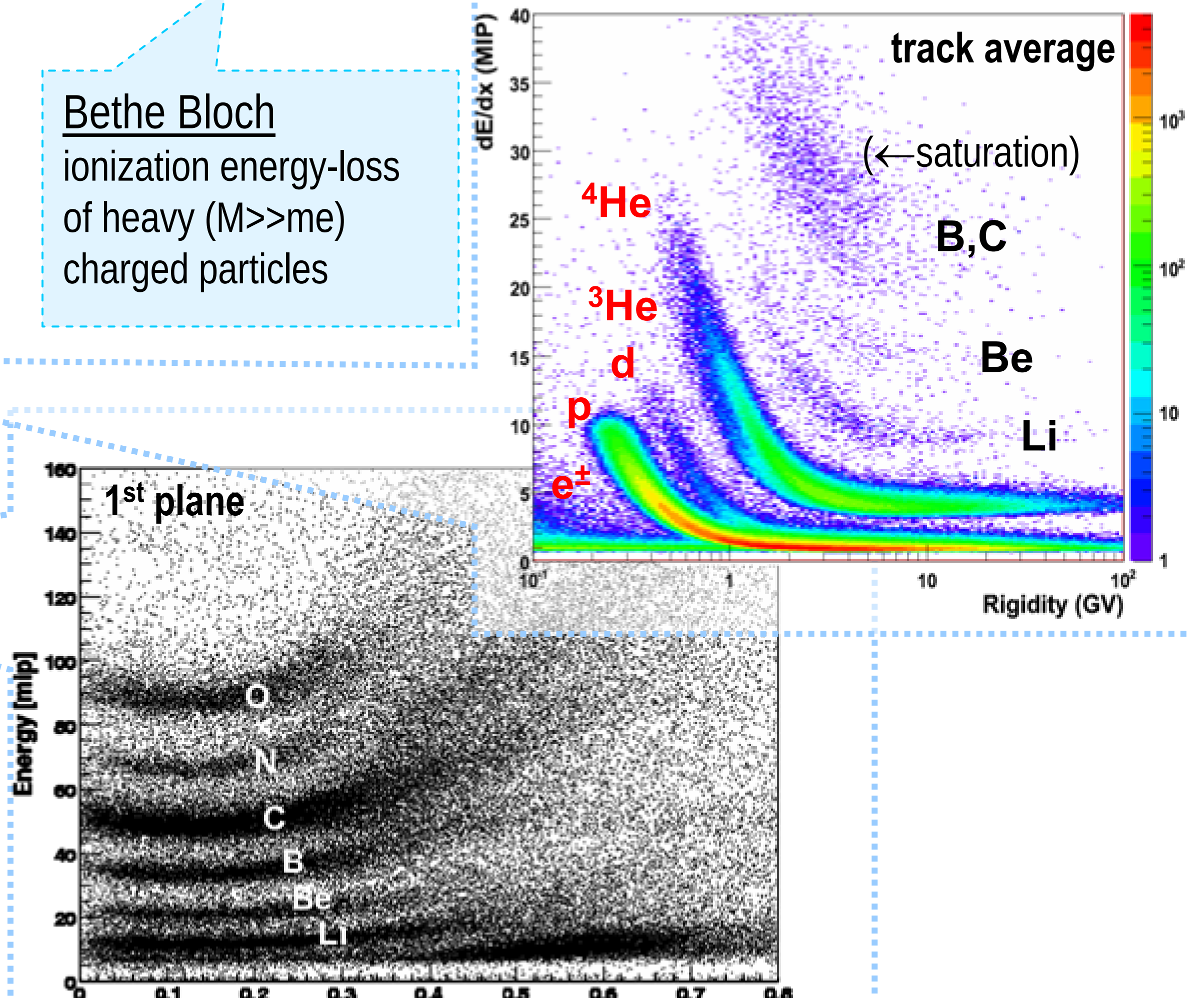

# Principle of operation

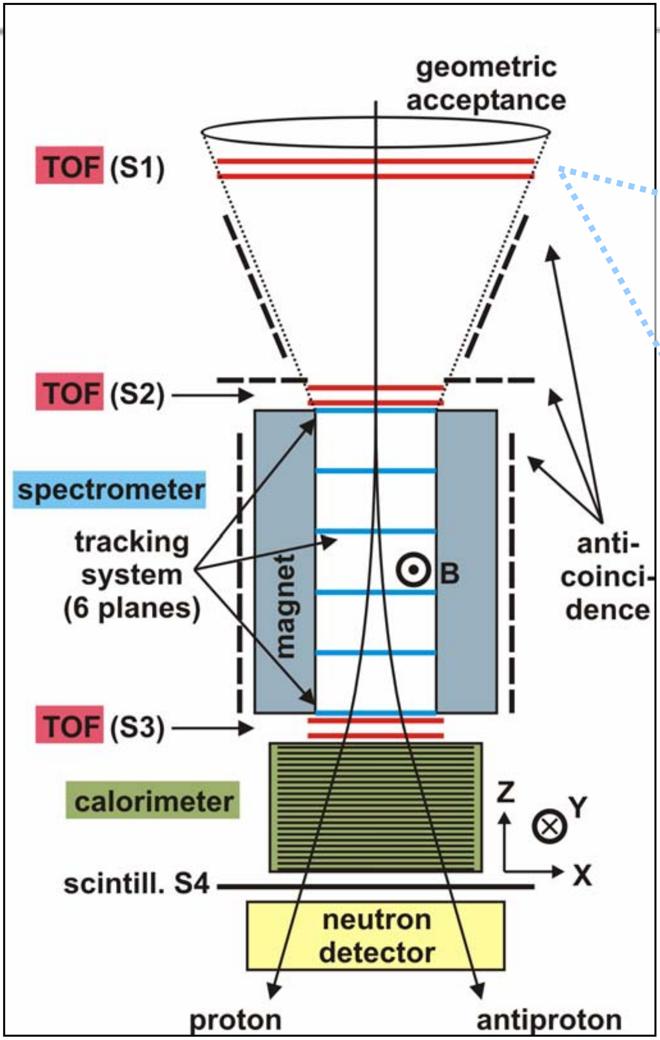


## Velocity measurement

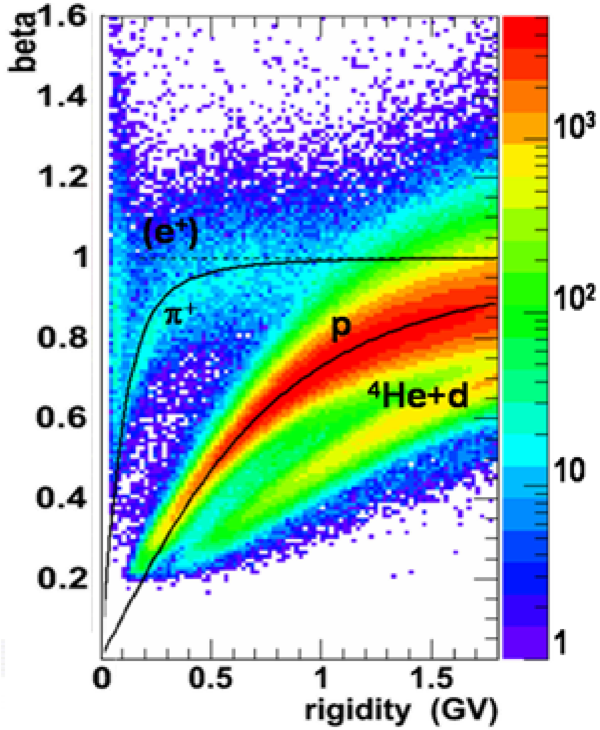


- Particle identification @ low energy
- Identify **albedo** (up-ward going particles $\rightarrow \beta < 0$ )

→ NB! They mimic antimatter!

# Principle of operation

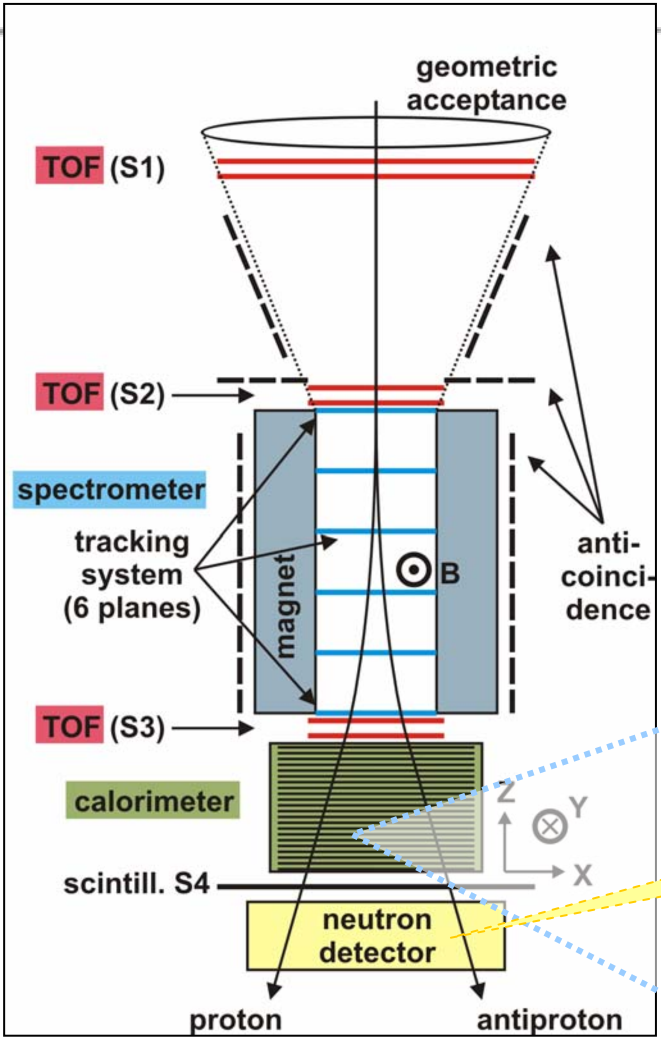


## Electron/hadron separation

- **Interaction topology**

e/h separation

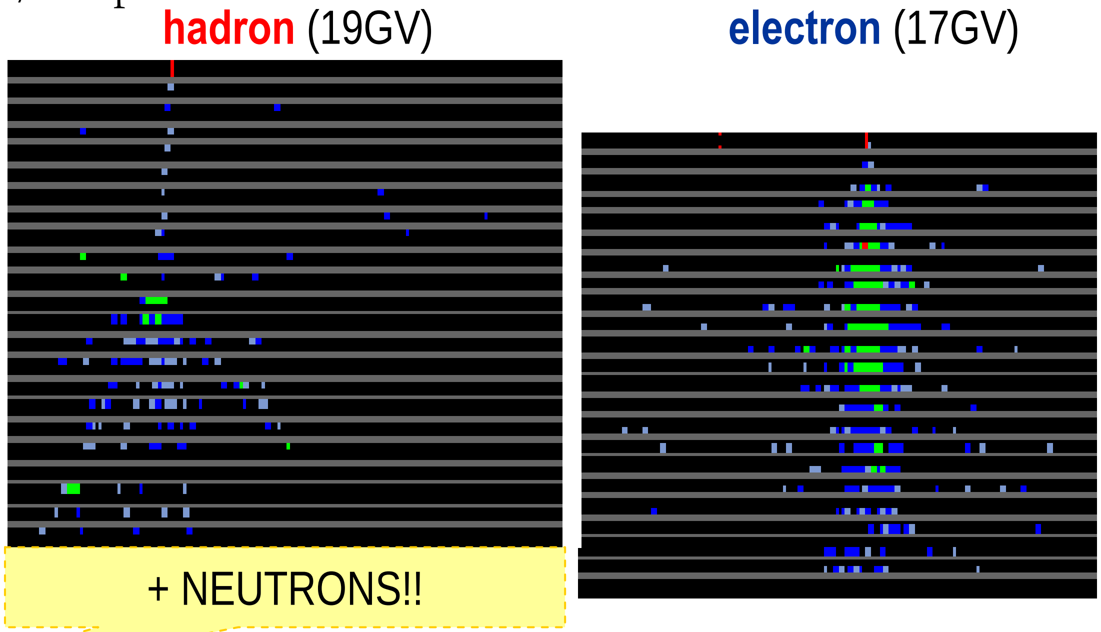


- **Energy measurement of electrons and positrons**

(~full shower containment)

$$\frac{\sigma_E}{E} = a \oplus \frac{b}{\sqrt{E}} \qquad \rightarrow a < 5\%$$

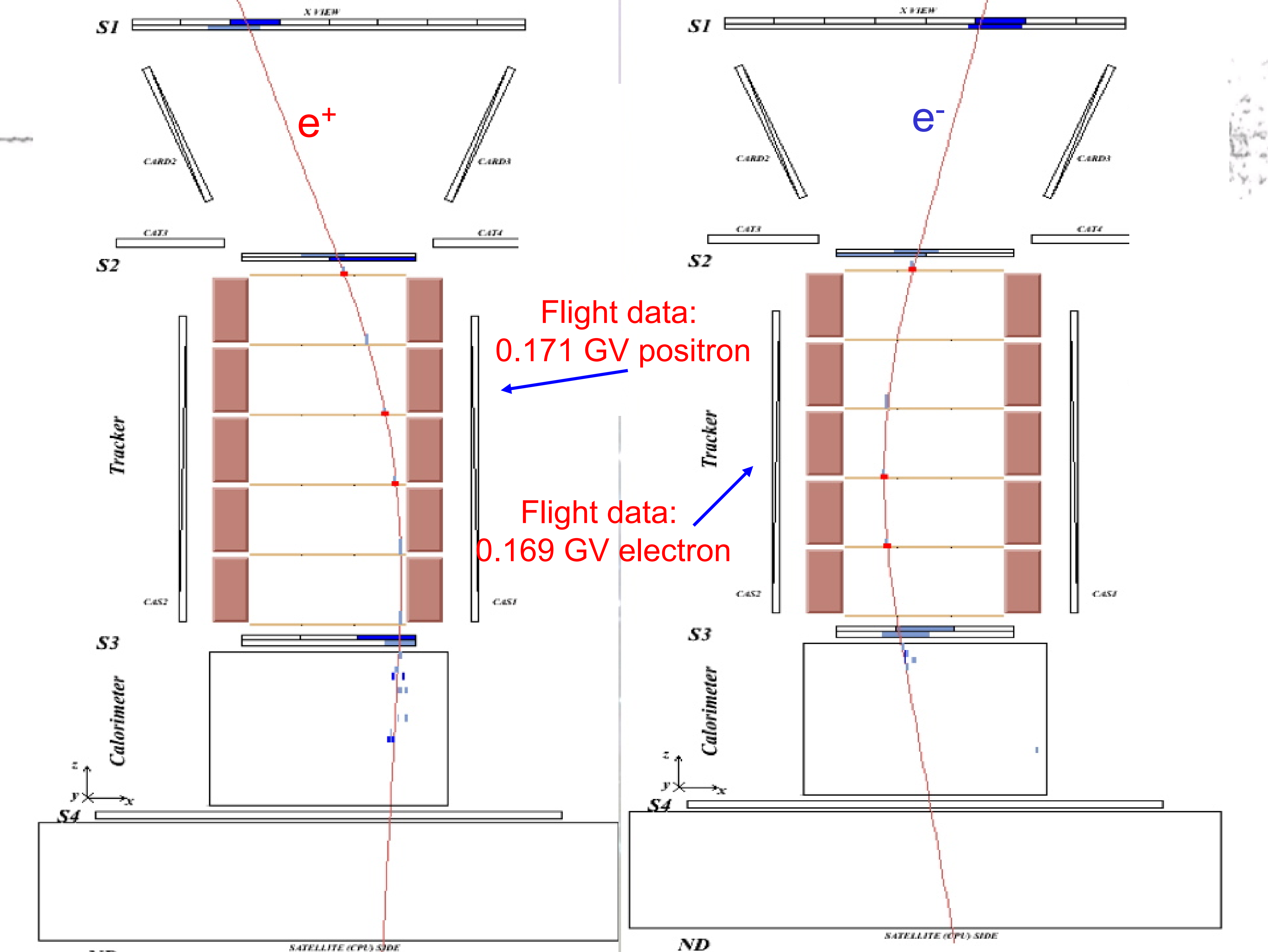
X VIEW
S1
e+
e-
CARD2
CARD3
CAT3
CAT4
S2
Flight data:
0.171 GV positron
Tracker
Flight data:
0.169 GV electron
CAS2
CAS1
S3
Calorimeter
S4
ND
SATELLITE (CPU) SIDE

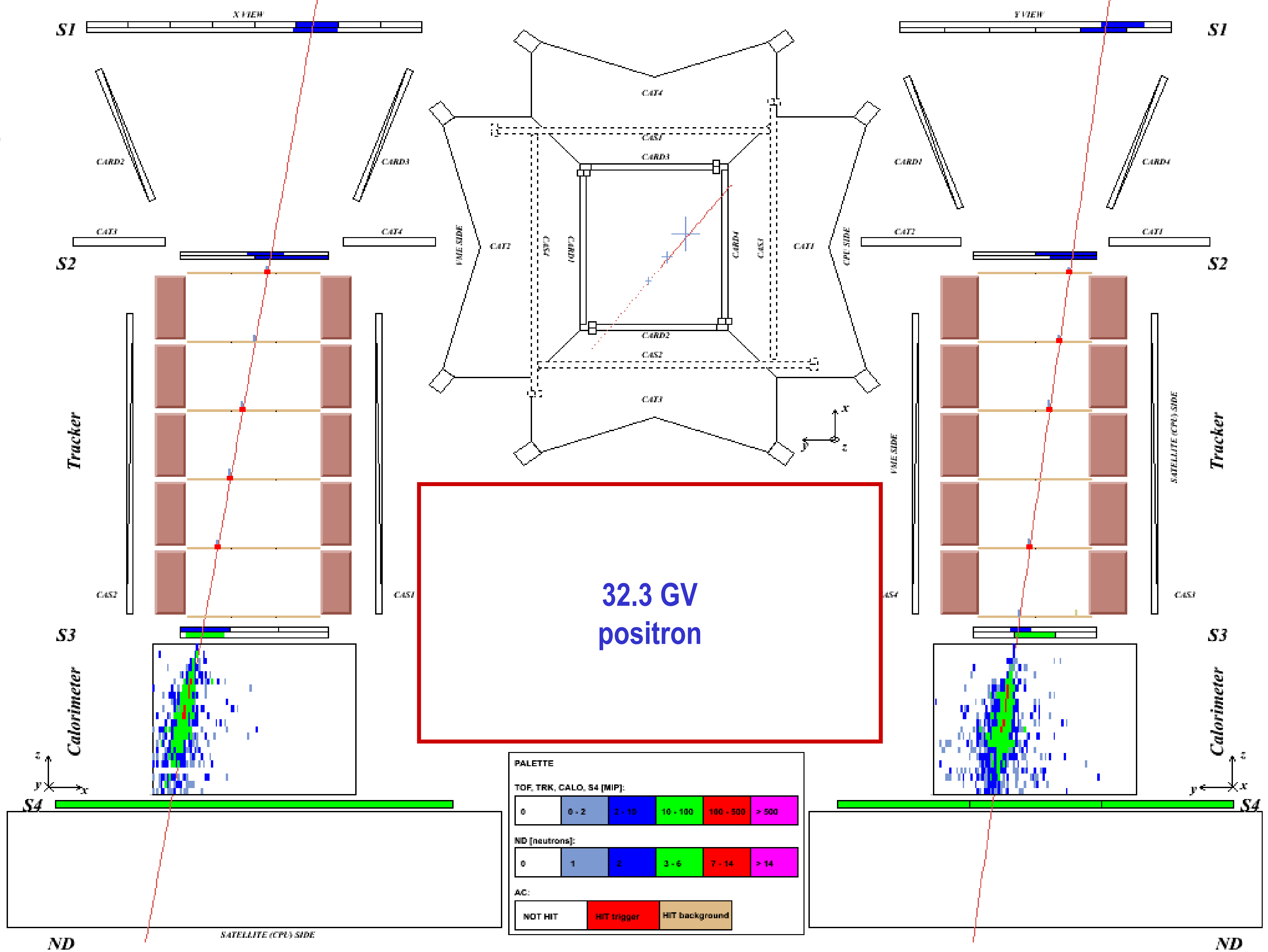
X VIEW
Y VIEW
S1
S2
S3
S4
ND
Tracker
Calorimeter
CARD1
CARD2
CARD3
CARD4
CAT1
CAT2
CAT3
CAT4
CAS1
CAS2
CAS3
CAS4
VME SIDE
CPU SIDE
SATELLITE (CPU) SIDE
32.3 GV
positron
PALETTE
TOF, TRK, CALO, S4 [MIP]:
0
0 - 2
2 - 10
10 - 100
100 - 500
> 500
ND [neutrons]:
0
1
2
3 - 6
7 - 14
> 14
AC:
NOT HIT
HIT trigger
HIT background

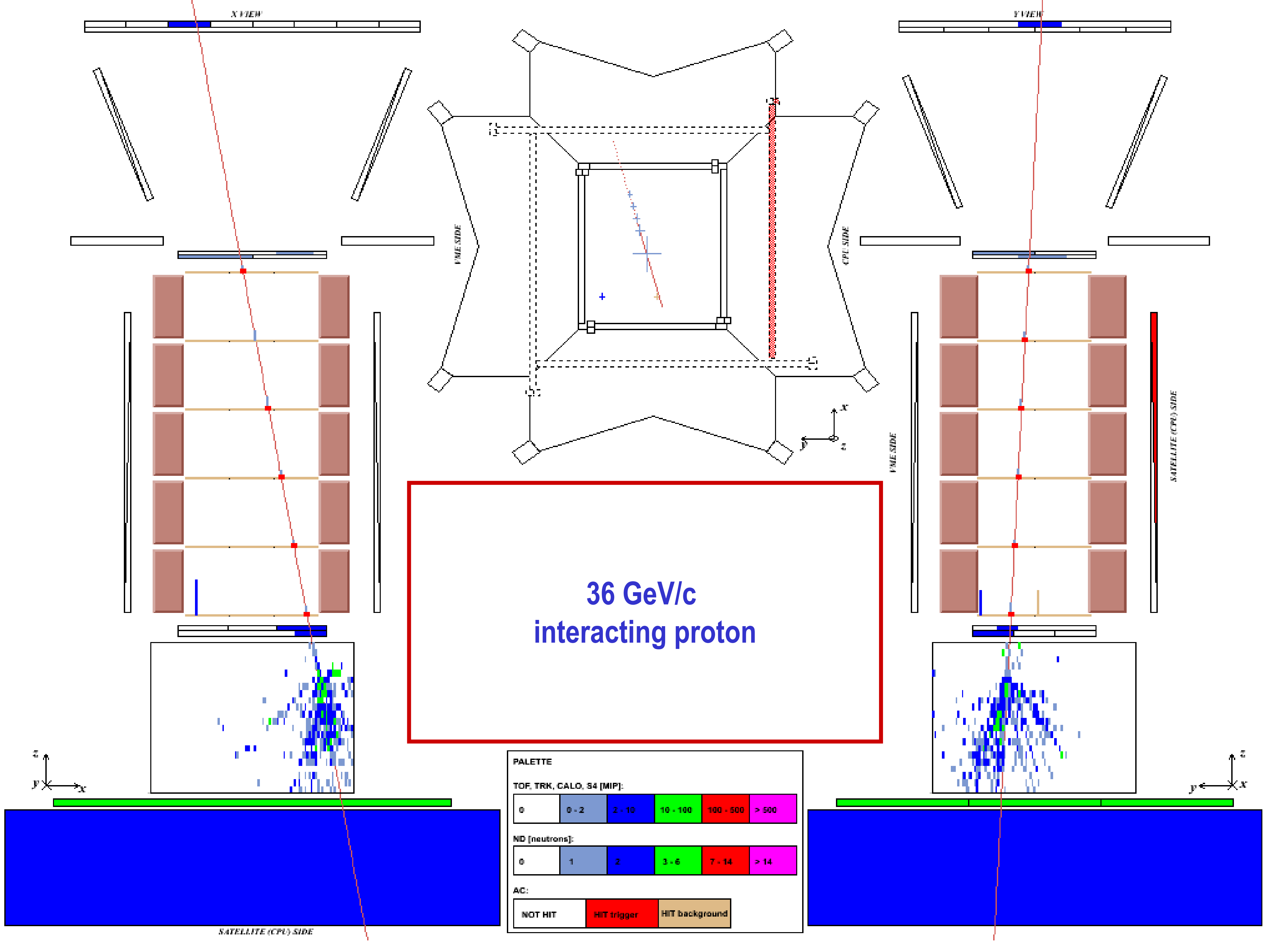
X VIEW
Y VIEW
VME SIDE
CPU SIDE
SATELLITE (CPU) SIDE
36 GeV/c
interacting proton
PALETTE
TOF, TRK, CALO, S4 [MIP]:
0
0 - 2
2 - 10
10 - 100
100 - 500
> 500
ND [neutrons]:
0
1
2
3 - 6
7 - 14
> 14
AC:
NOT HIT
HIT trigger
HIT background

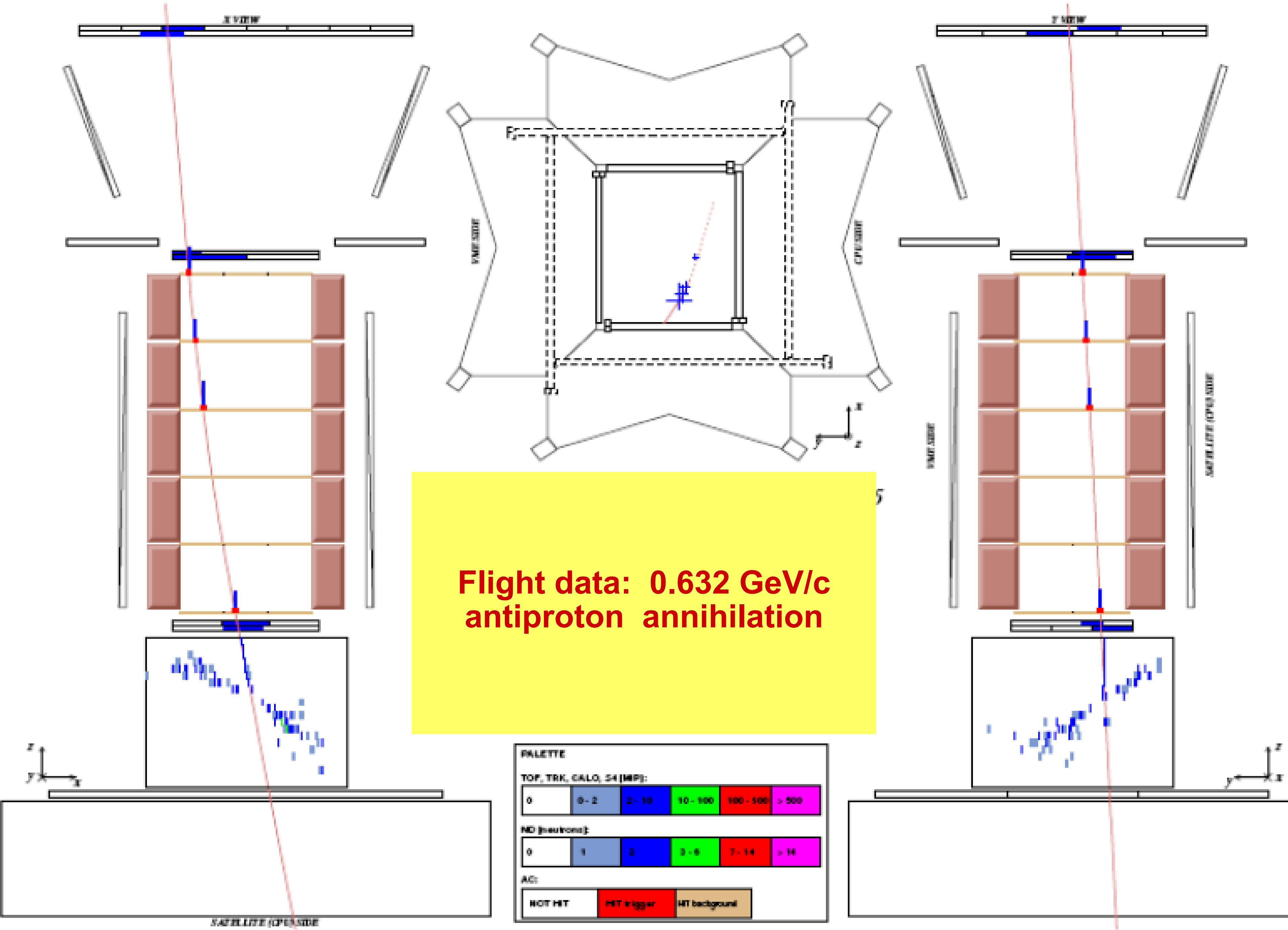


**Flight data: 0.632 GeV/c antiproton annihilation**

# Positron identification

The main difficulty for the positron measurement is the **interacting-proton background**:

- fluctuations in hadronic shower development $\Rightarrow \pi_0 \rightarrow \gamma\gamma$ might mimic pure EM showers
- proton spectrum harder than positron $\Rightarrow$ p/$e^+$ increase for increasing energy

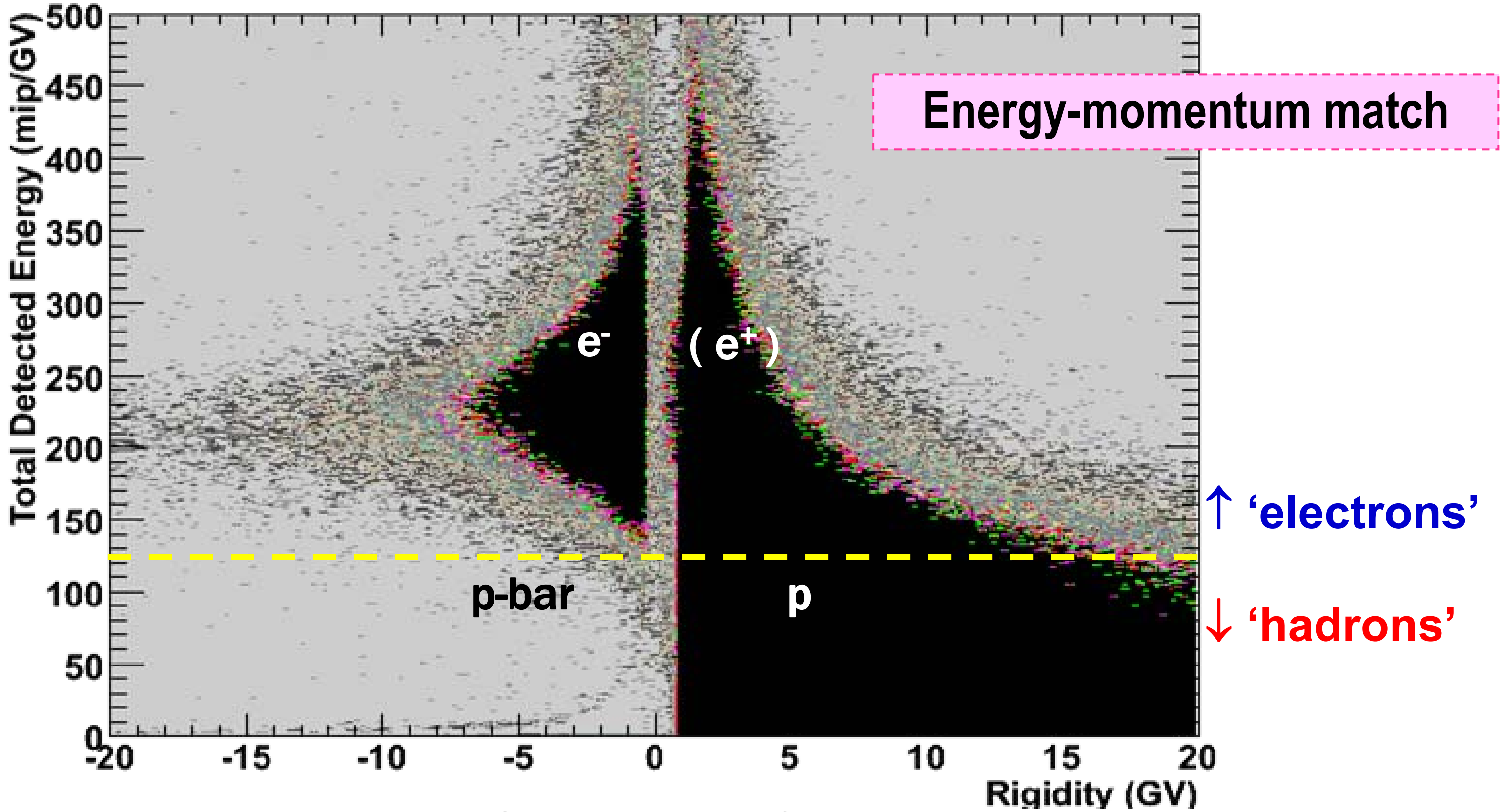

# High energy positron analysis

~500 days of collected data

Calorimeter plays a crucial role

Identification based on:

- **Shower topology**
  - lateral and longitudinal profile
  - shower starting point
- **Total detected energy**
  - energy-rigidity match

Analysis key points:

- **Tuning/check of selection criteria with:**

  test-beam data / simulation / flight data

  Selection of pure proton sample from flight data ("pre-sampler" method)

51 GV positron

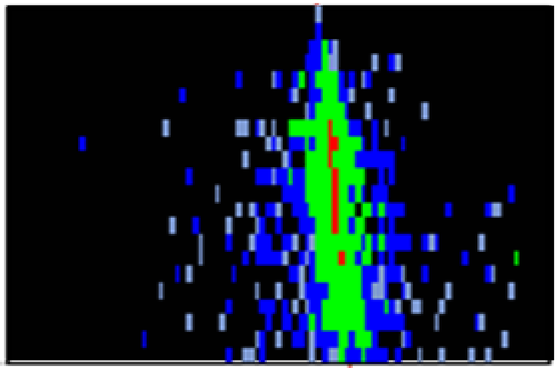

80 GV proton

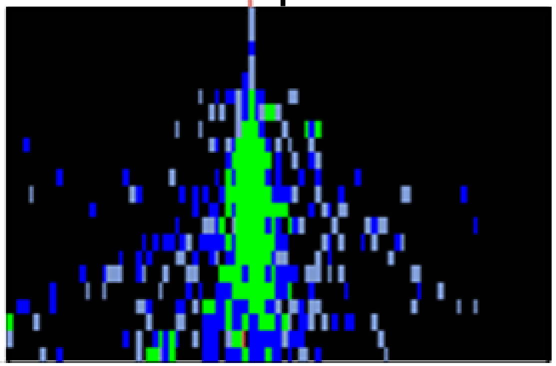

**Final results make <u>NON USE</u> of test-beam and/or simulation calibrations.**
**The measurement is based only on flight data**
**with the <u>background-estimation</u> method**

# The "pre-sampler" method

Selection of a pure sample of protons from flight data

**CALORIMETER: 22 W planes: 16.3 $X_0$**

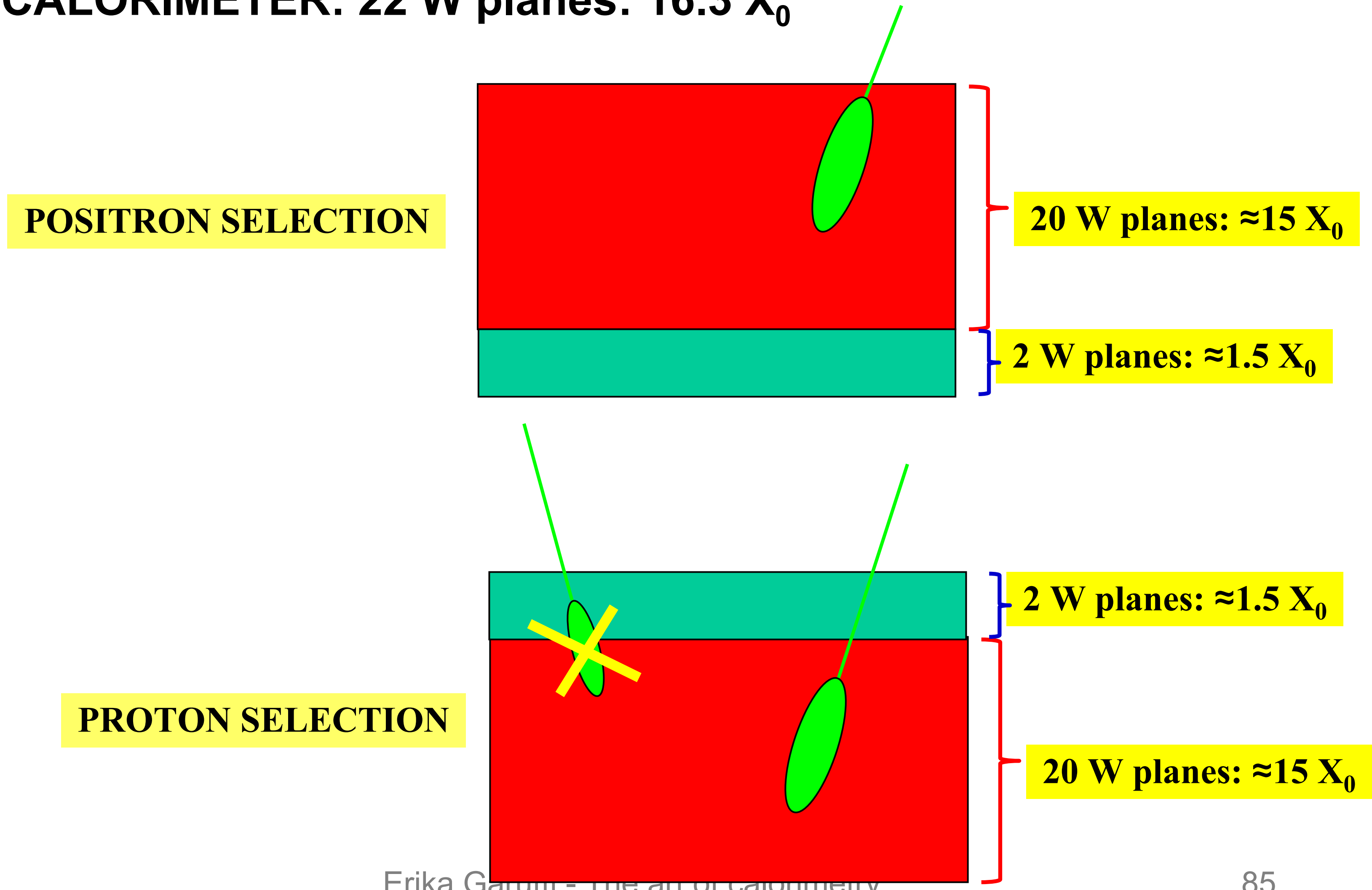

# Measuring anti-matter

## Antiprotons

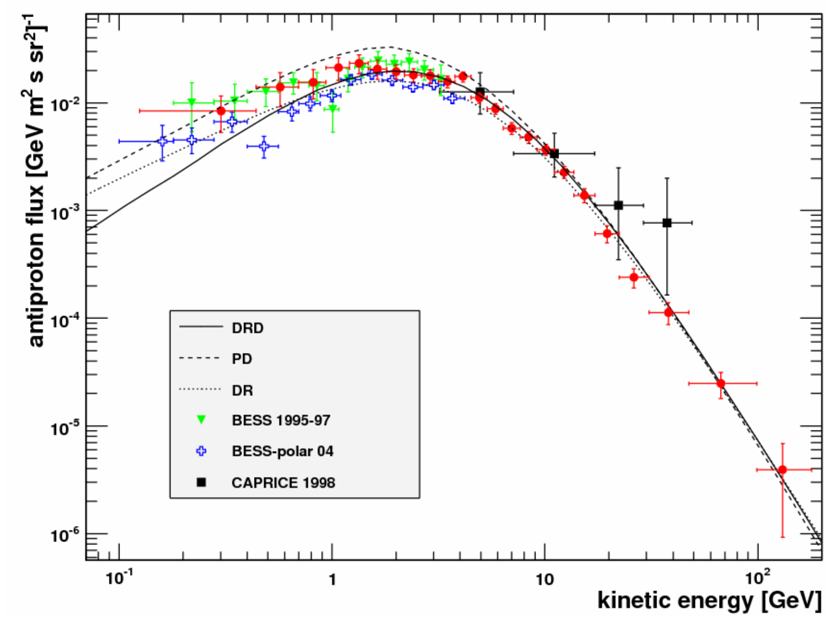


## Positrons

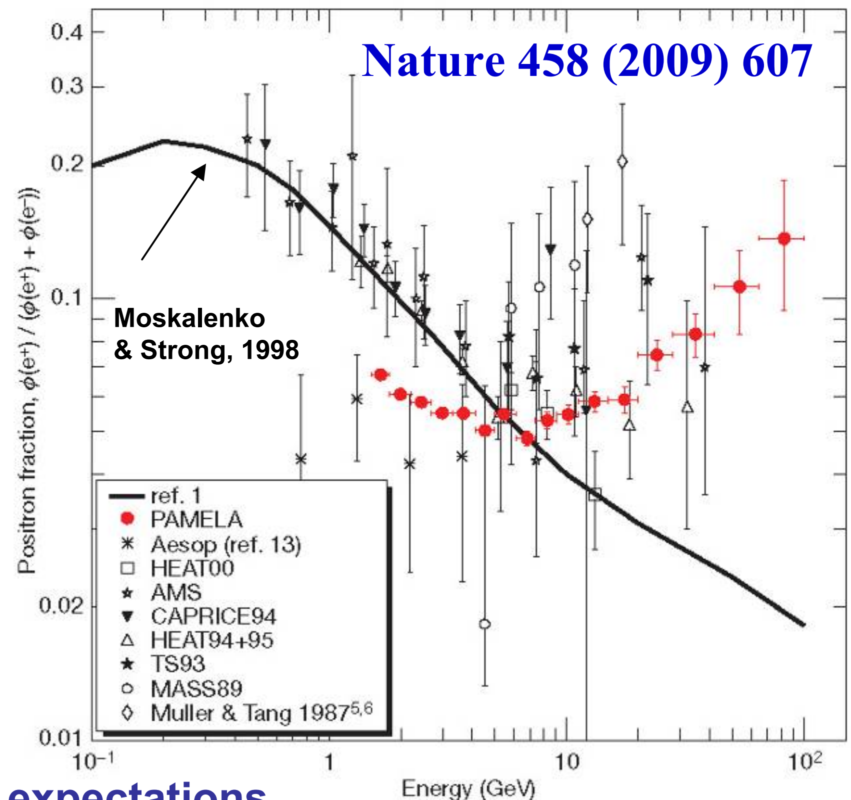


**Antiproton flux (~0.1 GeV ÷180 GeV)**

➔ **no evident deviations from secondary expectations**

**Positron charge ratio (~1 GeV ÷100 GeV)**

➔ **Clear excess with respect to secondary production models**

More data to come at lower and higher energies (up to 300 GeV)

PAMELA run extended till 2011

# Calorimeters at non-collider experiments

1) Calorimeters in space: PAMELA

2) Calorimeters for neutrino physics: Cuoricino/Cuore

# A quick look into neutrino physics

Since 1998, SuperKamiokande, SNO, and KamLAND have shown:

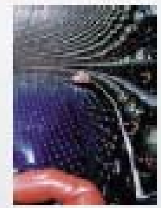

- Neutrinos undergo flavor-changing oscillations
- Neutrinos have finite masses

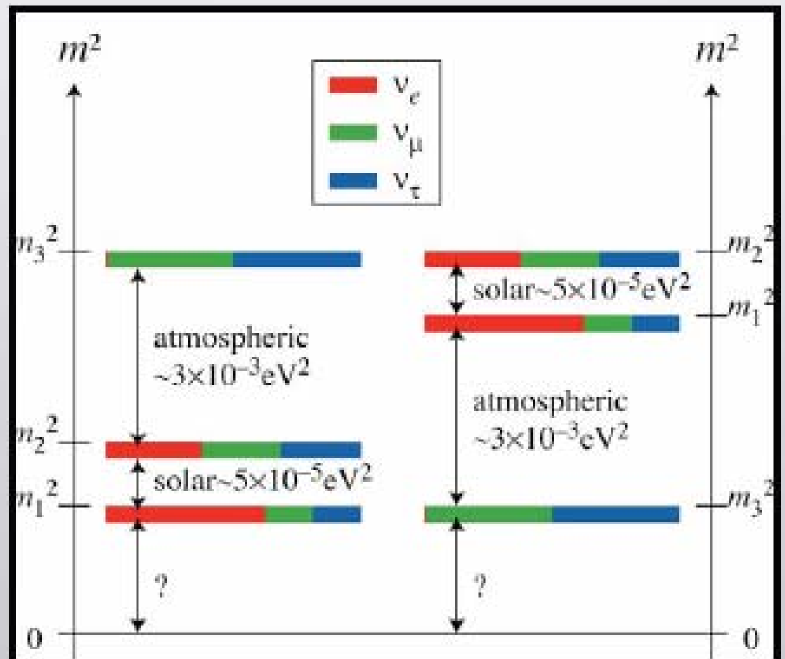


Two Open Questions in ν Physics:

- What is absolute scale of the ν mass?
- Are they Majorana or Dirac particles?

ββ0ν can address these

# Neutrino-less double beta decay (ββ0ν)

$(A,Z) \rightarrow (A,Z+2) + 2e^- + 2\nu_e$ ← allowed by the Standard Model $\tau \geq 10^{19}$ y

$(A,Z) \rightarrow (A,Z+2) + 2e^-$ ← open discussion on its observation $\tau \geq 10^{25}$ y

$(A,Z) \rightarrow (A,Z+2) + 2e^- + \chi$ ← Majoron (light neutral boson)

**Observation of ββ0ν implies Physics beyond the Standard Model**

- Violation of lepton number
- Rate of decay sets ν mass scale
- Process only occurs if neutrinos are Majorana particles

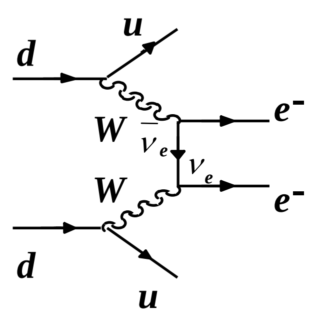

0ν - ββ decay

# Calorimeter for ββ0ν search: The Bolometer

**Bolometer operating principles:**

$\Delta T = E/C$ ⇒ **Low Temperature**

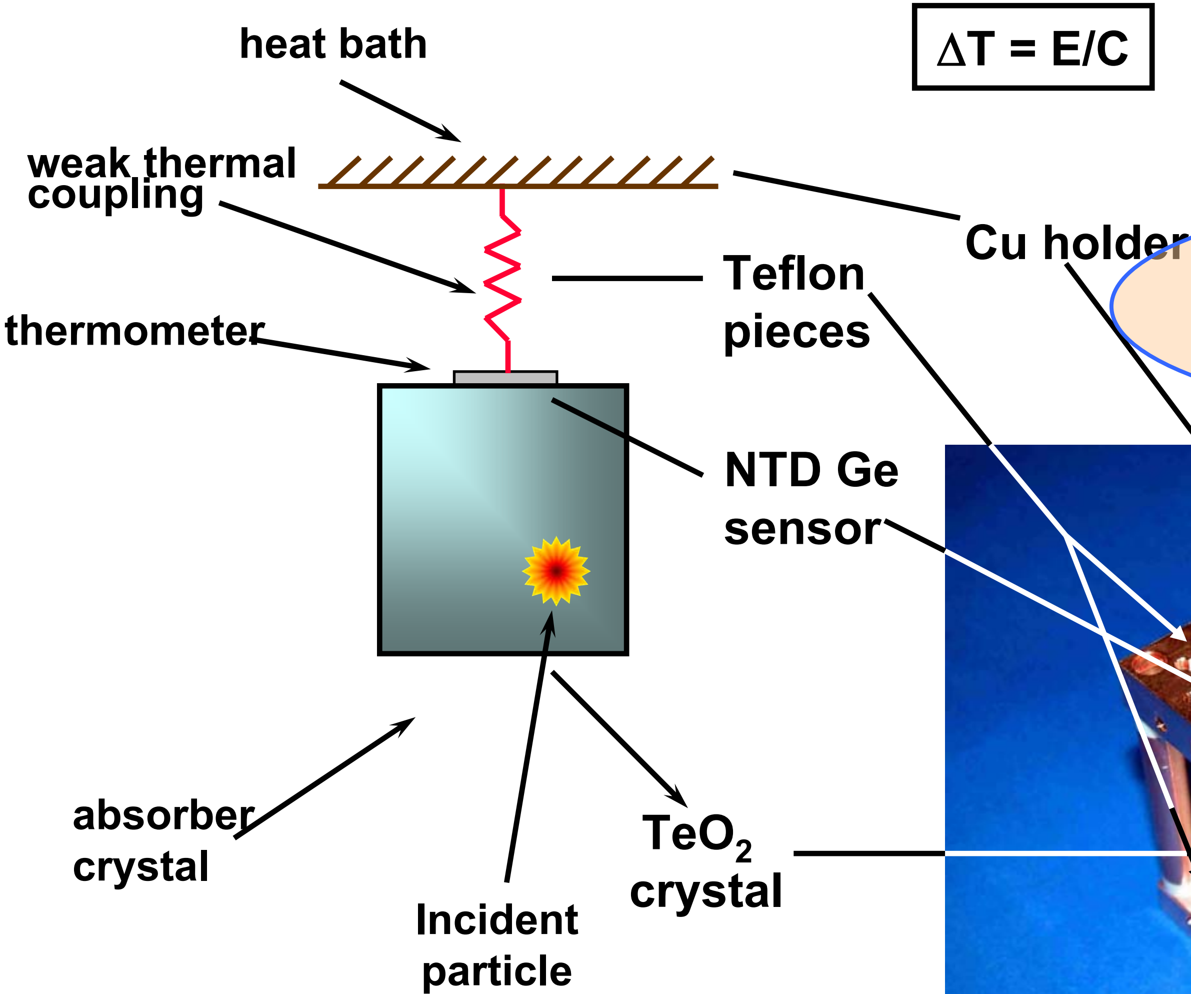


**Absorber material $TeO_2$** low heat capacity large crystals available radiopure

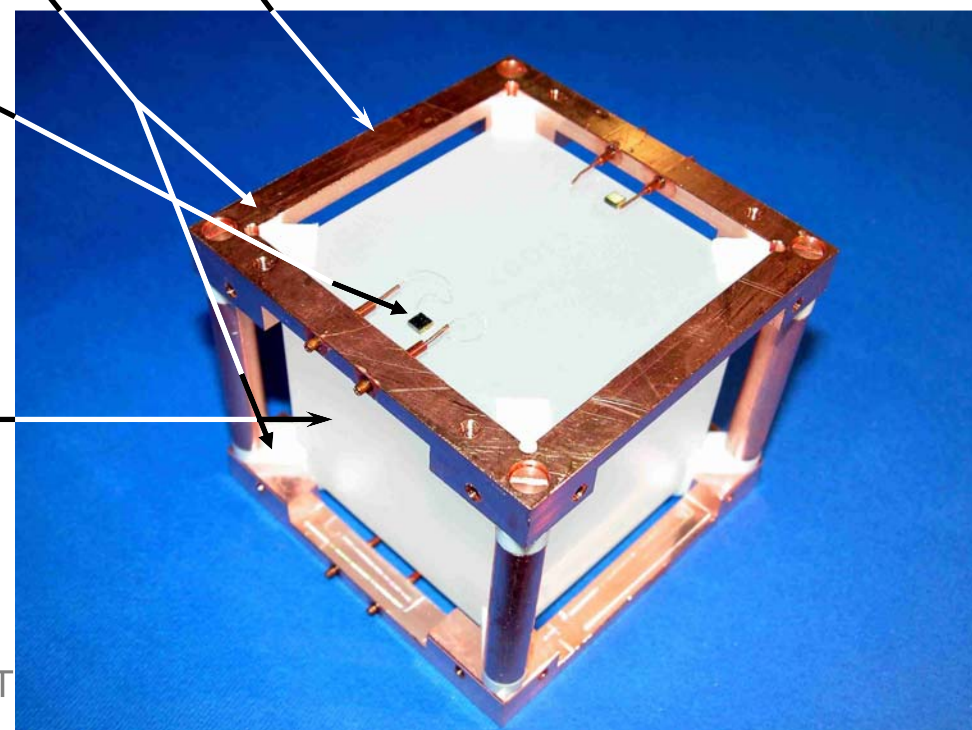

# Cryogenic bolometer

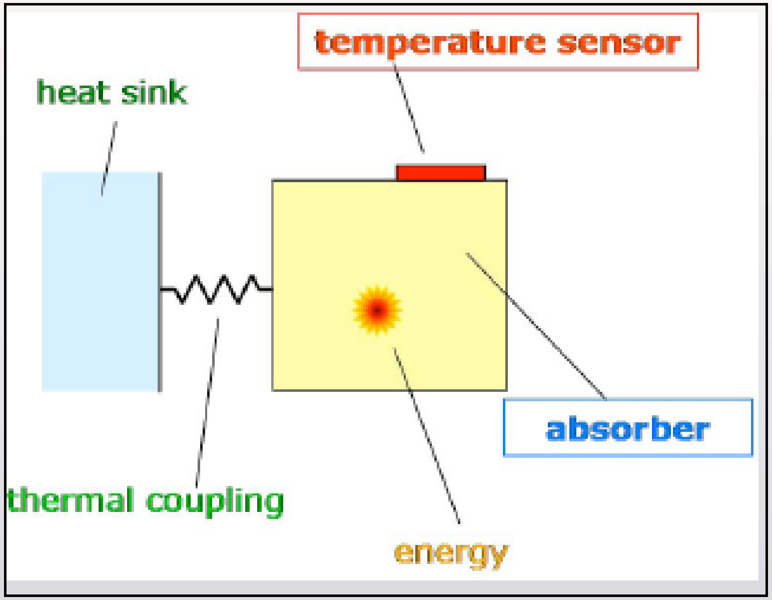


Heat sink: 8-10 mK

Weak thermal coupling (teflon holders):
$G = 4$ pW/mK

Thermister: NTD Ge-thermistor
$R \cong 100$ MΩ, $dR/dT \cong 100$ kΩ/μK

Crystal absorber: $TeO_2$ crystal
$C \cong 2$ nJ/K $\cong 1$ MeV / 0.1 mK

| | |
|---|---|
| Temperature signal for E=1 MeV: → | **$\Delta T = E/C \cong 0.1$ mK** |
| Signal size: $\Delta V = I \times dR/dT \times \Delta T$ → | **1 mV/1 MeV** |
| Signal recovery time: $\tau = C/G$ → | **0.5 s** |
| Noise over signal bandwidth (few Hz): → | **$V_{rms} = 0.2$ μV** |

Energy resolution (FWHM): $\cong$ 1 keV (in theory)

# Laboratori nazionali del Gran Sasso

Shielding: ~3500 m.w.e.

Two dilution refrigerators:

1. Hall A (Cuoricino) ⇒ Running!
2. Hall C (R&D final tests for CUORE)

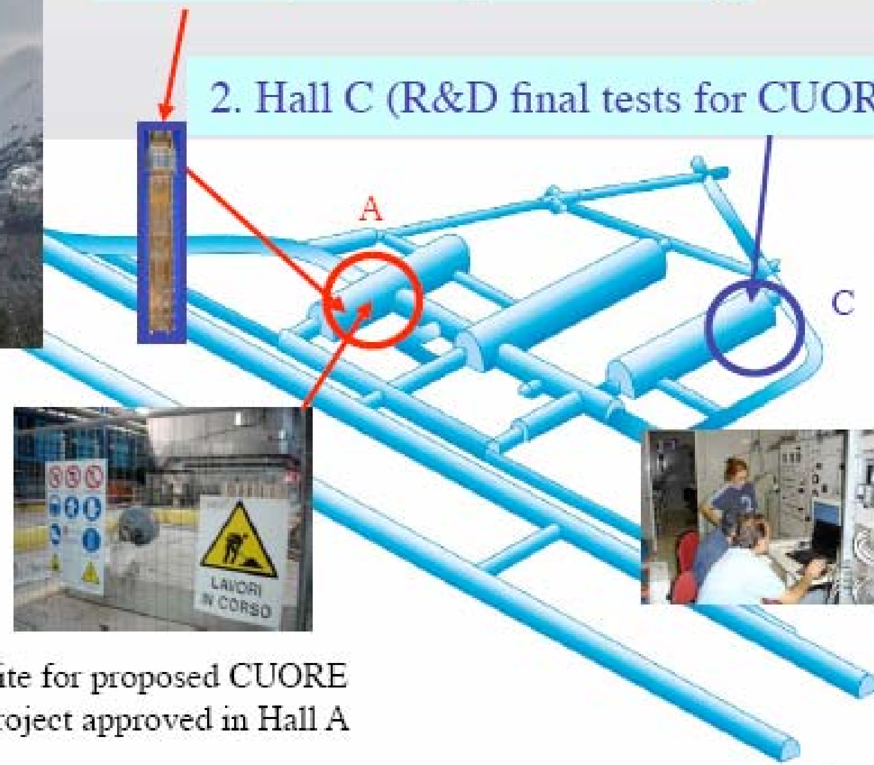


Site for proposed CUORE project approved in Hall A

Cuoricino is currently the largest operating bolometer in the world

# Cuoricino

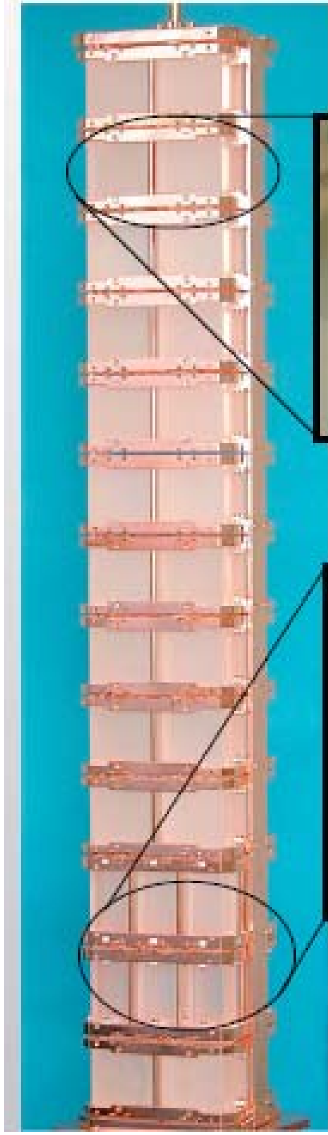

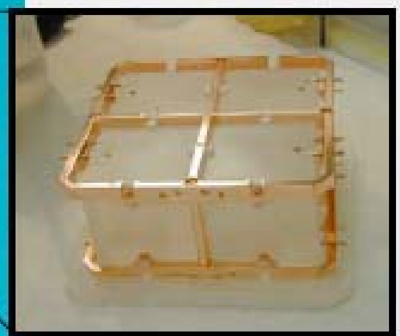

11 modules, 4 detector each,
crystal dimension: 5x5x5 $cm^3$
crystal mass: 750 g
$44 \times 0.79 = 34.76$ kg of $TeO_2$

Encased in a lead shield, nitrogen box, neutron shield, and Faraday cage

2 modules x 9 crystals each
crystal dimension: 3x3x6 $cm^3$
crystal mass: 330 g
$18 \times 0.33 = 5.94$ kg of $TeO_2$

Total detector mass: 40.7 kg $TeO_2$ $\Rightarrow$ **11.64 kg $^{130}Te$**

# Cuoricino results: No peak

Exposure
= 10.85 kg y

Resolution:
FWHM at 2615 keV
= 9.2 ± 0.5 keV

Background:
In the ββ0ν region
= 0.18 ± 0.01 counts /(keV kg y)

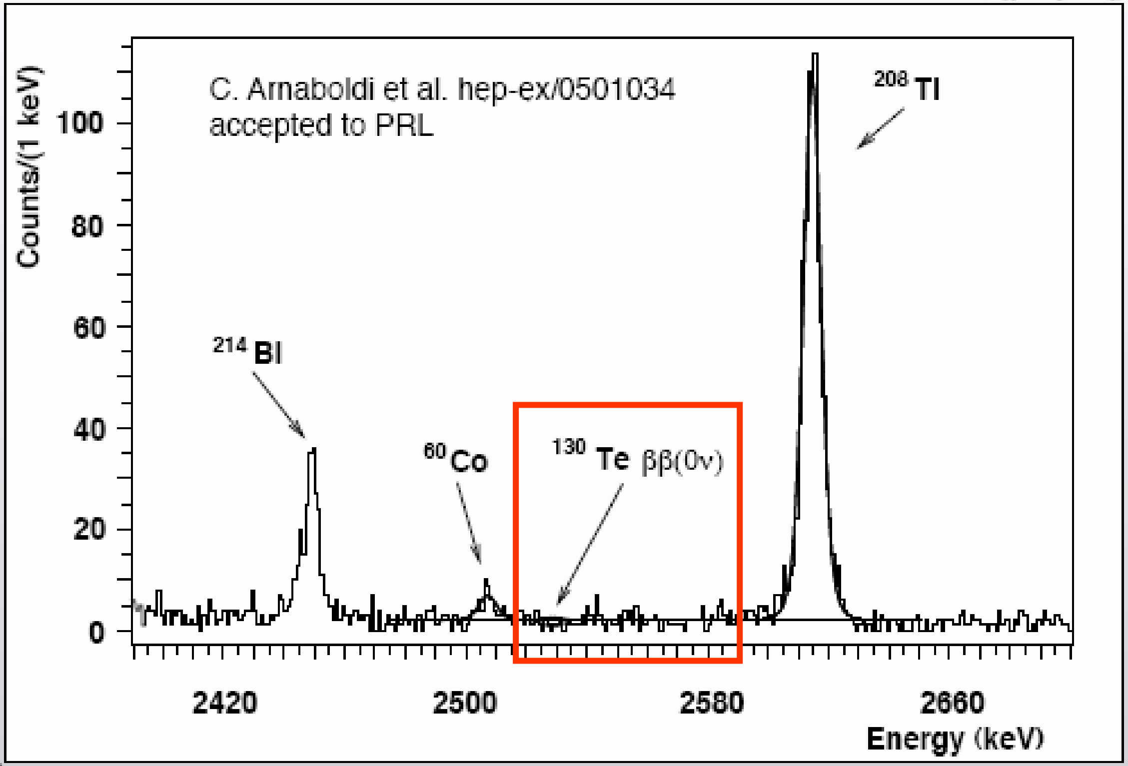


- Anticoincidence spectrum
- ϵ~85%
- Maximum Likelihood+flat+$^{60}$Co (2505)
  - energy region: 2470-2560 keV
- ~5% systematic error upon parameter variation
- N-Gaussian response function with individual FWHM detector resolution

No peak found

$\tau^{0\nu}_{1/2} > 1.8 \times 10^{24}$ y at 90% C.L.

$m_\nu < 0.2 - 1.1$ eV

# Next step: Cuore

- Array of 988 $TeO_2$ crystals
- 19 Cuoricino-like towers suspended in a cylindrical structure
- 13 levels of 4 5x5x5 $cm^3$ crystals (750g each)
- $^{130}Te$: 33.8% isotope abundance
- Time of construction: 4 years
- Total cost: 14-17M USD (depends on Euro…)
- 1st Data target: Jan 1, 2010

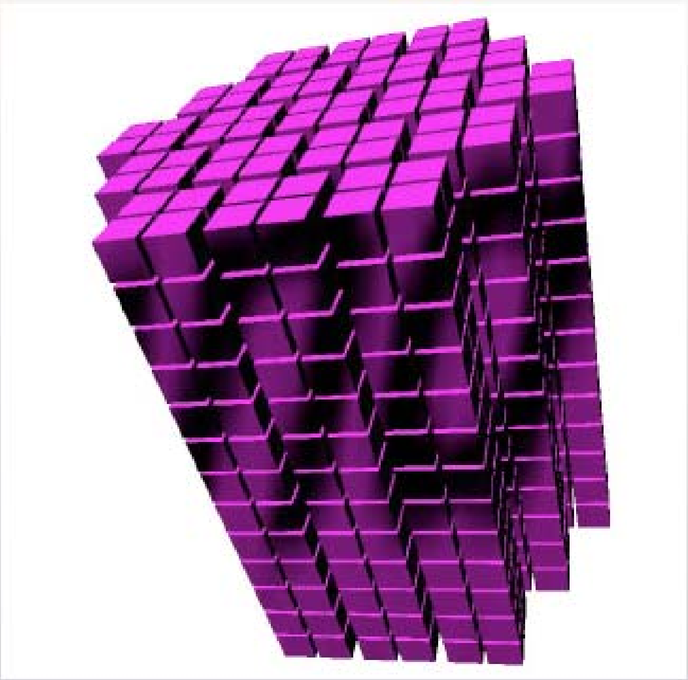

Acts as a single, highly segmented, detector

750 kg $TeO_2$ => 200 kg $^{130}Te$

Approved by the Science Counsel of Gran Sasso Laboratory and by INFN

With bolometry we are back to the original meaning of calorimetry !

# Conclusion: the future of calorimetry

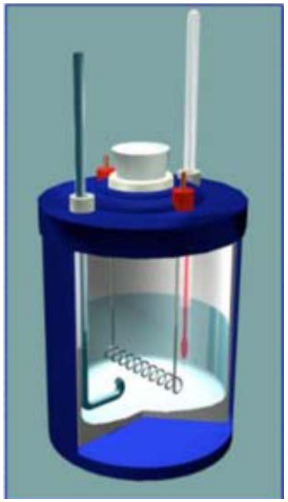

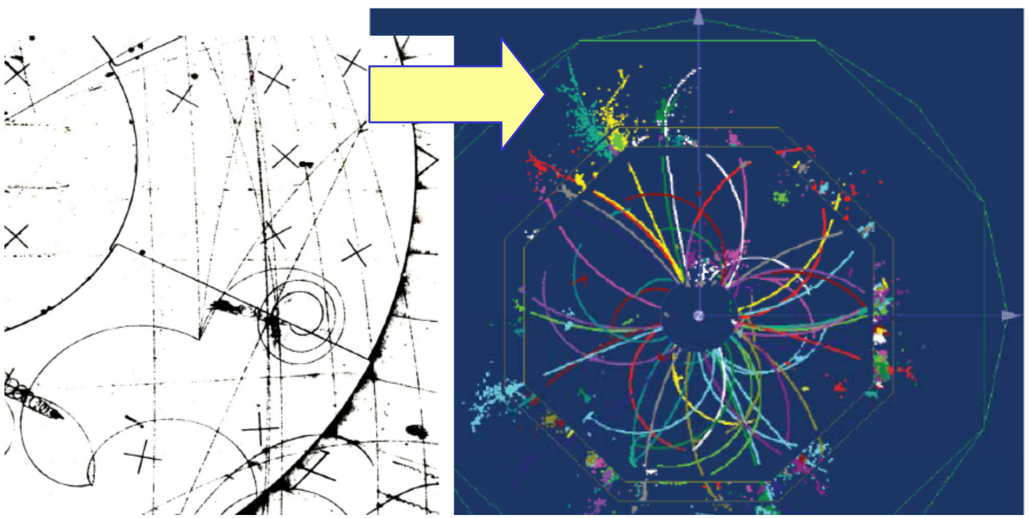

Calorimetry is an art evolved with more than a century of experience

New key issues for calorimetry:
- Extreme segmentation
  ➔ Imaging calorimeters
- Compensation in large volumes (inside magnet)
  ➔ Pflow / dual-readout
- Ultimate resolution

Thank you all for your attention and participation during these lectures!

# Acknowledgments

For these slides I have to give credit to the work of  the GEANT4 group,
O. Adriani, C. D'Ambrosio, T.D. Gutierrez, Dieter Renker,
the CALICE collaboration

from whom I have taken many plots and figures

# Backup

# G4 – hadronic shower models

models for the FIRST interaction of projectile-nucleon collision:

- Theory based models

QGS: Quark-Gluon String model (E>(12*)20GeV) *for p, n, pi, k on nuclei

FTF : Fritiof-like String model (E>20GeV)

- Parameterizations of data (from GHEISHA)

HEP: High Energy Parameterization (E>25GeV)

LEP: Low Energy Parameterization (E<55GeV) range not covered in the theory models for some particles (Σ, Ω)

➔ LHEP: in the interval 25<E<55GeV random selection between LEP and HEP

- FIRST interaction for E<10GeV

Bertini cascade (includes de-excitation via evaporation)

Binary cascade

# After the first interaction

After the first interaction the nucleus is left in a highly excited state
➔ de-excitation models:
P: pre-compound model (as in QGSP)

➔ final processes at low energy:
fission, Fermi breakup, multi-fragmentation and evaporation

➔ re-absorption in the nucleus, photo- and electro-nuclear inter., stopping part.
CHIPS: Chiral Invariant Phase space model

low energy processes (E<20MeV)
high-precision neutron processes and photo-evaporation

# QGS

- interaction of p, n, pi, k with nuclei for 12GeV<E<50TeV
- need to couple to other models for fragmentation and de-excitation of nucleus after initial interaction

nucleon targets is implemented as 3D model

after first interaction projectile and target are split into quarks and form excited quark-gluon strings

longitudinal string fragmentation

longitudinal momentum distribution sampled from fragm. functions

➔ principal model for incident particles above 12 GeV in LHC exp.

# Chiral Invariant Phase Space Model

used in some phys. lists for the fragmentation and de-excitation part

basic block: quasmon = massless free partons forming the hadronic system

hadronization via quark fusion and quark exchange

u,d,s quarks are massless and related by chiral symmetry

quark exchange and fusion are one-dimensional processes

used ideally in combination with QGS model

idea: absorb the soft particles produced in the fragmentation of the QGS by the residual nucleus

summed up energy of absorbed particles is T(b) * dE/dx

in QGSC dE/dx = 1.0 GeV/fm = each absorbed hadron interacts independently with nuclear matter and creates its own "quasmon"

in QGSC_EFLOW dE/dx = 1.5 GeV/fm all absorbed hadrons are combined in an E-flow and create only one "quasmon"

# Bertini cascade

handles incident N, pi, k, hyperons for E<10GeV

uses experimental cross-sections and angular distributions

can be extended to more hadrons (if exp. data available)

projectile (and secondaries) are transported on straight lines through the nuclear medium

first interaction

interaction by free-hadron model cross-section

nuclear medium = concentric shells of constant density

at shell boundary the particle is either reflected or transmitted

de-excitation of remnant nucleus

includes the de-excitation routine

Fermi breakup and fission channels are provided

nuclear evaporation for neutrons and alpha

final gamma emission a the lowest energies (<0.1 MeV)

# Binary cascade

incident p and n for E<3GeV, pi for E<1.5 GeV, light ions for E<3GeV/A

in some cases extended up to 10GeV

based on two-body to two-body or two-body to one-body interactions in the target nucleus

nucleon-nucleon scattering by resonance formation and decay

includes elastic nucleon-nucleon scattering

particle-particle collisions within a 3D target nucleon by free cross-section

projectile (and secondaries) are transported on curved paths (calculated from the integration of the equation of motion) through the nuclear medium

after the Binary cascade the G4 Pre-compound package is used to de-excite the residual nucleus